



Terms and Conditions of Use of Digitised Theses from Trinity College Library Dublin

Copyright statement

All material supplied by Trinity College Library is protected by copyright (under the Copyright and Related Rights Act, 2000 as amended) and other relevant Intellectual Property Rights. By accessing and using a Digitised Thesis from Trinity College Library you acknowledge that all Intellectual Property Rights in any Works supplied are the sole and exclusive property of the copyright and/or other IPR holder. Specific copyright holders may not be explicitly identified. Use of materials from other sources within a thesis should not be construed as a claim over them.

A non-exclusive, non-transferable licence is hereby granted to those using or reproducing, in whole or in part, the material for valid purposes, providing the copyright owners are acknowledged using the normal conventions. Where specific permission to use material is required, this is identified and such permission must be sought from the copyright holder or agency cited.

Liability statement

By using a Digitised Thesis, I accept that Trinity College Dublin bears no legal responsibility for the accuracy, legality or comprehensiveness of materials contained within the thesis, and that Trinity College Dublin accepts no liability for indirect, consequential, or incidental, damages or losses arising from use of the thesis for whatever reason. Information located in a thesis may be subject to specific use constraints, details of which may not be explicitly described. It is the responsibility of potential and actual users to be aware of such constraints and to abide by them. By making use of material from a digitised thesis, you accept these copyright and disclaimer provisions. Where it is brought to the attention of Trinity College Library that there may be a breach of copyright or other restraint, it is the policy to withdraw or take down access to a thesis while the issue is being resolved.

Access Agreement

By using a Digitised Thesis from Trinity College Library you are bound by the following Terms & Conditions. Please read them carefully.

I have read and I understand the following statement: All material supplied via a Digitised Thesis from Trinity College Library is protected by copyright and other intellectual property rights, and duplication or sale of all or part of any of a thesis is not permitted, except that material may be duplicated by you for your research use or for educational purposes in electronic or print form providing the copyright owners are acknowledged using the normal conventions. You must obtain permission for any other use. Electronic or print copies may not be offered, whether for sale or otherwise to anyone. This copy has been supplied on the understanding that it is copyright material and that no quotation from the thesis may be published without proper acknowledgement.

The effect of processing on the solid state characteristics of selected sulphonamides and their sodium salts, alone and as drug-salt composites

Presented by

Stefano Bianco, B.Sc. (Pharm.)

being a thesis submitted for the degree of
Doctor of Philosophy in Pharmaceutics

at the

University of Dublin, Trinity College

under the direction and supervision of

Professor Anne Marie Healy, B.Sc. (Pharm.), Ph.D., M.P.S.I., F.T.C.D.

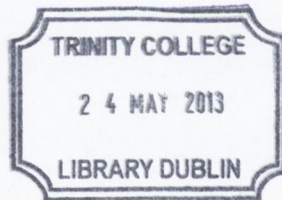
and

Lidia Tajber, B.Sc. (Pharm.), Ph.D., M.P.S.I

and

**Professor Owen I. Corrigan,
B.Sc. (Pharm.) (N.U.I.), M.A., Ph.D. (N.U.I.), F.T.C.D., F.P.S.I.**

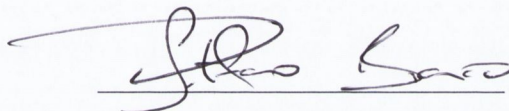
Aprile 2013



Thesis 9896

DECLARATION

This thesis is submitted by the undersigned to the University of Dublin, Trinity College, for examination for the degree of Doctor of Philosophy. This thesis has not been submitted as an exercise for a degree at any other university. It is entirely the work of the undersigned author, except where duly acknowledged. This manuscript was completely written by the undersigned author, with the aid of editorial advice from Prof. Anne Marie Healy and Dr. Lidia Tajber and Professor O.I. Corrigan. It is agreed that the library may lend or copy this thesis upon request.

A handwritten signature in black ink, appearing to read 'Stefano Bianco', written over a horizontal line.

Stefano Bianco

TABLE OF CONTENTS

Acknowledgements	<i>i</i>
Presentations and publication associated with this thesis	<i>iv</i>
Abbreviations and Symbols	<i>vi</i>
Summary	<i>x</i>

INTRODUCTION

Chapter 1 Introduction	1
1.1 Origin and scope	3
1.2 Aims and objectives	5
1.2 Spray drying	7
1.3 The sulphonamides	11
1.4 Background to drugs used in the current work	12
1.5 Solid state characteristics of API materials	13
1.6 Polymorphism	13
1.6.1 Classification of Polymorphs: Enantiotropism and Monotropism	14
1.6.2 Pseudo-polymorphism (Solvates and hydrates)	16
1.7 Amorphous state	18
1.7.1 Amorphous solids by rapid cooling of melt (quench cooling)	18
1.7.2 Stability of the amorphous state	20
1.8 Water-solid interaction mechanism	21
1.9 Physicochemical characterisation	22

1.9.1 Thermal analysis	22
1.9.2 FTIR Analysis	25
1.9.3 Powder X-Ray Diffraction (PXRD)	28
1.9.4 Inverse gas chromatography (IGC)	29
1.9.5 Water vapour sorption analysis (DVS)	30

Chapter 2 Materials and Methods

2.1 Materials	35
2.2 Methods	36
2.2.1 Spray drying	36
2.2.2 Spray drying of sulfadimidine (SD) and sulfadimidine sodium (SDNa)	37
2.2.3 Spray drying of sulfadimidine and sulfadimidine sodium composite systems	38
2.2.4 Spray drying of sulfathiazole (ST) and sulfathiazole sodium (STNa)	38
2.2.5 Spray drying of sulfathiazole and sulfathiazole sodium composite systems	40
2.2.6 Thermal Analysis Methods	41
2.2.6.1 Differential scanning calorimetry (DSC)	41
2.2.6.2 Modulated temperature differential scanning calorimetry (MTDSC)	41
2.2.6.3 Thermogravimetric analysis	41
2.2.7 Powder X-ray diffraction (PXRD)	42
2.2.7.1 Crystalline content evaluation by PXRD	42
2.2.8 Powder density (Helium pycnometry)	43
2.2.9 Scanning Electron Microscopy (SEM)	43
2.2.10 Fourier Transform Infra-Red Spectroscopy (FTIR)	43
2.2.11 Attenuated total reflectance Fourier Transform Infra-Red Spectroscopy (ATR-FTIR)	44
2.2.12 Water sorption analysis	44

2.2.12.1	Dynamic vapour sorption (DVS)	44
2.2.13	Surface free energy measurement	46
2.2.14	Tg prediction of composites using the Gordon and Taylor equation	47
2.2.15	Solid-state stability study	48
2.2.16	Solubility studies of sulfathiazole	48
2.2.16.1	Solubility in acetone and acetone:water solvent systems	48
2.2.17	Solubility studies of sulfadimidine	49
2.2.17.1	Solubility in acetone	49
2.2.18	Statistical analysis	50

Results and discussion

Chapter 3 Amorphisation of sulfadimidine and sulfadimidine sodium upon spray drying

3	Introduction	53
3.1	Spray dried Sulfadimidine (SD) and sulfadimidine sodium (SDNa)	56
3.2	Physicochemical properties of Sulfadimidine	56
3.2.1	PXRD, thermal and solubility analysis	58
3.3	Sulfadimidine spray dried from water and ethanol /water mixtures	58
3.3.1	Open cycle mode (OCM)	58
3.3.1.1	SD spray dried from water	61
3.3.1.2	SD spray dried from ethanol:water co-solvent systems	64
3.3.2	Closed cycle mode (OCM)	64
3.3.2.1	SD spray dried from acetone and acetonic solutions	67
3.4	FTIR analysis	70
3.5	DVS analysis	72
3.6	Physical stability upon storage at different temperature and RH conditions	74

3.7	SEM analysis	76
3.8	Key findings on sulfadimidine	77
3.9	Sulfadimidine sodium (SDNa)	77
3.9.1	Introduction	78
3.9.2	Sulfadimidine sodium spray dried from pure water and ethanol:water mixtures	78
3.9.3	SDNa spray dried from water	82
3.9.4	Sulfadimidine sodium spray dried from ethanol:water co-solvent systems.	86
3.9.5	SDNa spray dried from acetonic solutions	87
3.9.6	SEM analysis	89
3.10	FTIR analysis of amorphous SDNa	90
3.11	DVS analysis	96
3.12	Stability studies of spray dried SDNa at 4 and 25°C, under desiccated conditions / 60% RH / 70% RH	98
3.13	Key findings on sulfadimidine sodium	
3.14	SD and SDNa co-spray dried systems	99
3.15	Co-spray dried SD:SDNa	101
3.15.1	SEM analysis	104
3.15.2	DVS analysis	105
3.16	Conclusion	107

Chapter 4 Modification of the solid state nature of sulfathiazole and sulfathiazole sodium via spray drying

4	Introduction	111
4.1	Sulfathiazole	113
4.2	Results	113

4.3	Solubility	113
4.4	PXRD analysis	114
4.4.1	Open cycle mode (OCM)	114
4.4.2	Closed cycle mode (CCM)	117
4.5	Thermal analysis	117
4.5.1	Open cycle mode (OCM)	117
4.5.2	Closed cycle mode (CCM)	119
4.6	FTIR analysis	120
4.6.1	Open cycle mode (OCM)	120
4.7	SEM analysis	121
4.7.1	Open cycle mode (OCM)	121
4.7.2	Closed cycle mode (CCM)	122
4.8	DVS analysis	123
4.9	Discussion on Sulfathiazole	124
4.10	Sulfathiazole sodium	129
4.10.1	PXRD analysis	129
4.10.1.1	Open cycle mode (OCM)	129
4.10.1.2	Closed cycle mode (CCM)	130
4.11	Thermal analysis	130
4.11.1	Open cycle mode (OCM)	130
4.11.2	Closed cycle mode (CCM)	133
4.12	DVS analysis	134
4.13	Discussion on sulfathiazole sodium	137
4.14	Conclusion	140

Chapter 5 Bulk, surface properties and water uptake mechanisms of salt/acid amorphous composite systems

5.1	Introduction	145
5.2	Results and discussion	147
5.3	FTIR analysis	151
5.4	iGC analysis	153
5.5	DVS analysis	157
5.6	Conclusions	164

Chapter 6 General discussion

6.1	Introduction	167
6.2	Spray drying of sulfadimidine (SD) and sulfathiazole (ST)	169
6.3	Comparing differences in the tendency to crystallisation of SD and ST from the amorphous state	172
6.4	Comparison of solvent mediated polymorphic transformation and spray drying of ST	174
6.5	(Water mediated) Recrystallisation from the amorphous state	177
6.6	Comparing hydration of crystalline and amorphous salts	180
6.7	Amorphous dispersions	182
6.8	Main findings	184
6.9	Suggestions for future work	186

References	189
-------------------	-----

Appendices	205
-------------------	-----

Appendix I	207
------------	-----

ACKNOWLEDGEMENTS

First and foremost, I would like to thank my supervisors Prof. Anne Marie Healy, Dr Lidia Tajber and Prof. Owen Corrigan for their kind and constant encouragement, help and support over the last few years. In particular, I wish to thank Prof. Anne Marie Healy for giving me the opportunity of being part of her research group and for her untiring patience, together with Dr Lidia Tajber, in supervising me and suggesting improvements for this work. I am grateful to the Solid State Pharmaceutical Cluster (SSPC) and Science Fund Ireland (SFI) for their support and for giving me the opportunity to participate at international conferences on innovative pharmaceutical research in Europe and in USA. I would also like to extend my thanks to the academic, secretarial and technical staff of the School of Pharmacy and Pharmaceutical sciences and in particular to Betty, Liesa, Conan, Brian, Pat, Ray, Catherine, Derek for their assistance and help during the course of my research. Acknowledgements would not be complete without thanking all PhD students and post Docs: Vincent, Christine, Krzysztof, Anita, Joanne, Youness, Ines, Clare, Stephany, Arun, Shadeed, Bo, Maria, Janani, Adrian, Pat, Brian, Bozena, Keith, Sid, Ika, Fery, Connor, Andy, Katerina, Tadhg, Jason, Shona, Mike, Juan, Gary, Cathal, Park, Manuel, Serena and all the others I have left out of this list for being friends and not only colleagues. Grateful thanks to Vincent and Frederic (and Emma Rose) and Evelyn for their help, for the interesting scientific discussions we always engaged in, and for the fun and good times we always had outside these walls (too many Guinness though). Special thanks to Antonio, Mattia, Raffaella, Andrea and Anne Marie, Alessandra, Luis and Declan for being my family over the last four years and for their help and support when events seemed to be 'precipitating' together with my solutions. Finally, thanks to Roberta for her encouragement, patience and support, without which most probably, I would not

have brought this project to completion. Thanks in conclusion, to Mom and Dad, and to Daniel and Jessica for being there whenever I needed them.

To Maureen and Giuseppe

PRESENTATIONS AND PUBLICATIONS ASSOCIATED WITH THIS THESIS

Oral Presentation

“Amorphisation of sulphonamide-sulphonamide sodium salt composite systems via spray drying” presented at APSGB, University of Nottingham, Nottingham, April 2010. [S. Bianco, L. Tajber, O. I. Corrigan and A. M. Healy]. (Oral presentation award)

Poster Presentations

“The Physico-chemical characterisation of spray dried sulphonamide compounds and their sodium salts” presented at All-Ireland Schools of Pharmacy 30th Research Seminar, Trinity College, Dublin, April 2009. [S. Bianco, V. Caron, L. Tajber, O. I. Corrigan and A. M. Healy].

“Physico-chemical characterisation of spray dried sulphonamide compounds and their sodium salts” presented at AAPS Annual Meeting, October, 2009, Los Angeles, California, U.S.A. [S. Bianco, V. Caron, L. Tajber, O. I. Corrigan and A. M. Healy]

“Characterisation of co-spray dried sulphonamide-corresponding sodium salt composite systems” presented at All-Ireland Schools of Pharmacy Research Seminar, Queens University of Belfast, Belfast, April 2010. [S. Bianco, C. Bourke, V. Caron, L. Tajber, O. I. Corrigan and A. M. Healy]

“Modification of the solid state of sulfathiazole-sulfathiazole sodium composite systems via spray drying” presented at AAPS Annual Meeting, October, 2011, Washington Convention Center, Washington DC, U.S.A. [S. Bianco, F. Tewes, V. Caron, L. Tajber, O. I. Corrigan and A. M. Healy]

“Bulk and surface properties and water uptake mechanisms of salt/acid amorphous composite systems” presented at CGOM, June, 2012, University of Limerick, Limerick, Ireland. [S. Bianco, F. Tewes, V. Caron, L. Tajber, O. I. Corrigan and A. M. Healy]

Publications

“Modification of the solid state nature of sulfathiazole and sulfathiazole sodium via spray drying”, AAPS PharmSciTech. 2012 Jun;13(2):647-60. [S. Bianco, V. Caron, L. Tajber, O. I. Corrigan, L. Nolan, Y. Hu and A. M. Healy].

"Bulk, surface properties and water uptake mechanisms of salt/acid amorphous composite systems", [S. Bianco, F. Tewes, L. Tajber, V. Caron, O. I. Corrigan and A. M. Healy]. (in the process of being submitted to the International Journal of Pharmaceutics).

ABBREVIATIONS AND SYMBOLS

A	amorphous
A_c	area under peaks of processed/spray dried sample
A_x	area under peaks of unprocessed/raw material
API	active pharmaceutical ingredient
ATR	attenuated total reflectance
ρ	true density
C	crystalline
CCDC	Cambridge crystallographic data centre
C_s	solubility of solute
CM	closed mode configuration of spray dryer
DSC	differential scanning calorimetry
DVS	dynamic vapour sorption
EtOH	ethanol
Exo	exothermic direction
FTIR	Fourier transform infrared spectroscopy
g	grams
H	enthalpy
hr	hour/hours
HPLC	high performance liquid chromatography
iGC	inverse gas chromatography

J/g	joules per gram
K	degrees Kelvin
KBr	potassium bromide
kV	kilovolts
L/hr	litres per hour
M	molar
m	metres
mA	milliamperes
mbar	millibars
mg	milligrams
min	minute/minutes
mL	millilitres
mm	millimetres
MTDSC	modulated temp. differential scanning calorimetry
n	number of replicates
NaCl	sodium chloride
nm	nanometres
OM	open mode configuration of spray dryer
<i>p</i>	total vapour pressure
pH	minus log of hydrogen ion concentration
Ph. Eur.	European Pharmacopoeia
r^2	correlation of coefficient
RH	relative humidity

r.p.m	revolutions per minute
SD	sulfadimidine
sd	standard deviation
sec	seconds
SEM	scanning electron microscopy
t	time
T	temperature
TGA	thermogravimetric analysis
T_K	Kauzmann temperature
T_m	melting temperature/point
T_g	glass transition temperature
V	volume
v/v	volume in volume
w/v	weight in volume
w/w	weight in weight
x	mole fraction
PXRD	(powder) X-ray diffraction
%	percent
°	degree
°C	degree Celsius
±	plus or minus
~	approximately
α	alpha

β	beta
γ	gamma
δ	delta
ρ	density
θ	angle of incidence
Σ	sum of
ΔH	change in enthalpy
ΔH_c	enthalpy of crystallisation
ΔH_f	enthalpy of fusion
ΔT	temperature difference
μm	micrometers
μl	microlitres
μg	micrograms

SUMMARY

The purpose of the research presented in this thesis was to produce metastable active pharmaceutical ingredients (API) by spray drying and to analyse, physico-chemically characterise these forms and develop strategies to enhance their physical stability. The solid state properties of two spray dried drugs and their sodium salt forms together with co-spray dried API/salt composites were investigated and compared to the unprocessed materials. The drugs investigated were the sulphonamide compounds, sulfadimidine and sulfathiazole. The compounds were spray dried from water, ethanol, acetone and mixtures of these organic solvents with water.

The methods of analysis employed to characterise the resulting spray dried powders were conventional and modulated differential scanning calorimetry (DSC/MTDSC), thermogravimetric analysis (TGA), Fourier transform infrared spectroscopy (FTIR), attenuated total reflectance-FTIR (ATR-FTIR) and powder X-ray diffraction (PXRD). Surface properties were analysed by inverse gas chromatography (IGC) and morphology by scanning electron microscopy. Hygroscopic properties and water interactions were studied by dynamic vapour sorption (DVS).

All APIs were crystalline prior to spray drying. Both sulfadimidine and sulfathiazole could be spray dried into X-ray amorphous materials by tuning specific process parameters - the selection of an inlet temperature resulting in an outlet temperature of the process below the glass transition of the API and the use of the spray drier in the open mode configuration rather than the closed mode configuration resulted in amorphous product. Some reduction in crystallinity was detected for sulfadimidine when a higher inlet temperature or the closed mode configuration was used, whereas sulfathiazole did not form amorphous phases when the latter configuration was employed, but resulted in

the metastable polymorph I. The physical stability of the two amorphous APIs was considerably different, with sulfadimidine being stable for up to 5 months on storage under dry conditions at 5 °C, whereas sulfathiazole started to crystallise within an hour from the end of the spray drying process. Physical stability studies on amorphous sulfathiazole under different temperatures and relative humidities showed that the API can be tuned to crystallise into a specific polymorph by selecting the conditions of storage and that the crystallisation of amorphous sulfathiazole in the solid state follows Ostwald's rule of stages.

Spray drying of salt solutions resulted in amorphous materials, regardless of the solvent and the spray drier configuration employed. Enhanced physical stability characterised the amorphous salt powders compared to the non-ionised forms under dry conditions of storage. No detection of crystalline material was possible even after more than three years storage in dry conditions. However, the amorphous salts were highly hygroscopic materials and moisture induced crystallisation of the salts to hydrates was determined through intermediate/transitory viscous/liquid solutions.

In the case of API/salt co-spray dried systems, amorphous dispersions of sulfadimidine/sulfadimidine sodium and sulfathiazole/sulfathiazole sodium could be produced over a wide composition range. Augmented proportions of salt raised the T_g , enhancing the storage stability, however an enhanced hygroscopicity also resulted. For example, the addition of only 10% w/w salt to sulfathiazole resulted in a considerable increase in stability from 1 hour to approximately 2 months when stored in desiccated conditions. Tuning the properties of amorphous salt/acid composites by optimising the API:salt ratio appears potentially promising to improve the physical stability of amorphous formulations.

Chapter 1
Introduction

1.1 Origin and scope

Solid state characterisation of a drug following pharmaceutical processing and upon storage is a fundamental aspect in the development of drug formulations.

Nowadays the pharmaceutical industry is faced with many challenges. Problems occur when active pharmaceutical ingredients (API) and excipients undergo phase transformations during development and processing which influence the physical, chemical and mechanical properties of solids. The solid-state properties of the API have to be fully characterised and understood in order to tackle unpredictability and to ensure consistent product performance. Most solid drug formulations use APIs in their stable crystalline state. This is to guarantee quality, stability, safety and therapeutic efficacy. Although it is generally advantageous to produce a drug substance in its most stable form, to avoid undesirable changes occurring during processing or storage, the most stable form is not always the one characterised by the best biopharmaceutical properties (Rodríguez-Spong *et al.*, 2004). A key aspect of innovation in drug product development is to produce a drug in its most useful solid state form for the successful development of pharmaceutical preparations, even at the cost of reduced stability. Notwithstanding, adequate stability of a dosage form must be ensured and maintained within the limits imposed by pharmaceutical regulations (Mortko *et al.*, 2010). In addition, with the increasing number of newly discovered poorly soluble drugs, it may be worthwhile to use either metastable crystalline or amorphous states which, due to their higher level of energy, are characterised by greater apparent solubility. Unfortunately, drugs in the non-equilibrium state are much less stable than their crystalline counterparts and tend to revert back to the more stable crystalline state, often precluding the use of amorphous state in solid oral dosage forms. Consequently one of the most significant challenges for the

industry is to guarantee similar product performance (including stability) at least for the shelf life of the product.

Traditionally, pharmaceutical processes were optimised to prevent or reduce the insurgence of metastable forms. Nowadays there is a tendency to employ and exploit techniques such as milling or spray drying which may result in the generation of metastable pharmaceuticals. However a more in depth understanding of the phenomenon of amorphous / metastable form generation is needed to be of use from a pharmaceutical perspective.

Several studies reported in the literature have been carried out on the crystallisation of sulfathiazole from solution by means of different solvents (solvent mediated polymorphic transformation). These studies highlighted that the choice of process parameters used affected the final polymorphic form (Aaltonen et al., 2003; Blagden et al., 1998; Parmar et al., 2007). However, no amorphous sulfathiazole has been produced so far except by melt quench techniques (Caron et al., 2011; Kerč and Srčić, 1995; Threlfall, 1995). Furthermore, attempts by Caron et al., (2011) to obtain an amorphous form of this API via spray drying proved unsuccessful (Caron et al., 2011). In contrast, sulfamidine, despite having a similar chemical structure to that of sulfathiazole, is known to amorphise upon spray drying (Caron et al., 2011). Therefore, it was thought of interest to investigate the reasons underlying this inconsistency. Subsequently, it was hypothesised that modifying spray drying parameters could result in the production of sulfathiazole in its amorphous state as occurs for sulfadimidine. It was also hypothesised in line with (Tong and Zografī, 1999), that the use of the corresponding sodium salt forms of the two APIs would result in an amorphous phase on processing.

The scope of this work was to investigate the properties of the two selected APIs when subjected to spray drying through systematic studies involving the impact of feed

composition, configuration of the spray drier and process parameters. Moreover, the sodium salt forms were also processed and compared to their corresponding non-ionised forms.

Finally it was investigated whether performance of the materials in terms of physical stability could be improved by co-processing the acid form together with the salt form.

1.2 Aims and objectives

In the preformulation stage of drug development, full characterisation of the physicochemical properties of active pharmaceutical ingredients (APIs) is crucial. The importance of this stage lies in the opportunity to minimise unexpected formulation problems in the later stages of product development which will induce an increase in time and costs involved in delivering optimised dosage forms and mainly affect therapeutic efficacy, safety and quality issues. In this context, to widen the limited scientific understanding of phenomena such as crystallisation, polymorphism, phase transformation, generation of amorphous substances, desolvation and dehydration involved in pharmaceutical processes such precipitation, drying, milling and compression is essential.

Nowadays, with the increasing tendency of new drugs to possess low aqueous solubility, the interest in amorphous formulations is growing considerably. The potential advantage deriving from formulating drugs in the amorphous form, would consist in the increased apparent solubility with a potential improvement in APIs bioavailability. Unfortunately the great potential of amorphous formulations is opposed to their physical instability.

The general aim of this research concerned examining the changes in the solid state properties of selected APIs as a consequence of the spray drying process. In particular,

the ability to generate amorphous forms following the spray drying process was considered an interesting area of analysis and investigated in depth.

The specific objectives of the work presented in this thesis were:

1. To investigate the impact of the spray drying process on the physicochemical properties of poorly soluble APIs, sulfadimidine and sulfathiazole, both acidic molecules belonging to the class of sulphonamides, and to characterise these in the context of the corresponding behaviour of their sodium salt forms.

2. To examine the solid state changes and other physico-chemical properties of the drug substances on spray drying through systematic studies involving the impact of feed composition, configuration of the spray drier and other influential process parameters.

The ability of these APIs to generate amorphous substances was also investigated.

3. To study, investigate and develop new strategies to increase the physical stability of amorphous substances without adding any polymeric excipient to the formulation.

1.3 Spray drying

Spray drying is a one step process used to dry a liquid feed (solution, suspension or emulsion) into a solid powder (Master, 2002). The applications of this technique are many and it is widely used in the food and chemical industry, and also in the pharmaceutical and biopharmaceutical industry. Spray drying processes are characterised by rapid solvent evaporation, frequently resulting in the transformation of a crystalline structure to its amorphous counterpart (Caron et al., 2011; Chidavaenzi et al., 1997; Corrigan et al., 1984; Tajber et al., 2005) or resulting in (a) different polymorphic phase(s) within the material (Beckmann and Otto, 1996). Variations of feed concentration have been found to be relevant to the outcomes of spray drying processes. A study carried out by (Chidavaenzi et al., 1997) showed that by modifying this parameter, various solid state compositions of the final products were obtained. In another study, Buckton et al. (2002) showed that amorphous lactose, produced by using different feed temperatures in the process, crystallised to different solid state compositions after exposure to identical conditions of relative humidity (Buckton et al., 2002). Furthermore, Beckmann and Otto, (1996) showed that different polymorphic forms of abecarnil, could be produced by using different solvents in the feed solutions.

The process therefore can be used to control the physical state of pharmaceuticals, provided that the operating parameters are carefully optimised. The spray drying process involves five stages (Master, 2002), the first of which is the atomisation of the feed into a spray. Contact of the spray with the hot drying medium, followed by drying of the droplets represents the second and third stage, respectively. The last two stages include the separation of the particles from the drying gas and the collection of the dried product. The properties of the resulting spray dried powder particles and the physicochemical characteristics of the materials are controlled by the settings employed in the spray drying

equipment. The Büchi-290 spray drier (schematically represented in Figure 1.1) employed in this work is equipped with a two-fluid nozzle atomiser. Different atomisers are available depending on the nozzle design including two-fluid, ultrasonic nozzles and rotary atomisers (Master, 2002).

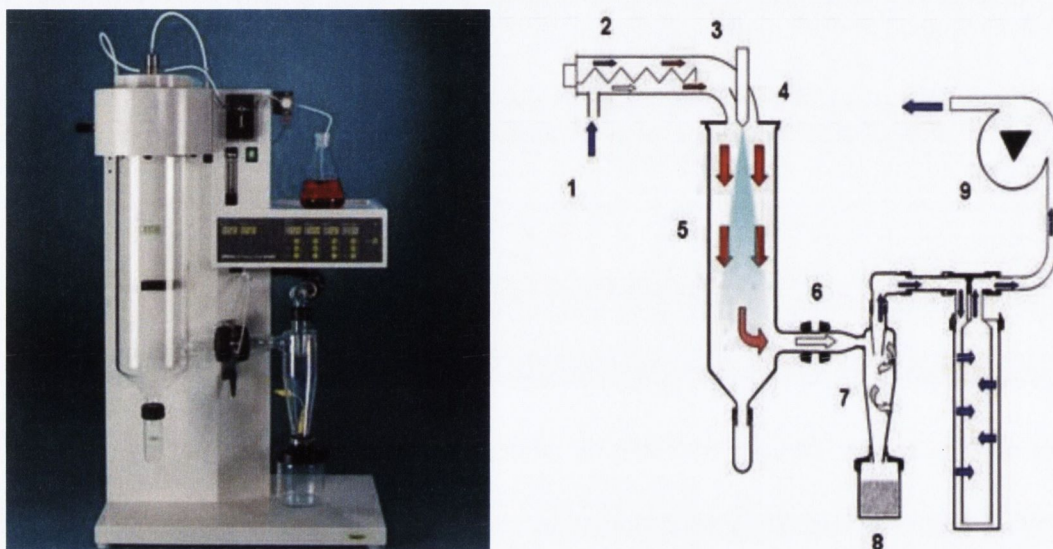


Figure 1.1 Spray drier (Büchi-290) and the drying medium flow pattern (co-current flow) (red arrows): 1 – drying medium intake (electric heating of the drying medium), 2 – nozzle (atomisation of the feed into fine droplets), 3 – temperature sensor (air inlet), 4 – drying chamber (spray/drying medium contact), 5 – temperature sensor (air outlet), 6 – cyclone (separation of product from drying medium), 7 – collecting vessel (collection of dried particles), 8 – outlet filter to remove fine particles, 9 – aspirator (adapted from Büchi-290 technical specifications).

According to the type of atomiser used, the characteristics of the spray of droplets will change leading to different properties of the final powders (Oakley, 1997). Atomisation involves the dispersion of a liquid in a gaseous medium to increase the surface area to mass ratio of the liquid (Islam and Langrish, 2010). As the droplet surface area exposed to the heat is high, drying is characterised by an intense heat and mass transfer which results in a fast and efficient process. In the Buchi 290, the spray drying procedure involves the electrically heated atomisation gas (air or N_2) and feed liquid entering the nozzle from the top independently and their releasing as a spray into the chamber through

the nozzle tip and cap orifice. The diameter of the orifice influences the size of the droplets and consequently the size of the final particles. The diameter orifices of the tip and cap used in this study measured 0.7 mm and 1.5 mm respectively. The use of a fixed diameter enables the uniformity and reproducibility of the spray cone. Therefore particles, obtained using this technique, are generally uniform in morphology and size (Büchi-290 technical specification, 2007).

Contact of the spray with the hot drying gas, followed by the drying of the droplets - the second and third stages of the process - take place in the drying chamber (Figure 1.1).

When the droplets come into contact with the drying gas, evaporation occurs at the surface and the surface solute concentration increases (Oakley, 1997). Until the solvent diffuses from the core of the droplet to the surface, evaporation takes place at a constant rate (Master, 2002). When the solvent content becomes too low, the solute at the surface develops a dried shell forming a particle, with the subsequent rate of evaporation dependent on the rate of moisture diffusion through the dried surface shell (Masters, 2002). The thickness of the shell depends on the drying rate. High initial drying rates lead to larger particles with thin shells and low density. Conversely, low initial drying rates will lead to smaller particles with thick shells and high density (Oakley, 1997).

The separation of the dried product from the drying medium -the fourth stage of the process- takes place in the cyclone while the final stage consists of the collection of the product from the collecting vessel placed underneath the cyclone (Figure 1.1).

Several solvents can be employed in the spray drying process and the type of solvent used will determine the spray dryer configuration. Spray dryers are available as open cycle and closed cycle systems. In the open cycle system, used to process non-inflammable solvents, the drying gas (air, N₂) is exhausted to the atmosphere after the spray drying process is completed. In contrast, the use of flammable, organic solvents necessitates the

closed mode configuration. With this configuration the drying gas (N_2) is filtered of solvent vapours at low temperature and recycled (Buchi-B-290, 2007; Islam and Langrish, 2010; Master, 2002). The use of different configurations was seen to impact on various properties including the crystallinity of lactose (Islam and Langrish, 2010) and solvent content of the spray dried particles of chlorothiazide sodium and potassium (Paluch et al., 2012).

Both configurations (open and closed cycle) were used to carry out the experimental work in this thesis. Other processing parameters were also varied to analyse the influence of these on the final properties of the API investigated. These included the inlet/outlet temperatures, feed concentration and temperature, composition of the feed and type of solvent used.

When spray drying a solution, emulsion or dispersion, process variables may impact on the final product and in particular the inlet temperature (temperature at which the drying gas is heated) can be considered a key parameter. Variation of this parameter results in the modification of the outlet temperature, i.e. the temperature of the air with the solid particles before entering the cyclone. The relevance of the outlet temperature consists in the fact that it can alter several product powder characteristics such as residual solvent levels and physical state characteristics. Spray drying at a lower outlet temperature (below the boiling point of the solvent) for example will yield powders exiting the spray dryer with high residual solvent levels which can adversely affect both short and long term physical stability of amorphous solid dispersions. Specifically, residual solvents can plasticise the solid dispersion particles, leading to the formation of small levels of crystallinity that can act as nucleation sites for crystal growth during storage. Consequently, the outlet temperature must be carefully evaluated and once this parameter has been optimised or determined, the inlet temperature should be ranged accordingly to

determine the effect on powder properties. The relevance of this study lies in the prospect of utilising the findings from lab scale spray drying techniques for potential application at industry scale.

1.4 The sulphonamides

The sulphonamides are a class of drugs whose molecular structures contain the sulfanilamide moiety (Figure 1.2a) or a sulfanilamide analog (Adsmond and Grant, 2001; Yang and Guillory, 1972).

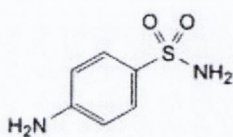


Figure 1.2a Chemical structure of sulfanilamide.

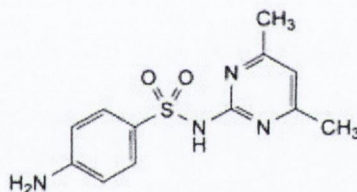


Figure 1.2b Chemical structure of sulfadimidine

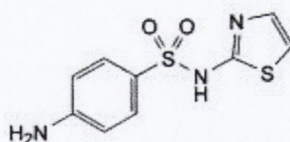


Figure 1.2c Chemical structure of sulfathiazole

Sulfadimidine and sulfathiazole differ from each other in the kind of substituent on the -SO₂NH₂ group, presenting a pyrimidinic and a thiazolic ring respectively. The structural resemblance between the sulfanilamide grouping and PABA (p-aminobenzoic acid) enables the sulphonamides to block the synthesis of folic acid in bacteria which accounts for the antibacterial action of these drugs. By interrupting this process sulphonamides inhibit bacterial growth and activity. The sulphonamide compounds used in this thesis are

specifically antimicrobial agents primarily used in veterinary medicine and to a lesser extent in human medicine. The structures of sulfadimidine and sulfathiazole are shown in Figure 1.2 b-c.

1.5 Background to drugs used in the current work

Sulphonamides have a strong tendency toward crystal polymorphism because of the high number of donor and acceptor chemical groups within their structures (Yang and Guillory, 1972; Caira, 2007). The possibility of development of various interactions, especially hydrogen bonding, between these groups, enhances the possibility of the drugs to crystallise in multiple forms. In particular, sulfathiazole has long been the subject matter of several studies on polymorphism due to its high propensity to solidify into different polymorphs from various solvents, with five forms identified to date (Parmar et al., 2007). In addition, amorphous sulfathiazole obtained only by quench cooling techniques has been described (Caron et al., 2011; Threlfall, 2003, Kerc and Srcic, 1995).

In contrast, sulfadimidine does not present polymorphism but merely changes in crystal habit when it solidifies from different solvents (Maury et al., 1985). The drug can however be made amorphous via spray drying as described by Nolan, (2008) and more recently by Caron et al., (2011).

The sodium salt forms of sulfathiazole and sulfadimidine used to carry out the experimental work in this thesis were supplied in a crystalline anhydrous state. Sulfathiazole sodium, like the corresponding free acid, is also known to be highly (pseudo) polymorphic and, a monohydrate, a sesquihydrate, a $4.6 \cdot \text{H}_2\text{O}$ hydrate and an exahydrate have been reported in the literature (Crusellas, 1943; Rubino, 1989). In contrast, only a single dihydrate form of sulfadimidine sodium has been described (Patel, 1995). To date no amorphous forms for both salts have been reported.

1.6 Solid state characteristics of API materials

In the pharmaceutical field, the majority of drugs are administered in the form of powder, tablets or capsules. During product development, changes in temperature, pressure and relative humidity can occur at any stage and may cause problematic phase transitions in the solid state, impacting on the physicochemical properties, the therapeutic efficiency and toxicity of the pharmaceuticals.

In particular, specific problems related to POLYMORPHISM and AMORPHISM in the pharmaceutical context can be assessed through polymorph screening and amorphous state characterisation. Adequate characterisation of the physicochemical properties of active pharmaceutical ingredients is a prerequisite to minimise risks of undesirable findings during clinical phases (Giron et al., 2004) and forms an essential part of pre-formulation studies.

1.7 Polymorphism

Crystalline solids consist of atoms, molecules or ions arranged in a regular lattice characterised by long-range tridimensional symmetry (Datta and Grant, 2004). The ability of a substance to exist in at least two crystalline forms originating from a different arrangement of the molecules in the solid state is defined as polymorphism (Aaltonen et al., 2003; Khoshkhoo and Anwar, 1993; McCrone, 1965). A third of organic substances under normal conditions of pressure and temperature are polymorphic (Threlfall, 1995).

From a pharmaceutical perspective, the interest provoked in this phenomenon derives from the fact that various polymorphs, albeit presenting the same chemical composition, can have different chemical, physical and mechanical properties (Table 1.1) (Datta and Grant, 2004; Parmar et al., 2007).

Table 1.1 Categorisation of properties that can be affected by polymorphic changes (adapted from Datta and Grant, 2004)

Physical and thermodynamic properties	density, refraction index, hygroscopicity, thermal and electric conductivity, melting point, chemical potential, free energy, thermal capacity, vapour pressure, solubility and thermal stability
Kinetic properties	Stability, dissolution rate, melting rate
Mechanical properties	Hardness, compressibility, thermal expansion
Surface properties	Free surface energy, crystalline habit, surface area

Consequently, the complete screening of a crystalline form is of primary importance since the ultimate properties of a specific pharmaceutical product depend mostly on the way in which the molecules are arranged in their solid state. Nowadays pharmaceutical regulatory guidelines demand that the pharmaceutical industries, besides knowing the exact solid state nature of a material obtained during the manufacturing process, know about product stability over time and have to ascertain the different physico-chemical properties related to the various polymorphic forms (Byrn et al., 1995; FDA, 2007).

1.7.1 Classification of Polymorphs: Enantiotropism and Monotropism

Polymorphs can be classified in two categories, monotropes and enantiotropes, depending upon their stability with respect to the range of temperatures and pressures (Threlfall, 1995). In a polymorphic system if one of the polymorphs is stable over a certain temperature range and pressure while the other polymorph is stable over a different temperature range and pressure, then the two polymorphs are said to be enantiotropes. In contrast, sometimes only one polymorph is stable at all temperatures below the melting point, while all the other polymorphs remain unstable. In this case these polymorphs are

linked by a monotropic relation. The thermodynamic relationship between enantiotropic and monotropic polymorphs is illustrated in Figure 1.3.

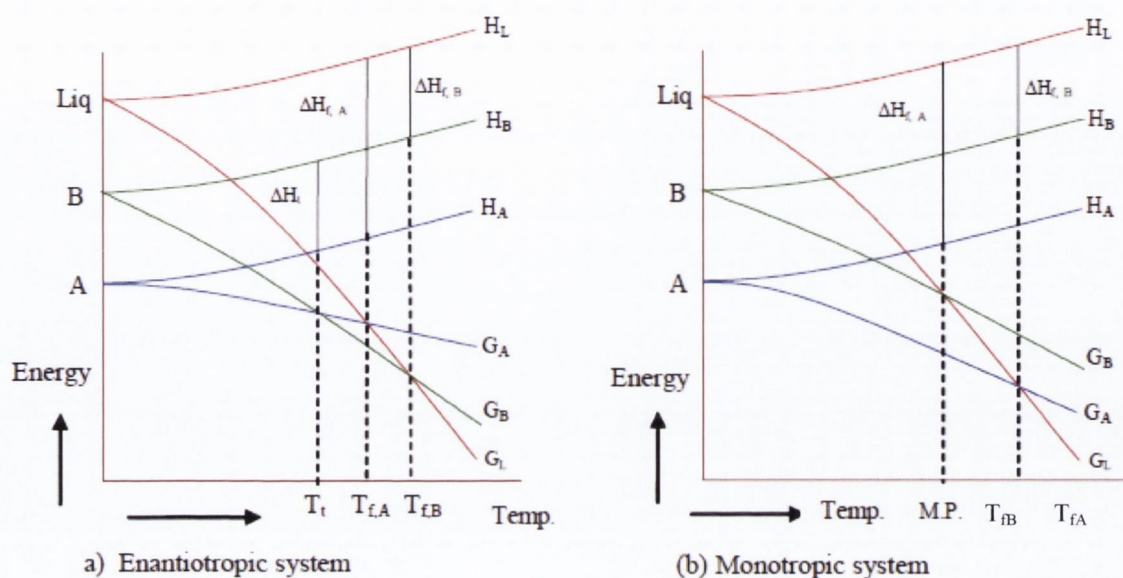


Figure 1.3 Variation of Energy with temperature for the solid and liquid phases (Liq) of a single compound, showing a) enantiotropy, and b) monotropy. Curves H_A , H_B and H_L are for enthalpy. Curves G_A , G_B and G_L are for Gibbs free energy. ΔH_{fA} and ΔH_{fB} represent enthalpy of fusion and ΔH_t represents enthalpy of transformation. T_t is for temperature of transition. T_{fB} and T_{fA} are the fusion temperatures of polymorphs A and B respectively. Adapted from (Giron, 2001)

In Figure 1.3a, polymorph A is stable below the temperature of transition (T_t), because of lower free energy G_A than polymorph B. On heating as the temperature increases and goes beyond T_t , free energy G_B of polymorph B becomes less than G_A and polymorph B becomes more stable than polymorph A. This represents an enantiotropic relation of the solid phases. For an enantiotropic system, a reversible transition can be observed at a particular transition temperature at which the free energy curves cross before the melting point is approached.

In a monotropic (Figure 1.3b) as opposed to an enantiotropic system, there is no point at which the two free Gibbs energy curves meet. As a result, the conditions of interconversion evidenced before cannot be verified and therefore no reversible transition from the metastable to the stable polymorph can be observed below the melting point.

However the implications of the latter are that a more thermodynamically stable form could remain concealed for kinetic reasons and then still show itself at a later stage, for example during handling or storage. This could cause problematic consequences.

1.7.2 Pseudo-polymorphism (Solvates and hydrates)

When a crystalline solid is made up from the combination of two different molecules, one of which is a solvent, it is known as pseudo-polymorph or solvate (Giron, 2001). Such forms originate from the process of crystallisation from solution when at nucleation the enthalpy of the crystal lattice including the solvent is lower than the enthalpy of the lattice consisting only in drug molecules.

Of particular interest are the hydrates, pseudo-polymorphs for which the solvent is water. Hydrates can occur following crystallisation from aqueous solution or by exposure of a crystal to an environment containing water vapour at various relative humidity values. Hydrates depending on their water content can be classified as stoichiometric or non-stoichiometric. In stoichiometric hydrates, the numbers of water and host molecules have a stoichiometric ratio, while the amount of water in non-stoichiometric hydrates depends on the relative humidity (RH) of the environment.

Moreover, based on the location of the solvent in the crystal hydrates, Morris and Hornedo (1993) (K.R. Morris, 1993; Rodríguez-Spong et al., 2004) classified these species as:

- 1) Channel hydrates: water molecules of contiguous unit cells are displayed beside one another along an axis of the lattice creating channels of solvent throughout the crystal structure.
- 2) Isolated site hydrates: water molecules are isolated by the presence of interposed drug molecules

- 3) Ion-associated hydrates: in this case water molecules complete the coordination shell of the ions fulfilling the stereo-chemical requirements of the ions included in the crystal.

In the pharmaceutical industry, hydrates can be used as APIs if their state of hydration is proven to be maintained following exposure to all the climatic conditions to which the substance might be exposed during its shelf life. Problems may occur if exposure to a dry environment or to low RH conditions occurs, in which case a hydrate may transform to a crystal characterised by a lower state of hydration, including an anhydrous form, by loss of water. Such changes can have a deep impact on the mechanical properties and solubility of the substance, therefore altering product performances (Giron et al., 2004).

Dehydration can modify, retain or destroy the crystalline structure of a hydrate depending on the impact of the water in stabilising the hydrate crystal structure.

Generally the development of a completely new anhydrous crystal occurs on the removal of the solvent, as water plays an important role in determining the final crystal structure of the hydrate by means of hydrogen bonding (McCrone, 1965). However, occasionally, if the structure is retained upon dehydration, the new anhydrate form developed will present only minor structural modifications compared to the original form and could even revert back to its original hydrate form under changing conditions of pressure and humidity. This process is typical of channel hydrates (McCrone, 1965). Furthermore frequently, dehydration may be followed by the complete loss of structural organisation and the development of an amorphous material (Taylor et al., 1998).

1.8 Amorphous state

Many pharmaceuticals often convert to partial or full amorphous materials on processing. Amorphous materials although presenting a disorganised liquid-like structure are however solids. Compared to crystals, the amorphous state is highly disordered and thermodynamically unstable (Caron et al., 2011; Hancock and Zografi, 1997). The molecular organisation of an amorphous solid lacks the long range order of molecular packing characteristic of the regular latticing typical of crystalline materials. Amorphous materials however, are characterised by a short range molecular order. This means that molecules in the amorphous state have a neighbouring environment similar to a molecule in the crystalline state, which is not repeated throughout the entire structure (Hancock and Zografi, 1997; Liu et al., 2006).

1.8.1 Amorphous solids by rapid cooling of melt (quench cooling).

Quench cooling a melted material below its melting temperature has the potential to inhibit the reorganisation of the molecules in a regular crystal lattice. In particular, molecules may be frozen in their random positions. The formation of an amorphous substance by cooling its liquid melt is schematically represented in Figure 1.4. Upon cooling a melted substance from a temperature above T_m , crystallisation can occur or be avoided depending on the properties of the material and/or the rate of cooling. If crystallisation takes place, the substance is characterised by changes in specific volume and enthalpy at T_m with the transition to an equilibrium (lower enthalpy and volume) crystalline state. In contrast, if no crystallisation takes place the substance remains in an out-of-equilibrium liquid state (higher enthalpy and volume) and is defined as a super-cooled liquid (Hancock and Zografi, 1997; Liu et al., 2006). Further cooling of the super-cooled liquid will result in the formation of an amorphous substance defined by several

authors as a glass (Baird and Taylor, 2012; Caron et al., 2011; Hancock and Zografi, 1997). This occurs at the liquid to glass transition temperature (T_g) (Baird and Taylor, 2012). The super-cooled liquid cannot remain in a liquid state without converting to an amorphous phase upon further cooling (Liu et al., 2006). The reason is that the enthalpy of a liquid phase below a certain temperature known as the Kauzmann temperature (T_K in the graph) would otherwise be lower than the enthalpy of a solid which is a thermodynamically impossible case (Liu et al., 2006) (Hilden and Morris, 2003).

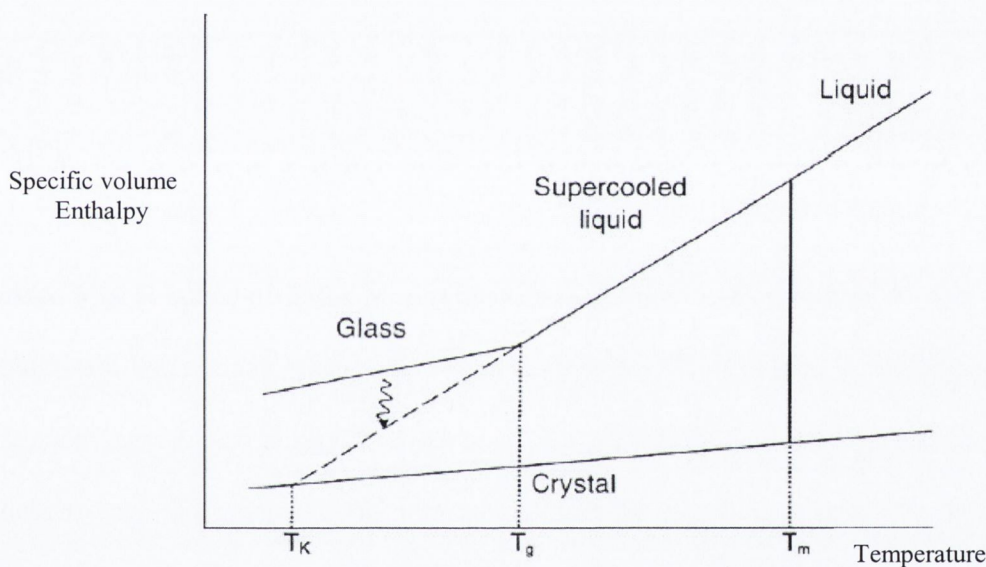


Figure 1.4- Schematic representation of temperature related variation of enthalpy and specific volume

The purpose of the quench cooling process is to cool the molten state to below the T_g rapidly enough to prevent formation of nuclei and growth, trapping the API in a kinetically disordered, amorphous state (Baird et al., 2010).

Besides spray drying, quench cooling and dehydration of pseudo polymorphs, other common pharmaceutical techniques are able to convert crystals to their corresponding amorphous phases, these include: milling, freeze drying and melt extrusion.

1.8.2 Stability of the amorphous state

The amorphous state is not in thermodynamic equilibrium, as its corresponding crystalline state is characterised by a lower energy level for any material below its melting point. This characteristic is adverse to the development of amorphous formulations because the change from an amorphous material to a crystal will lead to modifications in the physico-chemical and consequently, pharmaceutical properties of the substance. The improved apparent solubility and enhanced dissolution rate of the amorphous state compared to the corresponding crystalline form however, can be considered advantageous nowadays, as a growing number of new drugs are characterised by limited bioavailability due to poor solubility (Caron et al., 2011; Karmwar et al., 2012; Kaushal et al., 2004). Additional advantages consist in the fact that transformation to the amorphous state does not require chemical modification of the molecule and is applicable to any drug system (Caron et al., 2011). The T_g is a key factor in the stability of the amorphous state (Hancock et al., 1995; Yu, 2001). It represents the crossover between the liquid state, which is disordered with high molecular mobility and the glassy state which is disordered with greatly reduced molecular mobility (Caron et al., 2011). Therefore these materials should be stored at temperatures below the T_g to reduce the possibility of crystallisation (Hancock et al., 1995). As a consequence of the disordered arrangement of molecules and the lack of a regular crystal lattice, amorphous solids can sorb significant amounts of water within the material. Water sorbed into the amorphous solids can cause structural changes in amorphous materials such as swelling (Mikhailov et al., 2009). Moreover it is well known that water acts as a plasticiser i.e. it increases the molecular mobility by breaking the hydrogen bonds among the drug molecules which results in the reduction of T_g. A drastic lowering of T_g below the storage temperature causes the crystallisation of amorphous substances (Burnett et al., 2004; Burnett et al., 2006).

1.9 Water-solid interaction mechanism

Solid-water interactions consist of five different mechanisms, i.e. surface adsorption, capillary condensation, bulk absorption, hydrate formation and deliquescence (Ahlneck and Zografi, 1990; Hiatt et al., 2011).

Adsorption indicates the adhesion of water vapour molecules to the solid surface. The total amount of water adsorbed is related to several factors such as: the affinity between the surface and water molecules (hydrophilicity), temperature, RH and the surface area. Based on the forces involved in the interactions between the solid and vapour molecules, adsorption can be differentiated as either physical adsorption (physisorption) in which van der Waals interactions are involved, or chemical adsorption (chemisorption) where the adsorbed molecules are chemically bonded, usually by means of hydrogen bonding. Condensation of an adsorbed vapour within the pores which might be present at the surface of a solid is, instead, defined as capillary condensation.

In the process of absorption, water enters the bulk solid structure. Amorphous solids due to free void space and enlarged free volume are able to absorb water in the bulk. In contrast, crystalline solids due to their high molecular packing generally only adsorb water at the surface (Hancock and Shamblin, 1998; Mikhailov et al., 2009). However in particular conditions of RH it is possible for a crystal to absorb water and to develop a hydrate form (Newman et al., 2008).

On adsorption, soluble crystalline solids can undergo a first order phase transformation from solid to an aqueous solution known as deliquescence. This occurs at a relative humidity specific to the solid, generally defined as critical relative humidity (RH₀) (Hiatt et al., 2011). As the amount of moisture sorbed by amorphous solids is typically much greater than that adsorbed by crystalline solids below their critical RH₀, amorphous solids undergo deliquescence at a lower RH₀ (Hancock and Zografi, 1997; Hiatt et al., 2011).

Furthermore according to Mikhailov et al., (2009), when dealing with amorphous solids, deliquescence can be regarded as a non equilibrium phase transition like the glass transition (Mikhailov et al., 2009). Deliquescence is critical in a pharmaceutical context because the exposure of solids to humidity values above RH₀ results in the formation of a liquid phase where chemical reactions may be accelerated or physical changes catalysed (Hancock and Shamblin, 1998). For example in the case of formulations containing a substance undergoing deliquescence, the resulting condensed water can impact on the properties of other water-soluble components. Consequently processing and storage of either crystalline or amorphous materials require the determination of the conditions at which deliquescence takes place (Ahlneck and Zografı, 1990).

1.10 Physicochemical characterisation

The screening process requires the combined use of different analytical techniques which include thermal analysis, infrared spectroscopy, inverse gas chromatography and water sorption analysis, DVS.

1.10.1 Thermal analysis

Thermal analysis comprises a group of techniques in which changes of physical or chemical properties of the sample are monitored against time or temperature, while the temperature of the sample is programmed. The temperature program can be kept isothermal, involve heating/cooling stages at a determined rate or combine the two in sequences.

In the pharmaceutical industry in particular, differential scanning calorimetry (DSC) is a widely used technique. It enables several characteristic properties such as the purity of a material, melting point, phase transitions and transition enthalpies, degree of crystallinity

and decomposition to be measured and analysed (Clas et al., 1999; Lappalainen et al., 2006; Shah et al., 2006).

DSC measures the differential heat flow required to maintain a material sample cell and an inert reference cell (within a controlled environment) at the same temperature.

It is known that a material subjected to thermal stress may undergo changes in its physicochemical state. These are defined as phase transitions. During a phase transition if the process is endothermic (i.e. melting) or exothermic (i.e. crystallisation) the material will absorb or release heat respectively (Giron, 1998). Therefore to maintain both the sample and reference cells at the same temperature, less or more heat must flow to the sample depending on whether the process is exothermic or endothermic. DSC measures the amount of heat absorbed or released by the material during such transitions, providing information on its physical state as a function of temperature. Its capacity to measure transition temperature and corresponding enthalpies makes DSC a valuable tool in producing thermograms for various chemical systems. In this context, DSC is extremely useful in the identification of both amorphous and polymorphic substances (Caron et al., 2011; Giron, 1998).

For example during DSC analysis an amorphous solid will undergo a glass transition as the temperature is raised. On a typical DSC thermogram (Figure 1.5) of an amorphous material, T_g appears as a step change (heat flow deflection) in the baseline due to the sample undergoing a change in heat capacity.

Further heating will provide the molecules of the sample with enough energy to arrange themselves into a crystalline form. This transition from amorphous to crystalline results in an exothermic peak on the DSC thermogram. Beyond crystallisation as the temperature increases the sample reaches its melting temperature (T_m). In this case the peak is endothermic. In contrast DSC analysis of a monomorphic crystal will only display a

specific endothermic peak for each substance attributed to melting. Further endothermic or exothermic events may be recorded as a consequence of polymorphic transformation if the drug is polymorphic. Specifically the peak will be exothermic in case of enantiotropy and *vice versa*, endothermic, in case of monotropy. A peak on the DSC may result in the case of dehydration of solvated/hydrated structures. To distinguish between endothermic events caused by dehydration or polymorphic transitions, DSC data are usually complemented by thermogravimetric analysis (TGA).

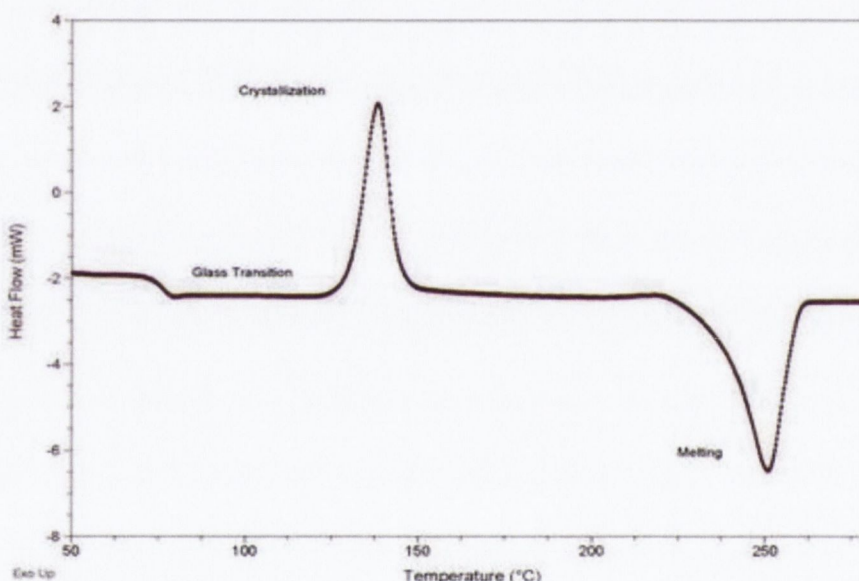


Figure 1.5 Typical DSC thermogram of an amorphous material

TGA is a technique that measures the mass variation of a sample located on a thermo-balance inside a controlled environment. The mass change is usually determined as a function of temperature. Therefore an endothermic event on a DSC thermogram related to loss of solvent, will be accompanied by corresponding mass loss in the same range of temperature provided that the two thermal analyses are carried out employing the same heating rate.

1.10.2 FTIR Analysis

Complete characterisation of pharmaceuticals includes vibrational spectroscopic infrared (IR) analysis which provides information on the solid state of pharmaceuticals at the molecular level (Kaushal et al., 2008). IR energy is a small portion of the electromagnetic spectrum which covers the wavelength range between 0.78 and 1000 μm . Wavelengths in IR spectroscopy are generally measured in wavenumbers which are the reciprocal units of the IR wavelength expressed in inverse cm (cm^{-1}).

The IR spectrum can be divided into three frequency regions which are:

- Near infrared (13.000-4.000 cm^{-1})
- Mid infrared (4.000-200 cm^{-1})
- Far infrared (200-10 cm^{-1})

The most common IR frequency used in physical characterisation is the Mid infrared.

The infrared spectrum of a substance is recorded by passing a beam of IR light through the sample. When a chemical substance is subjected to such energy, transitions between molecular vibrational and rotational energy levels cause the absorption of IR energy and gives rise to absorption bands at characteristic frequencies. Absorption however occurs only if two rules are satisfied:

1. when infrared radiation interacts with a molecule undergoing a change in dipole.
2. when the incoming infrared light has sufficient energy for the transition to the next allowed vibrational state.

The transmitted light i.e. not absorbed by the sample, is then detected by a spectrometer which reveals how much energy is absorbed at each wavelength by producing a characteristic spectrum for the substance. A spectrum consists of a sequence of absorption peaks/bands as a function of the wavelength (Figure 1.6). Each IR-active bond during the

molecular vibration will absorb IR energy at a particular/specific vibrational frequency

(v) according to the following formula:

$$\frac{1}{2\pi c} \times \sqrt{\frac{K}{\mu}}$$

Where c represents the speed of light, K is the force constant, and μ is equal to:

$$\mu = \frac{m_1 \times m_2}{m_1 + m_2}$$

with m_1 and m_2 respectively the mass of the two atoms bonded together.

According to this formula the higher the difference in electronegativity between two atoms bonded together, the higher the frequency of absorption.

A FTIR spectrum is therefore comprises a series of peaks each corresponding to specific functional groups included in the molecular structure and consequently useful for identifying the substance.

The diagram in Figure 1.6 gives an approximate outline of where specific types of bond stretches may be found.

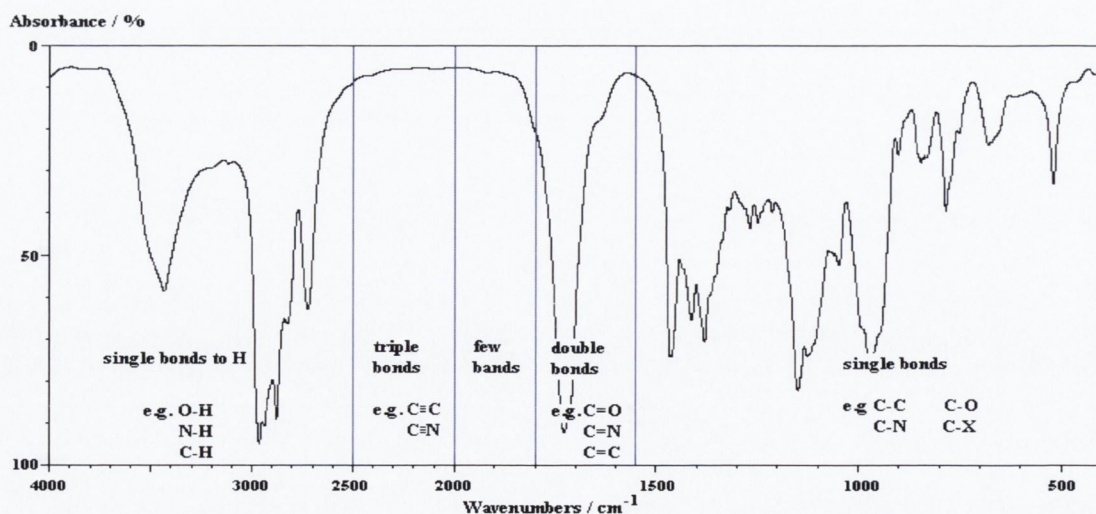


Figure 1.6 Diagram adapted from the literature, illustrating the wavenumber regions at which specific FTIR stretch peaks may be found.

IR analysis has been widely used to study crystals and the phenomenon of polymorphism. Given that in polymorphic forms the molecular structure is identical, modification in the FTIR spectra such as band shift or variation of absorption intensities can be attributed to differences in interactions within the polymorphs (Threlfall, 2003). In particular, the hydrogen bond, the strongest of all the intermolecular interactions, determines the most evident changes in the FTIR spectra (Kaushal et al., 2008). This particular bond originates from the attractive interaction between two electronegative atoms through a hydrogen bridge. Specifically, IR analysis can be used to investigate hydrogen bondings as the peak position of a stretching X-H bond (with X= oxygen, nitrogen or carbon etc.) is extremely sensitive to the extent of association (Tang et al., 2002). While an unbounded X-H gives a sharp peak on the IR spectrum of a molecule, the peak broadens and shifts to lower wavenumbers as a consequence of the formation of a X-H \cdots Y hydrogen bond (with Y being the acceptor atom). The shift is caused by the lengthening of the X-H bond which results on hydrogen bond formation. Hence the stronger the H-bond the greater the shift to lower wavenumbers. For this reason the FTIR technique is useful for polymorphic identifications (Threlfall, 1995). Several polymorphic substances have been identified by means of IR analysis (Hu et al., 2010; Threlfall, 2003; Threlfall, 1995).

With regard to amorphous solids, several authors have investigated their molecular structure by FTIR analysis (Kaushal et al., 2008; Tajber et al., 2005; Tang et al., 2002) as the molecular structure of an amorphous solid cannot be analysed in detail by X-ray diffraction (Kaushal et al., 2008). Amorphous materials are structurally very different from their crystalline counterparts however, they tend towards crystallisation. According to Tang et al. (2002), investigating the molecular associations in amorphous substances and the differences compared with those in the crystalline state can provide a more in depth understanding of the crystallisation tendency and how to prevent/reduce it by

selection of appropriate crystallisation inhibitors (Tang et al., 2002). Intermolecular interactions and in particular hydrogen bondings in amorphous solids are known to affect their molecular mobility, in particular by affecting the T_g (Taylor, 1998). Useful information about the reciprocal arrangement of the molecules and the nature of intermolecular interactions in the amorphous state can be obtained by IR spectroscopy. Mainly, by means of this technique, information on hydrogen bonding interactions in the amorphous state can be elicited and compared to those in the crystalline state. It is presumed that these interactions are different as limitations in crystal packing no longer exist. Furthermore, changes in the strength of molecular interactions or the formation of new interactions may result (Kaushal et al., 2008).

1.10.3 Powder X-Ray Diffraction (PXRD)

A useful technique complementing thermal and IR analysis in the physico-chemical characterisation of pharmaceuticals is PXRD. This method enables the characterisation of pharmaceutical powders and particularly the identification of drug polymorphs (Lu et al., 2005).

The PXRD technique is based on Bragg's law, which describes the diffraction of a monochromatic X-ray beam impinging on a plane of atoms (Brittain, 1999; Cullity, 1978). Basically, when X-rays irradiate crystal materials (the atoms of which are arranged in planes), radiation is scattered and then diffracted at angles related to the spacings between the planes of the molecules in the lattice. Therefore diffraction of X-rays by pharmaceutical crystals is exploitable for identification purposes for the reason that the three-dimensional spacing of planes constituting the crystal lattice is unique to each compound and each substance will provide a distinctive pattern. Moreover, PXRD is also a straightforward technique for the detection of amorphous forms. Generally amorphous

materials, devoid of a crystal lattice, will not reveal peaks but a characteristic diffuse halo.

Since solids can undergo phase transitions (polymorphic transformation or amorphisation) at any stage including handling and storage, this technique can be an important tool for monitoring the behaviour of the sample throughout the entire formulation process.

1.10.4 Inverse gas chromatography (IGC)

Inverse gas chromatography is a versatile and extremely sensitive technique which is widely used to measure surface thermodynamic properties of powders including the surface free energy (Newell et al., 2001) and is also employed to measure solubility parameters (Adamska and Voelkel, 2005; Price, 1988), glass transition temperature and its dependence on relative humidity (Ambarkhane et al., 2005; Buckton et al., 2004). Surface energy of powders is crucial in several industrial applications and processes. For example it is of primary importance in determining adhesion in composites and coatings (Langer and Kamiiska-Bach, 2011), it affects the particle wetting behaviour in several processes such as disintegration, dissolution, dispersion and solubilisation and it can also be used to determine the surface amorphous content (Brum and Burnett, 2011).

IGC involves the adsorption of a probe molecule in vapour phase (mobile phase) with known and specified physico-chemical properties onto the surface of a stationary phase (the powder we want to analyse) which, in this case, presents unknown physicochemical properties. This technique inverts the conventional relationship between mobile and stationary phase employed in analytical chromatography (Buckton and Gill, 2007). The stronger the interaction between adsorbate and probe, the more energetic the surface and the longer the retention time. Some thermodynamic parameters can be derived from the

retention behaviour of vapour molecules. IGC enables the dispersive and specific component of the surface energy of a solid substance to be determined. In acid-base theory, the total surface free energy of a solid (γ_s^T) has 2 main components: a dispersive contribution (γ_s^d) and a specific or acid-base contribution. The dispersive component is directly obtained from the retention times of a series of alkanes. In contrast, by injecting a range of polar probe molecules such as dichloromethane and ethyl acetate, it is possible to calculate the specific free energy. The latter can be converted to acid-base parameters if acid-base theories are applied. Several theories have been applied to date, all based on the Lewis acid-base concept including the Van Oss and Good theory (Van Oss and Good, 1989) employed in this thesis.

1.10.5 Water vapour sorption analysis (DVS)

Water vapour sorption isotherms indicating the water uptake by a sample at different relative humidity (RH) values at a fixed temperature, are widely used to evaluate the hygroscopicity of pharmaceutical solids (Newman et al., 2008).

The sorption/desorption isotherms can be obtained based on weight changes after equilibrating a substance at a fixed RH inside a sealed chamber. The apparatus used in this work to analyse the hygroscopic properties of unprocessed and spray dried sample was the DVS Advantage 1 apparatus (Surface Measurement Systems, UK). This instrument comprises a precise microbalance which records the mass changes of the sample over time. Using DVS the RH can be computationally modified by mixing water vapour with dry gas (nitrogen) in different proportions in order to simulate various RH conditions. On DVS analysis, the sample can either be exposed to a fixed RH ranging from 0 to 95% for a specific length of time or exposed to a sequence of RH step changes. In this case progression (to a subsequent step) can be time controlled or dependent on the

attainment of mass equilibrium ($\Delta m/\Delta T$) at each RH step. Another method of DVS analysis consists of exposing the sample to ramp changes in RH over time.

The use of this equipment is advantageous compared to the traditional use of different chambers containing saturated salt solutions as the RH chamber storage method is labour intensive and time consuming. Furthermore, several RH chambers are also necessary to cover a wide RH range and consequently more samples are required. DVS is faster because the attainment of equilibrium is accelerated by the use of small sample size (a single sample is sufficient) and by the dynamic environment provided by the humidified nitrogen gas purge.

With the DVS advantage apparatus the sample at each RH value can be further characterised by other techniques, such as DSC and XRD etc. This provides detailed information on the sample following water induced phase transitions such as crystallisation of polymorphic changes.

The applications of this technique are manifold and seen to be useful in the determination of the following:

1. Evaluation of hygroscopicity (Newman et al., 2008)
2. Analysis of surface adsorption and bulk absorption (adsorption) capacity (Agrawal et al., 2004; Alvarez-Lorenzo et al., 2000)
3. Measurement of water sorption/desorption isotherms (Tewes et al., 2010)
4. Quantification of amorphous content (Shah et al., 2006)
5. Determination of critical humidity of crystallisation (Burnett et al., 2004)
6. Measurement of critical humidity (RH₀) of solvate/hydrate formation or desolvation
7. Assessment of hysteresis: difference in water vapour uptake between the sorption and desorption isotherms (Alvarez-Lorenzo et al., 2000; Hiatt et al., 2008).

Chapter 2

Materials and methods

Materials and Methods

2.1 Materials

<i>Material (abbreviation or chemical formula)</i>	<i>Supplier/manufacturer</i>
Acetic acid glacial (CH ₃ COOH)	BDH Laboratory Supplies, UK
Acetone (CH ₃ COCH ₃)	Lab Scan Analytical Sciences, Ireland
Compressed air	Haug Kompressoren, Germany
Decane, iGC grade	Sigma, Ireland
Dichloromethane, iGC grade	Sigma, Ireland
Ethanol (EtOH)	Cooley distillery, Ireland
Ethyl acetate, iGC grade	Sigma, Ireland
Heptane, iGC grade	Sigma, Ireland
Hexane, iGC grade	Sigma, Ireland
Methanol, HPLC grade	Lab Scan Analytical Sciences, Ireland
Nitrogen gas (high purity, oxygen free)	BOC Gases, Ireland
Nonane, iGC grade	Sigma, Ireland
Octane, iGC grade	Sigma, Ireland
Potassium Bromide (KBr)	Sigma, Ireland
Silica gel	Merck, Germany
Sulfadimidine	Sigma, Ireland
Sulfadimidine sodium	Sigma, Ireland
Sulfathiazole	Sigma, Ireland
Sulfathiazole sodium	Sigma, Ireland
Water, deionised	Purite Prestige Analyst HP water
Water, HPLC grade	Purite Prestige Analyst HP water

2.2 Methods

2.2.1 Spray drying

All systems were spray dried as solutions or suspensions using a Büchi-290 Mini Spray Dryer (Büchi Laboratoriums-Technik AG, Flawil, Switzerland).

Systems were spray dried from water, organic solvent (pure ethanol or pure acetone) or from organic solvent:water cosolvent systems at different v/v compositions. The concentrations and constituents of the feed solutions, the spray drying parameters, the solvent(s) employed, and the drying gas for the various spray drying systems are detailed in Appendix I.

All stock and feed solutions were freshly prepared prior to spray drying. The selected quantity of API was dissolved in a suitable volume of the liquid medium. A sonicator (Fisher scientific FB 15053, Dublin, Ireland) was used to aid dissolution. The Büchi-290 Mini Spray Dryer allows for spray drying in both a closed mode (CM) and open mode (OM) configuration. Both configurations were employed in the experimental work carried out. When operating in the closed mode configuration the Büchi-290 spray dryer was used in conjunction with the Büchi-295 inert loop (Büchi Laboratoriums-Technik AG, Flawil, Switzerland). This modality is typically chosen with flammable or explosive solvents (i.e. organic solvents, toxic products or oxygen sensitive products) to be processed. The drying medium, nitrogen is constantly reused in the drying process through recycling within a closed system. A standard size cyclone was used in all spray drying experiments. After spray drying all samples were collected from the collecting vessel and cyclone of the spray dryer using a small brush and antistatic gun (Zerostat[®] 3, Sigma-Aldrich, UK). Samples were stored in amber screw top jars and stored in a sealed desiccator at 5 °C under low humidity conditions provided by silica gel, if not otherwise mentioned.

2.2.2 Spray drying of sulfadimidine (SD) and sulfadimidine sodium (SDNa)

Spray dried powders were obtained using a laboratory scale Buchi B-290 Mini Spray dryer (Buchi Laboratoriums-Technik AG, Flawil, Switzerland) operating either in an open cycle mode (OCM) configuration using air as the drying gas or in a closed cycle mode (CCM) configuration using nitrogen as the drying gas. 0.5% w/v SD feed systems were prepared by dissolving the active pharmaceutical ingredient (API) in ethanolic or acetonic solvents, prepared by mixing ethanol or acetone with deionised water at different v/v ratios: 9:1, 8:2, 7:3 and 6:4 for ethanolic and 9:1, 7:3 acetonic solutions respectively. SD was also spray dried as a solution from pure acetone. Due to the poor solubility of the drug in water, SD was additionally dissolved in water at 65 °C to generate a 0.1% w/v solution.

Spray drying of SD was performed using the following parameters: inlet temperature between 78 °C and 120 °C, gas flow of 40 mm (473 L/hr); aspirator rate of 100% and feed flow rate of 30% (8 mL/min).

SDNa solutions (0.5% w/v) were spray dried from pure water, ethanol:water solutions (9:1, 8:2, 7:3 v/v) in the OCM and from acetone:water solutions (9:1, 8:2, 7:3 v/v) in the CCM using identical spray drying parameters as for SD, except for the inlet temperature employed to spray dry the salt from water which was varied between 120 and 160 °C.

Additional details regarding process parameters used including feed concentrations and outlet temperatures for the spray dried systems are presented in Appendix I.

2.2.3 Spray drying of sulfadimidine (SD) and sulfadimidine sodium (SDNa) composite systems

Composite spray dried powders were obtained using a Buchi B-290 Mini Spray dryer (Buchi Laboratories-Technik AG, Flawil, Switzerland) operating in an open cycle mode configuration using air as the drying gas. 0.5% w/v feed solutions were prepared by dissolving the APIs in a mixture of ethanol and deionised water at a v/v ratio of 9:1 and spray drying with an inlet temperature of 78 °C using identical spray drying parameters as for SD.

2.2.4 Spray drying of sulfathiazole (ST) and sulfathiazole sodium (STNa)

Spray dried powders were obtained using a laboratory scale Buchi B-290 Mini Spray dryer (Buchi Laboratories-Technik AG, Flawil, Switzerland) operating either in an open cycle mode (OCM) configuration using air as the drying gas or in a closed cycle mode (CCM) configuration using nitrogen as the drying gas. 0.5% w/v ST feed systems were prepared by dissolving the active pharmaceutical ingredient (API) in ethanolic or acetonic solvents, prepared by mixing ethanol or acetone with deionised water at different v/v ratios: 9:1, 8:2, 7:3. ST was also spray dried as a solution from pure acetone and as a supersaturated solution from pure ethanol. Supersaturation was obtained by dissolving an amount of drug (greater than the limit of saturation) in ethanol with the aid of a sonicator. Due to the higher solubility of the drug in acetonic solutions, ST was additionally dissolved in acetonic solutions in order to achieve a comparable degree of saturation to the ethanolic solutions. Spray drying of ST was performed using the following parameters: inlet temperature of 78 °C, gas flow of 40 mm (473 L/hr); aspirator rate of 100% and feed flow rate of 30% (8 ml/min). Additional details regarding feed

concentrations, degree of saturation and outlet temperatures of the spray dried systems are presented in Table 2.1 and Appendix I.

Table 2.1 Spray drying parameters for sulfathiazole

Solvent	Spray dryer configuration	Volume ratio (v/v)	Outlet (°C) range	Feed conc.(w/v) %	Degree saturation %
Ethanol	Open	1/0	52-56	0.5%	120%
Ethanol:water	Open	9/1	49-55	0.5%	50%
Ethanol:water	Open	8/2	48-52	0.5%	35%
Ethanol:water	Open	7/3	45-50	0.5%	30%
Ethanol:water	Closed	9/1	51	0.5%	50%
Ethanol:water	Closed	7/3	48-49	0.5%	30%
Acetone	Closed	1/0	58-59	0.5%	42%
Acetone:water	Closed	9/1	49-54	0.5%	8%
Acetone:water	Closed	8/2	48-50	0.5%	7%
Acetone:water	Closed	7/3	47-50	0.5%	8%
Acetone	Closed	1/0	57-58	1.2%	100%
Acetone:water	Closed	9/1	54-55	3%	50%
Acetone:water	Closed	8/2	49-50	2.45%	35%
Acetone:water	Closed	7/3	50-51	1.95%	30%

STNa solutions (0.5% w/v) were spray dried from pure water, ethanol and ethanol:water solutions (9:1, 8:2, 7:3 v/v) in the OCM and from pure ethanol, ethanol:water and acetone:water solutions (9:1, 8:2, 7:3 v/v) in the CCM using identical spray drying parameters as for ST, except for the inlet temperature which was set to 160 °C. This inlet temperature was chosen to enable the recovery of a powder suitable for analysis as an inlet temperature lower than 160 °C resulted in wet and sticky powders. The resulting outlet temperature ranged between 98 and 108 °C.

2.2.5 Spray drying of sulfathiazole (ST) and sulfathiazole sodium (STNa) composite systems

Spray dried powders were obtained using a Buchi B-290 Mini Spray dryer (Buchi Laboratoriums-Technik AG, Flawil, Switzerland) operating in an open cycle mode configuration using air as the drying gas. 0.5% w/v feed solutions were prepared by dissolving the APIs (Table 2.2) in a mixture of ethanol and deionised water at a v/v ratio of 9:1. Spray drying of ST and ST-STNa systems was performed using the following parameters: gas flow of 40 mm (473 L/hr); aspirator rate of 100% and feed flow rate of 30% (8 ml/min). The inlet temperature for the mixtures was adapted to the amount of salt employed in the system, ranging from 85 to 90°C as reported in Table 2.2.

Table 2.2: Spray drying parameters for ST: STNa systems. (An inlet temperature higher than 85 °C for ST 9:1 resulted in partially crystalline materials. For the other systems inlet temperature lower than 90 °C resulted in wet powders).

ST: STNa Weight ratio (w/w)	Code	Inlet (°C)
9:1	ST 9:1	85
8:2	ST 8:2	90
3:1	ST 3:1	90
3:2	ST 6:4	90
1:1	ST 1:1	90
4:6	ST 4:6	90
1:3	ST 1:3	90
15:85	ST 15:85	90

2.2.6 Thermal Analysis Methods

2.2.6.1 Differential scanning calorimetry (DSC)

Differential scanning calorimetry (DSC) runs were conducted on a Mettler Toledo DSC 821^e using nitrogen as a purge gas. The method selected was similar to that previously reported by Caron *et al.*, (2011). Samples (3-7 mg) were placed in pin-holed aluminium pans and heated at a scanning rate of 10 °C/min from 25 °C (approximately room temperature) to 220 °C for SD and ST and from 25 °C to 320 °C or 280 °C respectively for SDNa and STNa, unless otherwise detailed. The recorded thermograms were analysed with Mettler Toledo STAR^e software (n≥2).

2.2.6.2 Modulated temperature differential scanning calorimetry (MTDSC)

Modulated temperature differential scanning calorimetry (MTDSC) scans were recorded on a QA-200 TA instruments MDSC calorimeter using nitrogen as a purge gas. Weighed samples (1.5-3.5 mg) were sealed in closed aluminium pans with one pin-hole. The method selected was similar to that previously reported by Caron *et al.*, (2011). A scanning rate of 1 °C/min, amplitude of modulation of 1 °C and modulation frequency of 1/60 Hz were employed for all the experiments. The temperature range was from 5 °C to 200 °C (n≥2).

2.2.6.3 Thermogravimetric analysis (TGA)

TGA experiments were conducted on a Mettler Toledo TG 50 apparatus using a method previously described by (Tajber *et al.*, 2005). Weighed samples (5-10 mg) were analysed in open aluminium pans placed on a Mettler MT5 balance. All samples were heated at a

scanning rate of 10 °C/min under nitrogen purge. Mass loss of the samples recorded were analysed by Mettler Toledo STARe software ($n \geq 2$).

2.2.7 Powder X-ray diffraction (PXRD)

X-ray powder diffraction measurements were conducted on samples mounted on a low background silicon sample holder, using a Rigaku Miniflex II, desktop X-ray diffractometer (Tokio, Japan). The method employed was previously described by Caron et al. (2011). The samples were scanned over a range of 5-40° in 2 θ scale using a step size of 0.05°/s. The X-ray source was a Cu K α radiation ($\lambda = 1.542 \text{ \AA}$) and the diffractometer was operated with a voltage of 30 kV and a current of 15 mA.

2.2.7.1 Crystalline content evaluation by PXRD

XRD was used to quantify the percentage crystallinity of spray dried (partially crystalline) powders. The same samples, stored for 3 years under dessicated conditions, were assumed to have fully crystallised and were used as the 100 % crystalline standards. This was deemed appropriate as these samples, relative to crystalline unprocessed material, would more closely resemble the processed materials in terms physical characteristics, such as particle size. The % crystallinity was calculated from equation 1 below:

$$\text{Crystallinity \%} = \frac{A_c}{A_x} (100) \quad (1)$$

where A_c and A_x are the total peak areas of the spray dried (partially) crystalline sample and of the recrystallised sample, respectively.

2.2.8 Powder density (Helium pycnometry)

True density was measured with an AccuPyc 1330 Pycnometer (Micromeritics®) using helium (99.995% purity) to determine the volume of the sample. The samples were dried for at least 24 hr prior to analysis using a vacuum oven operating at 600 mbar and 25 °C. Density measurements for amorphous ST were carried out immediately after collection of the powder from the spray dryer.

A 1 cm³ sample cup was used for sample analysis. A calibration check was run prior to analysis with an empty sample cup to check how close the average volume was to zero, expected to be within ± 0.05%. During each analysis the evacuation rate was 0.005 psig/min, the number of purges was 10 and the number of runs was 5. Measurements were carried out at least in duplicate.

2.2.9 Scanning Electron Microscopy (SEM)

Visualisation of particles was undertaken by scanning electron microscopy (SEM). SEM micrographs were recorded on a Mira Tescan XMU microscope (Tescan s.r.o., Czech Republic). Resolution: 3 nm at 30 kV, accelerating voltage: 5 kV, specimen stage: 300 mm by 330 mm (Compucentric), detector: secondary electron. Before analysis, the samples were fixed on aluminium stubs and coated with gold under vacuum. Different areas of each sample were analysed and photomicrographs were taken at different magnifications.

2.2.10 Fourier Transform Infra-Red Spectroscopy (FTIR)

Infrared spectra were produced using a Nicolet Magna IR 560 E.S.P. spectrophotometer controlled by OMNIC 4.1 software. The method used was as previously described by Caron *et al.* (2011). An average of 64 scans with a resolution of 2 cm⁻¹ over a wavenumber region of 4000-650 cm⁻¹ was used for each sample. Powder samples were diluted with KBr in a ratio 1:100 w/w, ground with a pestle in an agate mortar and then

pressed under 8 tons for 2 minutes in order to produce 13 mm KBr/drug discs. All spectra were baseline corrected. Analyses were carried out at least in duplicate.

2.2.11 Attenuated Total Reflectance Fourier Transform Infra-Red Spectroscopy (ATR-FTIR)

Infrared spectra of sulfathiazole: sulfathiazole sodium co-spray dried systems were produced using a PerkinElmer Spectrum 1FT-IR Spectrometer and evaluated using Spectrum v5.0.1 software as previously described (Grossjohann et al., 2012; Tewes et al., 2011). An average of 6 scans with a resolution of 4 cm^{-1} over a wavenumber region of $4000\text{--}650\text{ cm}^{-1}$ was used for each sample. All spectra were baseline corrected. Analyses were carried out at least in duplicate. When co-spray dried acid/salt composites were analysed, the spectrum of pure amorphous salt was subtracted from the mixture spectra, considering their molar ratio.

2.2.12 Water sorption analysis

2.2.12.1 Dynamic vapour sorption (DVS)

Water sorption behaviour of samples was determined using a DVS Advantage 1 apparatus (DVS Surface Measurement Systems, UK), as previously described (Tewes et al., 2010). Samples placed in a microbalance were exposed to three cycles of RH (0–90–0 %) at 25°C , with the following steps 3, 6, 10 and then every 10% RH ($n \leq 2$). Water sorption isotherms were calculated using the equilibrated mass ($dm/dt \leq 0.002\text{ mg/min}$ for 10 min) recorded at the end of each stage and expressed as a percentage of the dry sample mass.

The Young–Nelson equations were used to fit experimental equilibrium sorption and desorption data of the isotherms obtained for the sulfathiazole:sulfathiazole sodium co-spray dried systems (Tewes et al., 2010):

$$M_s = A(\beta + \theta) + B\theta RH \quad (2)$$

$$M_d = A(\beta + \theta) + B\theta RH_{\max} \quad (3)$$

where M_s and M_d are, respectively, the mass percentage of water contents of the system at equilibrium for each %RH during sorption and desorption. A and B are constants characteristic of each system. In this model, θ is the fraction of the surface covered by at least one layer of water molecules. It is defined as follows, with E a constant depending on the material.

$$\theta = RH/(RH + E(1 - RH)) \quad (4)$$

And β is defined by the following equation:

$$\beta = -E \times RH / (E - RH \times (E - 1)) + E^2 / ((E - 1) \times \ln[E - RH(E - 1)/E] - (E + 1) \times \ln(1 - RH)) \quad (5)$$

Thus, $A\theta$ is the mass of water in a complete adsorbed monolayer expressed as a percentage of the dry mass of the sample. $A(\beta + \theta)$ is the total amount of adsorbed water, and $A\beta$ is the mass of water which is adsorbed beyond the mass of the monolayer (i.e., in multilayer or cluster adsorption). B is the mass of adsorbed water at 100% of RH, and, hence, $B\theta RH$ is the mass of adsorbed water when the water coverage is θ for a given %RH. According to the model characteristics, from the estimated values of A , B , and E , the corresponding profiles of water adsorbed in monolayer ($A\theta$), multilayer ($A\beta$) and adsorbed ($B\theta RH$) were obtained.

2.2.13 Surface free energy measurement

Surface free energy measurements were carried out using inverse gas chromatography (iGC) (SMS Ltd., London, UK), as described previously (Tewes *et al.*, 2011). Powders were packed into silanised glass columns (300mm x 3mm). The columns were pre-treated for 1 h at 30 °C and 0% RH to remove any physisorbed molecules. Then, 250 µL of the elution mixture (probe vapour and helium) was injected into the carrier gas (helium) flow. All injections of probe vapours were performed at 0.03% v/v of the saturated probe vapour. A flame ionization detector was used to monitor the probes elution. Measurements were performed at 0, 10 and 20% of RH and 30 °C, (n = 2). In acid-base theory, the total surface free energy of a solid (γ_s^T) has 2 main components: a dispersive contribution (γ_s^d) and a specific or acid-base contribution (γ_s^{AB}), which are independent and additive, according to Eq. (6).

$$\gamma_s^T = \gamma_s^d + \gamma_s^{AB} \quad (6)$$

In order to calculate γ_s^d of the powders, alkane probes with a known dispersive contribution (γ_p^d) and a nil specific contribution (γ_p^{AB}) were used. Methane was used as inert reference to determine the dead volume of the system. At this low % of saturation (0.03% v/v), iGC was used in infinite dilution conditions and γ_s^d was calculated using the method developed by Schultz *et al.* (Schultz *et al.*, 1987). γ_s^{AB} was obtained indirectly via the measurement of the specific free energy of adsorption (ΔG^{SP}) of 2 monopolar probes and by using the acid-base theories developed by Van Oss *et al.* (vOCCG) (Van Oss *et al.*, 1988). In the vOCCG theories, γ_s^{AB} is subdivided into two non-additive parameters γ_s^+ and γ_s^- related according to Eq. (7), representing the electron acceptor (acid) and donor (base) properties, respectively.

$$\gamma_s^{AB} = 2 \cdot \sqrt{\gamma_s^+ \gamma_s^-} \quad (7)$$

By using ethyl acetate ($\gamma_p^- = 475.67$, $\gamma_p^+ = 0$ mJ/m², at 30°C) as the base probe and dichloromethane ($\gamma_p^- = 0$, $\gamma_p^+ = 124.58$ mJ/m², at 30 °C) as the acid probe with the acid and base component values calculated based on the Della Volpe and Siboni scale (Della Volpe and Siboni, 1997), γ_s^+ and γ_s^- of the powders surface were calculated. Polarity

index ($\frac{\gamma_s^{AB}}{\gamma_s^d}$) was then calculated.

Additionally the spreading coefficient (S_{SL}) was calculated using the dispersive contribution (γ_s^d) and the acid-base contribution (γ_s^+ and γ_s^-) of the total surface free energy of the solid and of the liquid (water) by the following equation.

$$S_{SL} = 2 \cdot \sqrt{\gamma_s^d \gamma_L^d} + 2 \cdot \sqrt{\gamma_s^+ \gamma_L^-} + 2 \cdot \sqrt{\gamma_s^- \gamma_L^+} - 4 \cdot \sqrt{\gamma_L^+ \gamma_L^-} - 2 \gamma_L^d \quad (8)$$

Where γ_L^d , γ_L^+ and γ_L^- are respectively the dispersive contribution (γ_L^d) and the acid-base contribution (γ_L^+ and γ_L^-) of the total surface free energy of the of the liquid (water) (Zdziennicka and Jańczuk, 2010).

2.2.14 Tg prediction of composites using the Gordon and Taylor equation

To measure the theoretical Tg values of co-spray dried composites the Gordon and Taylor equation was used:

$$Tg = \frac{w_1 \times Tg_1 + K \times w_2 \times Tg_2}{w_1 + K \times w_2}$$

Where Tg is the predicted glass transition temperature in Kelvin degrees of the amorphous composite mixture, Tg1 and Tg2 are the experimental glass transition temperatures for the individual amorphous components measured by MTDSC. w_1 and w_2

are the weight fraction of each substance in the mixture and k is a constant which was obtained by using the Simha-Boyer rule:

$$K = \frac{Tg_1 \times \delta_1}{Tg_2 \times \delta_2}$$

where δ_1 and δ_2 are the true densities of the individual amorphous components.

2.2.15 Solid-state stability study

The physical stability of the amorphous forms was investigated as a function of humidity and temperature. Spray dried samples were placed in weighing boats and positioned inside plastic humidity controlled chambers (Amebis Ltd. Ireland) providing a constant relative humidity of:

- $\leq 5\%$
- 35%
- 55%
- 60 %
- 75 %

The samples were stored at refrigerator temperature of 5 °C and at 25 or 40 °C using Gallenkamp incubators (Gallenkamp, UK).

At appropriate time intervals a sample of each solid material was removed for analysis by PXRD, SEM, DSC, and FTIR.

2.2.16 Solubility studies of sulfathiazole

2.2.16.1 Solubility in acetone and acetone:water solvent systems

The solubility of sulfathiazole was determined in acetone and three different acetone:water (v/v) ratios at 25 °C (9:1; 8:2; 7:3 v/v). Excess solid was placed in 12 ml

ampoules (closed with screw caps to prevent evaporation) placed in a temperature controlled (25 °C) water bath shaking at 100 cpm. The vials were kept under constant conditions for up to 60 hours and analysed at different time intervals (1 hr, 6 hr, 24 hr, 48 hr and 60 hr). The concentrations of API in filtrates, (obtained by using a 0.45 µm membrane filter (Titan 2, USA), from the acetonic systems were measured using a Shimadzu HPLC class VP series with a LC-10AT VP pump, SIL-10AD VP autosampler and SCL-10AVP system controller equipment operating with a SPD-10A VP UV-VIS spectrophotometer ($\lambda=254$ nm). A Hypersil BDS C18 5µm (length 150mm) column (Thermo scientific) and a flow rate of 1 mL/min were employed using a method previously reported in the literature (Capparella et al., 1995). The solubility of the drug in each solvent system was calculated as the average of the concentration values at the plateau of the corresponding concentration versus time curve (n=3).

The HPLC system used was a Waters HPLC, which consists of a Waters 600E pump, Waters 717 Autosampler and a Waters 2487 Dual λ Absorbance Detector. Data collection and integration were accomplished using Waters 746 Data Module. The mobile phase was filtered through a 0.45 µm membrane filter (Gelman Supor-450, USA) before use and degassed under reduced pressure during the run using a Phenomenex Degasser, model DG-4000.

2.2.17 Solubility studies of sulfadimidine

2.2.17.1 Solubility in acetone

The solubility of sulfadimidine in acetone was determined at 25 °C. Excess solid was placed in 50 ml glass beakers (n=3) containing acetone and stirred continuously for 3 hrs. The suspensions were then allowed to settle until a superficial clear solution was obtained. After sedimentation, samples of the filtered supernatant were placed in 1.5 mL

vials and dried in a Gallenkamp incubator oven at 40°C until complete evaporation of the acetone. The supernatant was filtered through a 0.45 µm membrane filter (Titan 2, USA).

The solubility of the drug (n=3) was calculated by gravimetric analysis.

2.2.18 Statistical analysis

iGC data were statistically evaluated by a two-way analysis of variance (ANOVA) test with Bonferroni test as post-hoc test. Significance level was $\alpha < 0.05$.

Chapter 3

Amorphisation of sulfadimidine and
sulfadimidine sodium upon spray
drying

3 Introduction

3.1 Spray dried Sulfadimidine (SD) and sulfadimidine sodium (SDNa)

The low solubility of some active pharmaceutical ingredients is a major hindrance to their use as effective pharmacological agents. In order to increase the solubility of such compounds, various chemical, physical and/or technological approaches can be employed such as the utilisation of their corresponding salt forms or particle size reducing processes such as the spray drying technique. This method has commonly been used in pharmaceutical technology; however a deeper understanding of the performance and properties of the processed materials is needed. In this work a model sulphonamide compound with low aqueous solubility sulfadimidine (SD) is spray dried, characterised and compared to the equivalent sodium salt system: sulfadimidine sodium (SDNa). Spray drying is a process capable of transforming a material from a liquid state (solution, suspension, emulsion) into a dry particulate. The physico-chemical properties of the resulting material including size, morphology and solid state nature can be modified upon processing. Corrigan et al., 1984, Tajber et al., 2005 and Chidavaenzi et al., 1997, for example have described the change on spray drying from crystalline to amorphous materials of the drugs employed in their respective studies upon spray drying (Chidavaenzi et al., 1997; Corrigan et al., 1984; Tajber et al., 2005).

From a pharmaceutical perspective, sodium salts are the most commonly used salt forms by virtue of their low toxicity compared to other salt forms (Ashford, 2002). However, little information on the behaviour of spray dried sodium salt systems is reported in the literature.

Chapter 3 Amorphisation of sulfadimidine and sulfadimidine sodium upon spray drying

For example, sodium cromoglycate was spray dried from ethanol, water and various compositions of these two solvents by Najafabadi et al., 2004 (Najafabadi et al., 2004) and then by Gilani et al., 2004 (Gilani et al., 2004). A correlation between the degree of crystallinity of the processed materials and the solubility of the API in the feed solution was noted. More recently, Paluch et al., (2012) (Paluch et al., 2012) found that spray drying chlorothiazide sodium resulted in an amorphous material regardless of the processing conditions employed. However, the findings from their study showed that the use of different spray drier configurations (closed versus open configuration) resulted in differences in the residual solvent content of the amorphous processed powders, noting a higher content for materials spray drying in the closed cycle configuration. Retained solvents including water may induce chemical reactions leading to degradation (Hancock and Shamblin, 1998), cause crystallisation of amorphous materials or also induce polymorphism. Polymorphic transitions induced by solvent-drug interaction have been extensively described in several studies (Aaltonen et al., 2003; Anwar et al., 1989; Croker and Hodnett, 2010; Parmar et al., 2007; Rodríguez-Hornedo and Murphy, 1999). Although drug-solvent interactions are an important consideration in the spray drying process, few studies have investigated directly the impact of a specific solvent on a drug, and in particular on the sodium salt form of a drug. This forms the basis for this chapter. Moreover, a range of other conditions were used to process SD and SDNa, and the impact of changing the operational mode of the spray dryer (open or closed mode configuration) and the inlet drying temperature on the characteristics of resulting materials was investigated.

SD was initially spray dried from water. Then ethanol and acetone were chosen to spray dry the API in a range of co-solvent concentrations with water on the basis of previous work by

Chapter 3 Amorphisation of sulfadimidine and sulfadimidine sodium upon spray drying

Nolan (Nolan, 2008) who spray dried SD from different co-solvent compositions. As no information on processing sulfadimidine sodium has been reported in the literature to date, initially the spray drying parameters considered were identical to those used to process the non ionised form. To increase the feasibility of obtaining an amorphous drug upon processing, SD and SDNa starting materials were spray dried only from solutions (Chidavaenzi et al., 1997). Due to poor solubility in water, a low concentration of 0.1% (w/v) was used when SD was spray dried from this solvent. For all the other systems, a 0.5% (w/v) feed solution was employed in the spray drying process. Solutions of SD and SDNa in ethanol:water and pure water were spray dried using a Buchi B-290 Mini Spray Dryer operating in the open mode configuration (OCM). In contrast, the closed cycle configuration (CCM) was used to spray dry the API from acetic solutions. The physico-chemical properties, including the physical stability, of both the processed and the starting materials were compared in order to evaluate the impact of the process.

3.2 Physicochemical properties of Sulfadimidine

3.2.1 PXRD, thermal and solubility analysis

The PXRD patterns of unprocessed SD (Figure 3.1) was characterised by Bragg peaks indicative of a crystalline structure and consistent with the pattern reported by Caron (Caron et al., 2011).

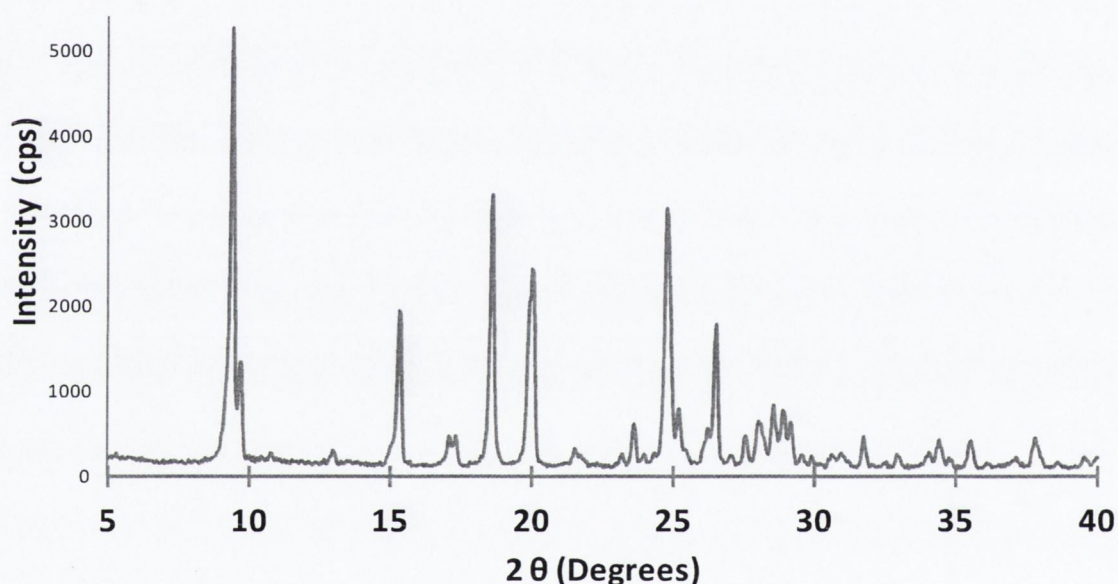


Figure 3.1 PXRD pattern of SD starting material.

The DSC thermogram (Figure 3.2) of SD showed a single endothermic event with onset at $197 \pm 0.5^\circ\text{C}$ which corresponds to the melting of the drug. The powder was dry, with a mass loss of $\sim 0.3\%$ up to 120°C attributed to adsorbed moisture as indicated by TGA analysis. Beyond the melting point, starting at $\sim 230^\circ\text{C}$ an abrupt mass loss was also recorded due to the degradation of the API (Figure 3.2).

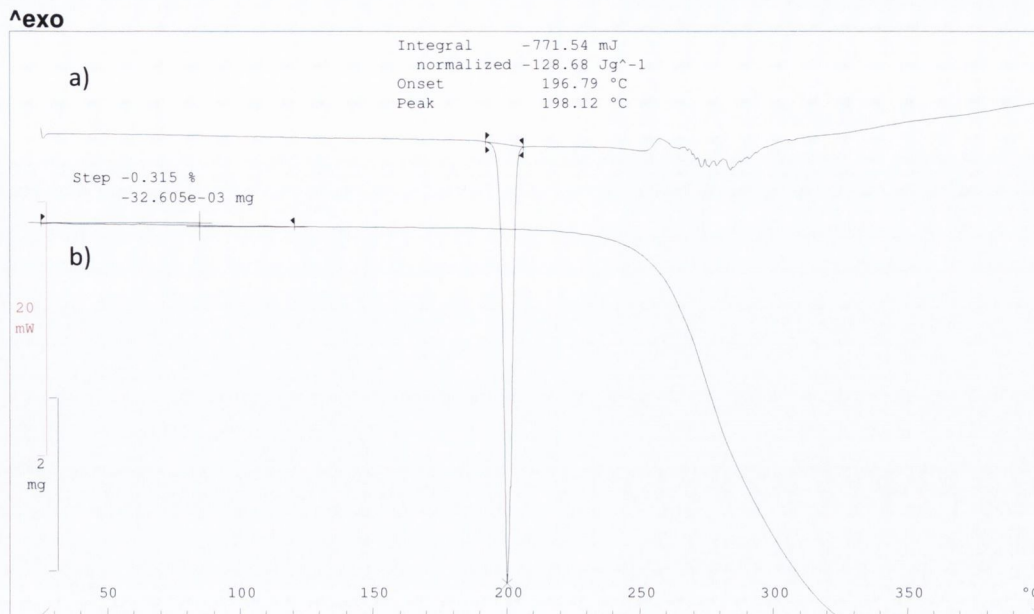


Figure 3.2 DSC (a) & TGA (b) thermograms of SD starting material.

The solubility of SD in water, ethanol and water:ethanol mixtures at different ratios was previously determined in this laboratory by (Nolan, 2008) and is plotted in Figure 3.3 as a function of the volume fraction of ethanol.

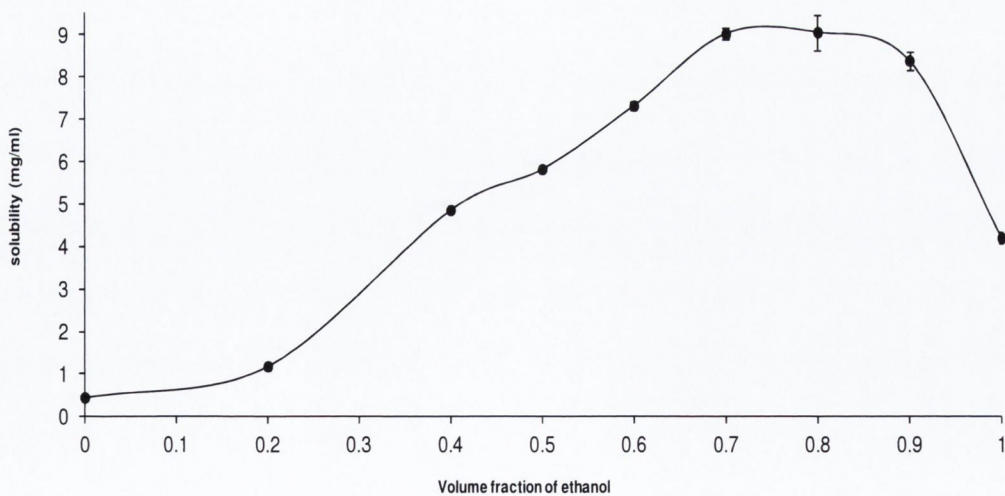


Figure 3.3 Ethanol:water solubility profile for sulfadimidine at 25°C, the solubility of the solute plotted against the volume fraction of the mixed system (ethanol:water) [from (Nolan, 2008)].

SD solubility in ethanol (4.205 ± 0.131 mg/mL) was approximately nine times higher than in water (0.453 ± 0.004 mg/mL). From the ethanol:water solubility profile by Nolan (Figure 3.3) it can be evinced that the addition of ethanol to water renders the solvating environment less polar, resulting in a more favourable solvation of the hydrophobic SD in the liquid phase. In particular, by adding a volume of ethanol between 50% and 90% v/v to the water, the solubility of the drug in the co-solvent mixtures was higher than in the individual solvents. The graph also showed that the highest level of solubilisation for SD was achieved with ethanol content between 70 and 90% v/v. At these volume fractions, the solubility of SD increased up to ~ twice the solubility in pure ethanol.

3.3 Sulfadimidine spray dried from water and ethanol:water mixtures

3.3.1 Open cycle mode (OCM)

3.3.1.1 SD spray dried from water

The spray drying technique involves the atomisation of a liquid feed which can be prepared either by dissolving or suspending a solid into a suitable solvent. However the study by Chidavaenzi *et al.* demonstrated that spray drying solutions or suspensions can impact on the final crystallinity of the processed material (Chidavaenzi *et al.*, 1997). Zhang *et al.* (2007) showed that the solubility of sulfadimidine in water could be increased by heating the solvent (Zhang *et al.*, 2007). Therefore a 0.1% (w/v) solution of SD in water was obtained when the temperature of the solvent was increased up to 65°C. Different inlet temperatures were tested between 78 and 100°C to spray dry SD from water. However the use of these inlet temperatures resulted mainly in low yields of wet powders stuck to the cyclone walls which therefore could not be analysed.

According to the technical specifications of the Buchi B-291 Mini Spray Dryer increasing the inlet temperature results in a corresponding increase in the outlet temperature. This consequently reduces the relative humidity in the spray dryer environment which can lead to an increase of yield by preventing stickiness (Buchi-B-290, 2007). When the inlet was finally set at 120°C, the collection of a powder suitable for analysis was possible. Spray dried SD analysed by PXRD did not show any characteristic Bragg peaks as for the starting material but a diffuse halo pattern indicative of an amorphous compound (Figure 3.4f). Thermal analysis by DSC of spray dried SD from water revealed initially a baseline deflection at 79°C, corresponding to the glass transition temperature (T_g) of amorphous SD. This value is in agreement with the T_g of SD reported by Caron et al. (Caron et al., 2011).

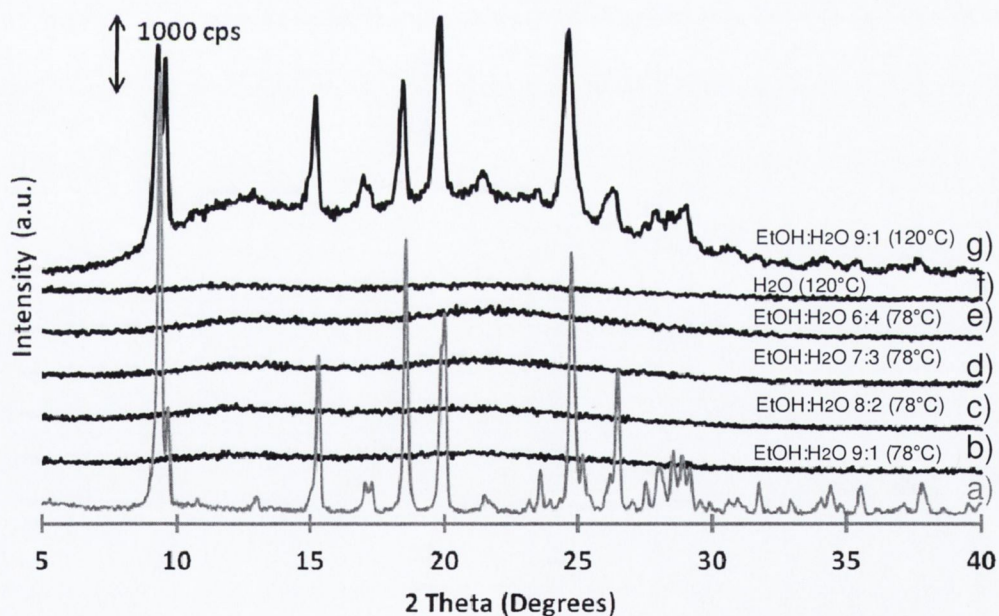


Figure 3.4 PXRD pattern of a) unprocessed SD, b) SD spray dried from ethanol:water 9:1 v/v; c) SD spray dried from ethanol:water 8:2 v/v; d) SD spray dried from ethanol:water 7:3 v/v; e) SD spray dried from ethanol:water 6:4 v/v; f) SD spray dried from water at inlet of 120°C; g) SD spray dried from ethanol:water 9:1 v/v at inlet of 120°C.

The T_g was followed by an exothermic peak with onset at 120°C , attributed to the crystallisation of the amorphous material (Figure 3.5B). Finally a melting endotherm with peak onset at $\sim 195^\circ\text{C}$ and ΔH of $\sim 120\text{ J/g}$ was observed. Onset of melting evaluated for the processed material was 3 degrees lower compared to the starting material values. In order to establish if amorphous SD crystallised on heating into its original solid state form, PXRD analysis was performed on the material immediately on heating beyond the endset of the exo-peak in the DSC. Bragg peaks corresponding uniquely to the unprocessed API were observed and no new peaks were evident. This was expected, as no polymorphic structures of SD are reported in the literature.

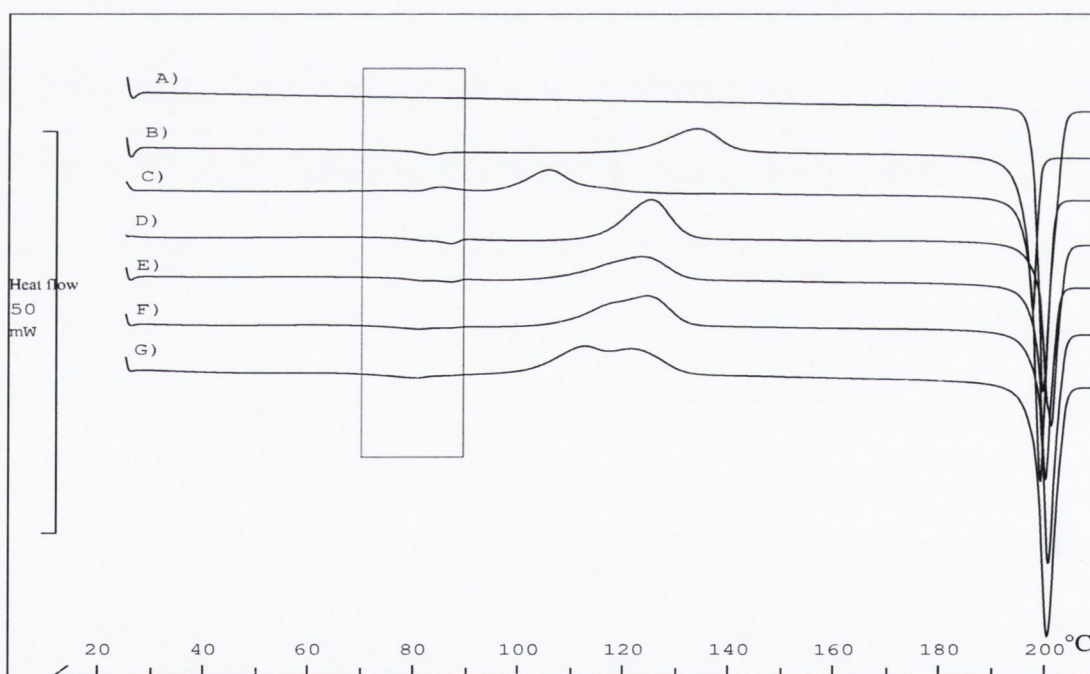


Figure 3.5 DSC curves of a) unprocessed SD; b) SD spray dried from water (Inlet 120°C); c) SD spray dried from ethanol:water 9:1 v/v (Inlet 120°C); d) SD spray dried from ethanol:water 9:1 v/v (Inlet 78°C); e) SD spray dried from ethanol:water 8:2 v/v (Inlet 78°C); f) SD spray dried from ethanol:water 7:3 v/v (Inlet 78°C); g) SD spray dried from ethanol:water 6:4 v/v (Inlet 78°C). T_g region highlighted.

3.3.1.2 SD spray dried from ethanol:water co-solvent systems

The improved solubility of SD in co-solvent mixtures of water and ethanol coupled with the possibility of dissolving the salt form in comparable solvents formed the basis of spray drying from these co-solvent systems.

The feed concentration was increased to 0.5% (w/v) to produce an appropriate amount of powder for further analysis in a reasonable period of time. Initially for comparison purposes the same inlet of 120°C was used and the drug was dissolved in an ethanol:water 9:1 v/v system. The PXRD pattern for SD processed from this co-solvent system was characterised by Bragg peaks of reduced intensity compared to the starting material which indicated that the drug was produced in a partially crystalline state (Figure 3.4 g). Partially crystalline systems produced upon spray drying have been previously reported for other spray dried substances (Chidavaenzi et al., 1997; Langrish, 2007). These biphasic or multiphase systems are considered adverse for pharmaceutical development purposes because the presence of a more stable crystalline form increases the tendency of the remaining amorphous material to crystallise during storage. Of particular concern is the release of the water absorbed in the amorphous phase upon crystallisation which increases the molecular mobility of the remaining amorphous fraction through plasticisation (Vehring, 2008).

Thermal analysis of SD was in agreement with the results from PXRD. No clear T_g could be detected for the system spray dried from the ethanolic solution, as a consequence of the increased crystallinity. Moreover the crystallisation exotherm was of reduced ΔH and at a lower onset temperature (~95 °C) compared to the system spray dried from water. The amorphous content calculated by PXRD was approximately 12%. The same samples, after

full crystallisation upon storage under desiccated conditions (3 years), were used as the 100 % crystalline standards to calculate the amorphous content in the spray dried material as indicated in Chapter 2 (Materials and methods, section 2.2.7.1).

It seems plausible that the outlet temperature could be the parameter which caused differences in the physical state of the drug. The outlet temperature is the temperature to which substances are subjected in the spray drier until completion of the process. This is an important parameter to be considered because an outlet above T_g may promote the crystallisation of the API. The outlet temperature for the system spray dried from water ($\sim 65^\circ\text{C}$) was below the temperature of the glass transition of amorphous SD while for the system spray dried from the ethanolic mixture ($\sim 85^\circ\text{C}$) it was above T_g . To assess that the different solid state outcomes were a consequence of the impact of the outlet temperature on processing SD, and not related to the spray drying of a heated solution, the inlet temperature was reduced to 78°C and SD was spray dried from ethanolic solutions prepared and held at room temperature. To fully dissolve SD to a concentration of 0.5% w/v, four different ethanol:water ratios 9:1, 8:2, 7:3 and 6:4 (v/v) were tested. SD was previously spray dried at this inlet temperature from ethanolic mixtures but at a lower concentration by Nolan (Nolan, 2008) who successfully produced amorphous particles. This temperature was chosen because of the boiling point of the main component of the mixture. All SD powder samples spray dried from ethanol:water solutions (inlet 78°C) at all compositions presented no diffraction peaks but a characteristic halo pattern in the PXRD diffractograms of the materials (Figure 3.4b-e).

DSC thermograms of spray dried SD at all compositions (Figure 3.5) showed a deflection of the baseline due to the glass transition event, with temperature onsets in agreement with

Chapter 3 Amorphisation of sulfadimidine and sulfadimidine sodium upon spray drying

those obtained on spray drying from water. Beyond T_g , a crystallisation peak was detected at a temperature between 100°C and 130°C for all systems, attributed to the crystallisation of the amorphous material (Figure 3.5). The onset temperature of this peak was lower compared to the amorphous system obtained from water, indicating a reduced thermal stability. The melting onset for all systems was at $\sim 197^\circ\text{C}$ and ΔH of $\sim 124\text{ J/g}$ which compares to both the onset and ΔH for the unprocessed material.

3.3.2 Closed cycle mode (CCM)

3.3.2.1 SD spray dried from acetone and acetic solutions

To analyse the impact of solvent on the physicochemical properties of spray dried SD dissolved in a different solvent, the API was spray dried from acetone and two different acetone:water co-solvent ratios 9:1 and 7:3 (v/v). To safely process inflammable solvents such as acetone the CCM with nitrogen (N_2) as drying gas was employed. This configuration allows the circulation of inflammable gases and solvent vapours under inert conditions. DSC analysis of SD spray dried from pure acetone did not detect any degree of amorphous material as just the melting endotherm ($\sim 196^\circ C$) was recorded on the thermograms of the spray dried drug (Figure 3.6b).

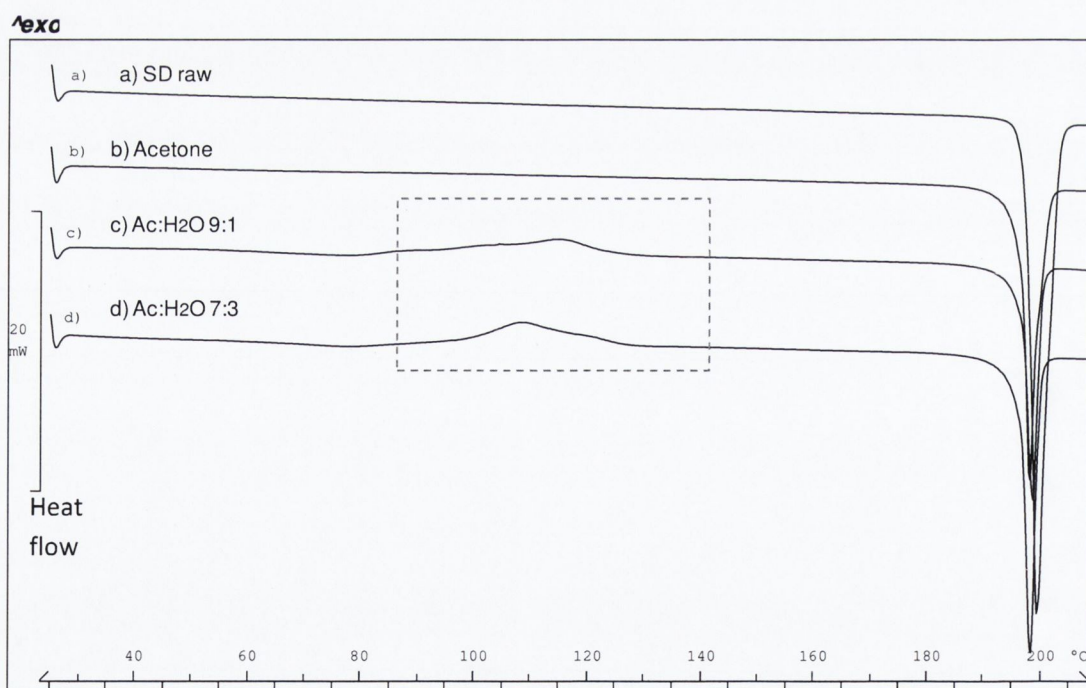


Figure 3.6 DSC curves of a) unprocessed SD, b) SD spray dried from pure acetone, c) SD spray dried from acetone:water 9:1 v/v, d) SD spray dried from ethanol:water 7:3 v/v.

In contrast, the thermograms of SD processed from the acetone:water co-solvent systems presented exothermic peaks with onset at $\sim 97^{\circ}\text{C}$ and ΔH of ~ 70 J/g (Figure 3.6 c-d). Both the melting point and enthalpy of crystallisation were lower compared to the corresponding systems processed from ethanolic solutions in the OCM and therefore indicative of the solidification of SD on spray drying into partially crystalline samples.

The production of partially crystalline SD was confirmed by the PXRD patterns of spray dried sulfadimidine from acetone:water co-solvent systems which displayed a small number of reduced intensity peaks, characteristic of crystalline sulfadimidine raw material (Figure 3.7 c-d).

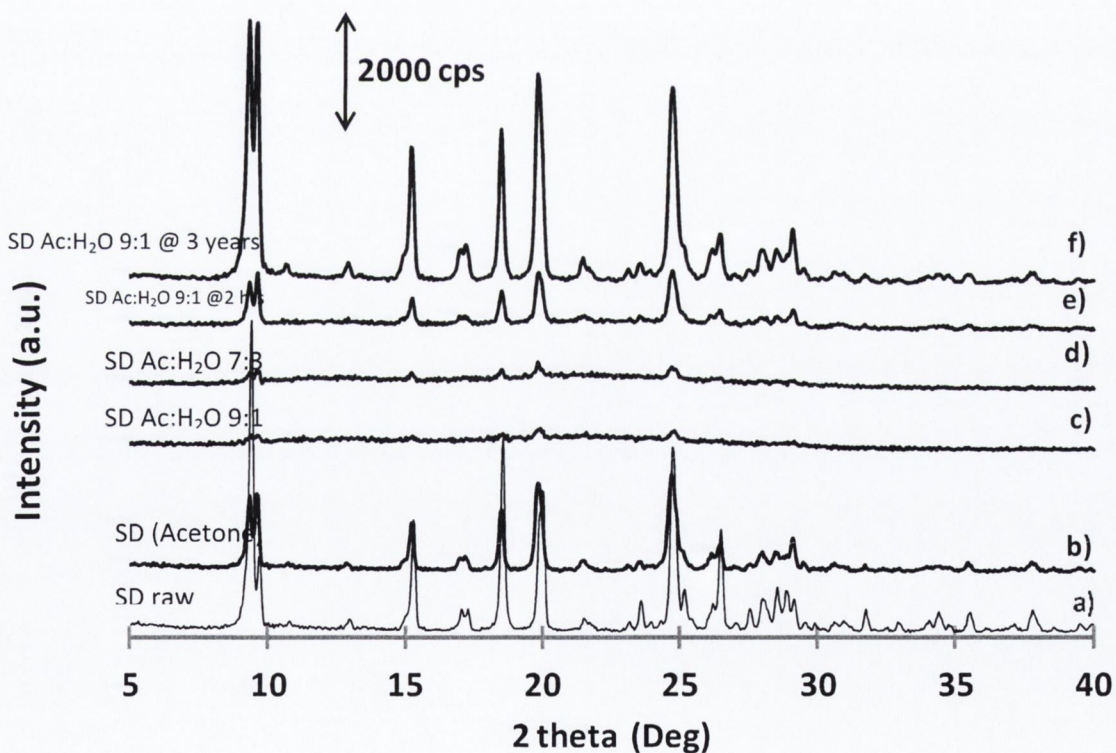


Figure 3.7 XRD pattern of a) unprocessed SD, b) SD spray dried from acetone; c) SD spray dried from acetone:water 9:1 v/v; d) SD spray dried from acetone:water 7:3 v/v; e) SD spray dried from acetone:water 9:1 v/v after 2 hour storage; f) SD spray dried from acetone:water 9:1 v/v after 3 years storage under desiccated conditions at 5°C .

Chapter 3 Amorphisation of sulfadimidine and sulfadimidine sodium upon spray drying

The crystallinity of the spray dried samples from acetone:water systems was calculated by PXRD at 75%, 9% and 6%, when spray dried from cosolvent concentrations of 100%, 90% and 70% (v/v) acetone respectively. Although no exotherm could be detected on the thermogram of SD spray dried from acetone, an amorphous content of 25% was calculated by PXRD. This percentage was above the limit of detection of amorphous content by the conventional DSC technique of ~10% (Saleki-Gerhardt et al., 1994). However, overestimation of the amorphous content by PXRD could be attributed to the production of nanocrystalline particles the dimension of which escape X-ray detection (Bates et al., 2006). Differences in crystallinity could also be attributed to subsampling procedures. Differing amounts of sample employed in DSC and PXRD experiments may affect the amorphous content estimation in non-homogeneous powders. For all spray drying runs the outlet temperature recorded was ~25 degrees below the T_g of the drug and, the concentration employed was below the maximum solubility of SD in acetone measured at 56.4 ± 0.6 mg/mL by gravimetric analysis. However Yoshioka and Tashiro (2004), highlighted that different solvents can plasticise amorphous systems to different extents and a correlation between the degree of plasticisation and solubility was noted (Yoshioka and Tashiro, 2004). Therefore it is hypothesised that due to the high solubility of SD in acetone, residual vapours of this solvent in addition to the residual water vapour in the spray dryer could plasticise the drug causing it to solidify into a (partially) crystalline substance.

Kinetics of evaporation are dissimilar among different spray dryer configurations due to different pressures and relative content of solvent in the drying gas (Dobry et al., 2009). Paluch et al., 2012 pointed out that powders produced in the CCM were characterised by a higher solvent residual than powders processed in the OCM (Paluch et al., 2012). In theory in

the closed loop system the gas stream of N₂ should be purified by the presence of the solvent by condensing the organic vapours at low temperature. The regenerated gas is then returned again in the spray drier (Büchi-290 technical specification, 2007). Nevertheless it is hypothesised that some impurities of solvent might contaminate the recycled carrier gas. Interestingly, the addition of water to acetone in the feed solution resulted in the production of partially amorphous powders of SD suggesting that the use of water, a co-solvent in which the drug is poorly soluble, might reduce the plasticising effect of the acetone on the drug.

3.4 FTIR analysis

The infrared spectrum of the crystalline starting material (Figure 3.8a) is compared with the spectra of the amorphous counterparts obtained by spray drying SD from pure water (Figure 3.8b) and from ethanolic co-solvent systems (Figure 3.8c).

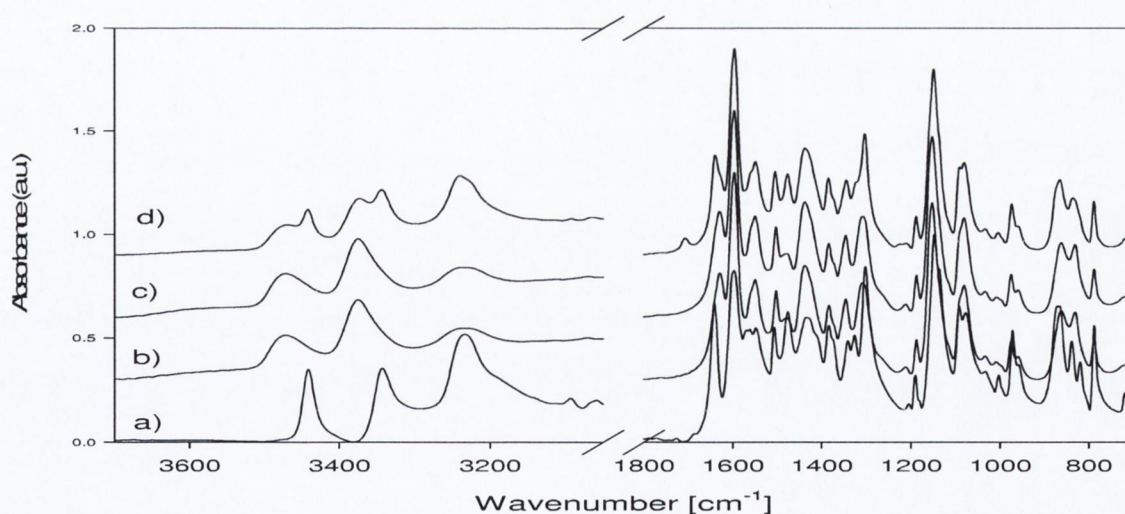


Figure 3.8 FTIR spectra of a) sulfadimidine raw material; b) spray dried sulfadimidine from water; c) spray dried sulfadimidine from ethanol:water 9:1 v/v inlet 78°C; d) spray dried sulfadimidine from acetone:water 9:1 v/v.

Regardless of the ethanol to water proportion employed in the spray drying process the amorphous spectra were identical. However a series of differences distinguished the spectra

of the crystalline and amorphous forms of SD. In addition to a general broadening and smoothening of the peaks in the amorphous samples, changes in peak shape and position were noticeable between the two physical states. The increased bandwidth of the spectra in the amorphous state is a known phenomenon that is generally attributed to the loss of crystal lattice as a consequence of the solidification of the drug into a disorganised state such as the amorphous state (Kaushal et al., 2008; Tajber et al., 2005; Tang et al., 2002). The main shifts were recorded in the 3390-3245 cm^{-1} region. In this region SD and sulphonamides in general have characteristic strong bands attributed to the stretching vibration of the N-H bonds (Socrates, 2001). The spectrum of pure crystalline sulfadimidine presented these characteristic peaks at 3442 and 3342 cm^{-1} for the asymmetric and symmetric NH (anilino) stretching vibration respectively (Yang et al., 2005). These peaks were broader and were shifted to higher wavenumbers in the spectra for the spray dried samples, indicating that the hydrogen bond strength decreased with loss of crystallinity (Tang et al., 2002). Simultaneously both the asymmetric (1302 cm^{-1}) and symmetric (1147 cm^{-1}) S=O stretching vibration peaks shifted to higher wavenumbers, confirming that the SO_2 group acts as a H-bond acceptor in the crystalline state (Caira, 2007; Kaushal et al., 2008). However the magnitude of the shift of the SO_2 peaks was lower compared to that of the NH stretching peaks. Variations in the magnitude of the shifts for the donor and acceptor group of H-bonds were discussed in the work of Kaushal et al. (2008). The author related the differences to a higher sensitivity of the frequency of the donor X-H stretching vibration to the formation/rupture of hydrogen bonds compared to the acceptor group (Kaushal et al., 2008). Furthermore it is also hypothesised that upon amorphisation, the SO_2 group, as consequence of the breakage of intermolecular hydrogen bonds with the NH_2 group, would be available to

form intra-molecular H-bonds. This type of intra-molecular interaction would also explain the downward shift of the bending NH (anilino) peak from $\sim 1641\text{ cm}^{-1}$ in the crystalline state to $\sim 1628\text{ cm}^{-1}$ in the amorphous state (Figure 3.9).

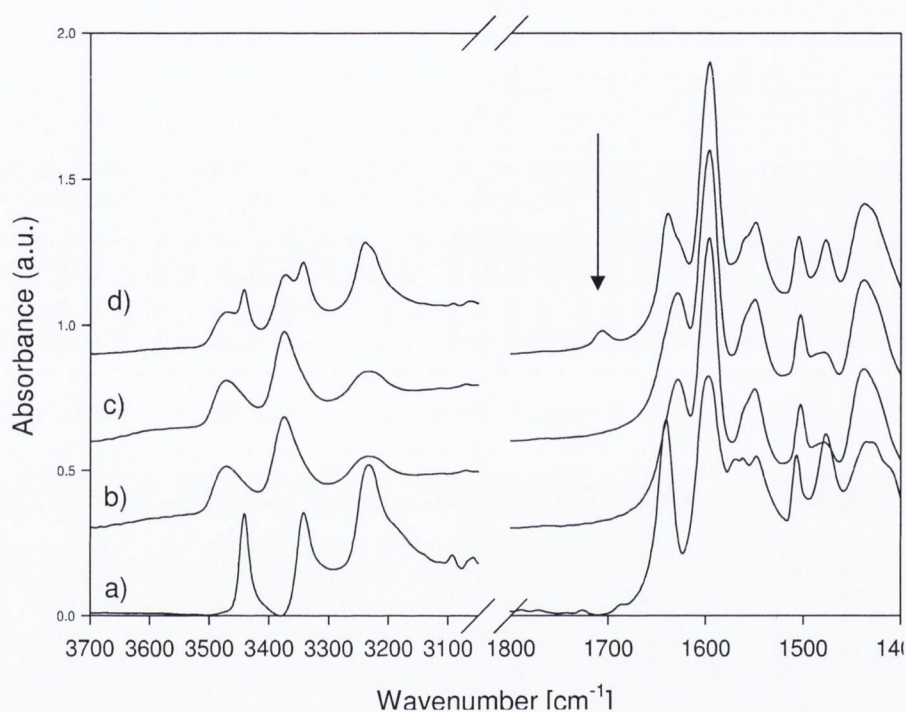


Figure 3.9 FTIR spectra of a) sulfadimidine raw material; b) spray dried sulfadimidine from water; c) spray dried sulfadimidine from ethanol:water 9:1 v/v inlet 78°C; d) spray dried sulfadimidine from acetone:water 9:1 v/v.

The FTIR spectrum of the partially crystalline SD processed from acetone:water (Figure 3.9d) presented an extra peak at $\sim 1700\text{ cm}^{-1}$. This peak, typical of the C=O stretching vibration of ketones (Socrates, 2001), was not found in the spectra of either the original material or the processed materials from water and ethanol:water solvent systems and therefore was attributed to acetone retained in the amorphous compound. The higher solubility of the drug in this solvent compared to ethanol might explain the high affinity of

acetone to the amorphous state of SD and why the drug solidified as a (partially) crystalline material when spray dried from this solvent.

3.5 DVS analysis

Investigating and understanding the behaviour of crystalline and amorphous drugs when exposed to various conditions of RH is a fundamental aspect of pre-formulation studies. The behaviour of both crystalline and amorphous SD at predefined relative humidity values was investigated by DVS analysis. Moreover this would allow for comparison studies as it was anticipated that similar studies would be performed on the corresponding amorphous salt form. Amorphous solids uptake relatively large amounts of water vapour compared to their corresponding crystalline phases. Sorbed water can act as a plasticising agent, lowering the glass transition temperature below the storage temperature and cause phase transitions. Several low molecular weight amorphous materials have been reported to convert to their more stable crystalline state if subjected to RH above the glass transition (Burnett, 2009; Burnett et al., 2004; Jouppila et al., 1998; Kedward et al., 2000) . When a material converts from an amorphous to a crystalline state, the water sorption ability decreases due to the lower hygroscopicity of the crystalline state compared to the amorphous state and the excess water will be desorbed during the phase transition (Burnett et al., 2006; Grisedale et al., 2011). Analysing the mass variation of an amorphous substance exposed to increasing conditions of RH can be used to determine the % RH at which water-induced phase transitions are favoured and provide guidelines for rational stabilisation strategies of amorphous materials. Experiments were performed using a dynamic vapour sorption (DVS) analyser which measures the uptake and loss of water vapour gravimetrically using a recording microbalance with a mass resolution of $\pm 0.1\mu\text{g}$ (DVS-training-guide, 2009). Figure 3.10 and 3.11 display

Chapter 3 Amorphisation of sulfadimidine and sulfadimidine sodium upon spray drying

the sorption-desorption isotherms (1st and 2nd cycle) and the corresponding sorption-desorption kinetic profiles for amorphous SD (spray dried from ethanol:water 9:1 v/v), respectively. Additionally Figure 3.10 displays the sorption isotherm for unprocessed crystalline SD up to 70% RH. After equilibration at each step of RH up to 70% the crystalline drug presented a maximum water uptake of less than 0.1% w/w at 70% RH indicating that the original unprocessed drug is a non hygroscopic substance. In contrast the isotherms showed that amorphous SD, when exposed to a series of 10% step changes of RH (0-90-0%), reached a maximum water uptake of ~4.3% at 90% RH.

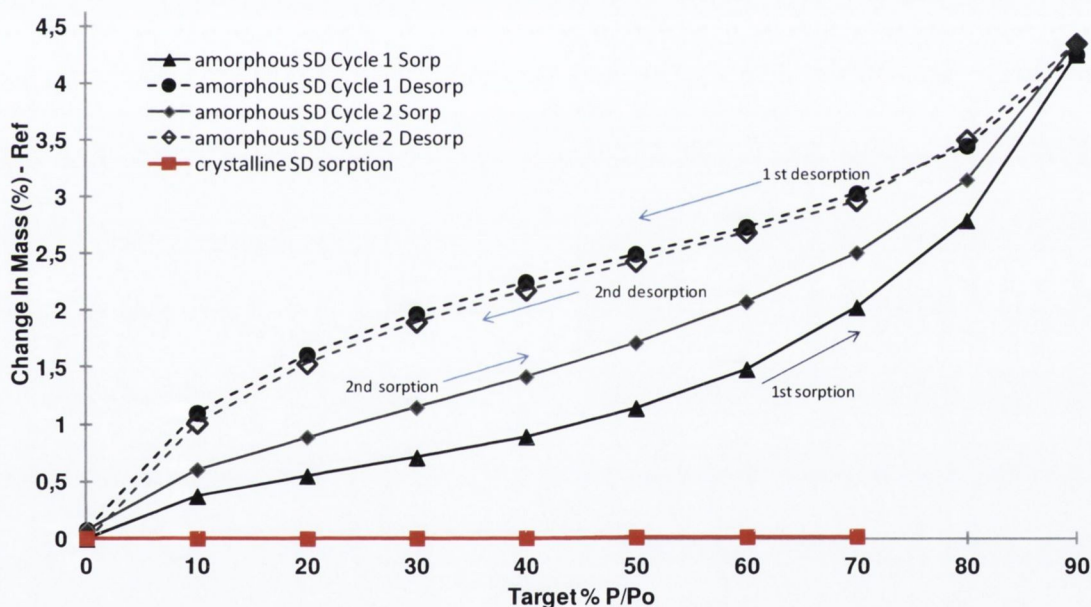


Figure 3.10 DVS sorption-desorption isotherm of unprocessed crystalline SD (red line) and amorphous SD (spray dried from ethanol:water 9:1 v/v).

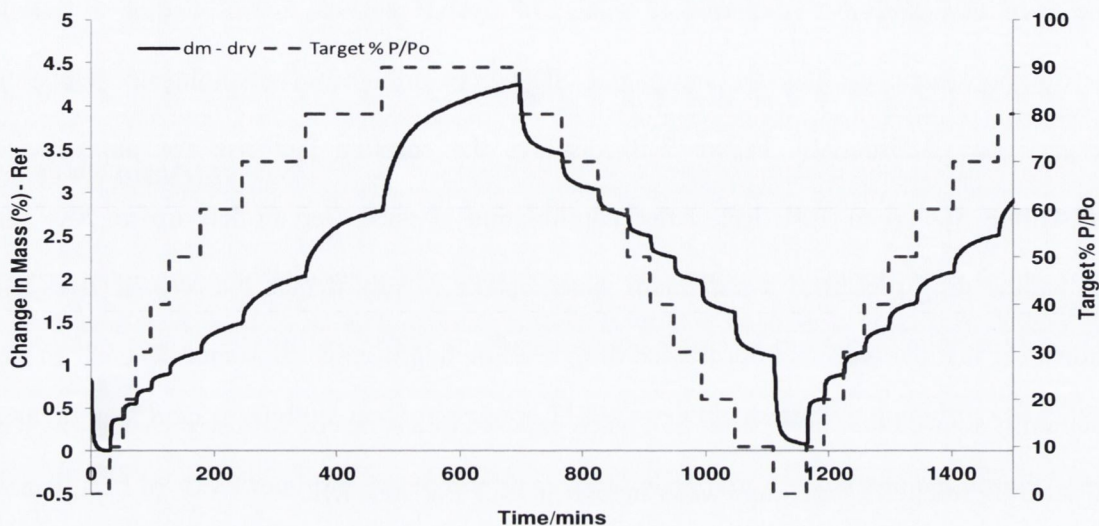


Figure 3.11 DVS sorption-desorption kinetic profile of amorphous SD.

Corresponding kinetic profiles (Figure 3.11) presented an increase in mass and then a plateau for each percentage of RH analysed for all cycles. This behaviour suggested that the amorphous drug did not crystallise during the duration of the experiment. PXRD analysis confirmed DVS results and no Bragg peaks were detected on the pattern produced by the powder after being subjected to three (0-90-0) sorption-desorption cycles.

3.6 Physical stability upon storage at different temperature and RH conditions

Nolan (2008) investigated the physical stability of amorphous SD (spray dried from ethanol:water solutions) under different storage conditions. SD remained XRD amorphous up to 8 weeks when stored in desiccated conditions at 4°C. In contrast at 25°C/60% relative humidity and 40°C/75% relative humidity, the API converted to a partially crystalline material after three days and ~1 day of storage respectively (Nolan, 2008). These results were not in complete agreement with the findings from the current study. In accordance with the

Chapter 3 Amorphisation of sulfadimidine and sulfadimidine sodium upon spray drying

work of Nolan, the amorphous drug crystallised between 2 and 3 days of storage when stored at 25°C and 60% RH and 40°C/75% RH. In contrast, several batches of amorphous SD spray dried from ethanol:water co-solvent systems at all compositions, and from pure water, stored at 4°C in desiccated conditions, were found to be physically stable over a period of 20 weeks. This was indicated by the lack of detection of Bragg peaks on the PXRD patterns. The physical stability of the drug was also investigated upon storage at 5°C and 60% RH. SD remained amorphous as indicated by PXRD analysis for 4 weeks. This result coupled with the high stability of amorphous SD following DVS studies suggesting that the degree of hydrophilicity and the solubility of the substance are important factors to be considered when taking decisions on the conditions of storage of amorphous substance. The differences in crystallisation kinetics (3 days versus 4 weeks) appear mainly to be due to the storage temperature. A higher storage temperature, besides facilitating crystallisation because it is closer to the T_g of the drug, at the same time increases the solubility of the drug in water.

In contrast, spray dried sulfadimidine from acetone:water 9:1 and 7:3 v/v co-solvent systems showed an increase in crystallinity from respectively 9 and 6% to ~80% for both systems after two days storage in desiccated conditions at 5°C. As previously reported for the ethanolic systems, the same samples (n=2) after 3 years storage in desiccated conditions at 5°C were taken as the 100% crystalline standards to calculate the amorphous content in the spray dried materials. The PXRD pattern of SD spray dried after 3 years storage is shown in Figure 3.7f.

3.7 SEM analysis

The particle morphology of spray dried SD varied in relation to the solvent or co-solvent mixture used in the process (Figure 3.12).

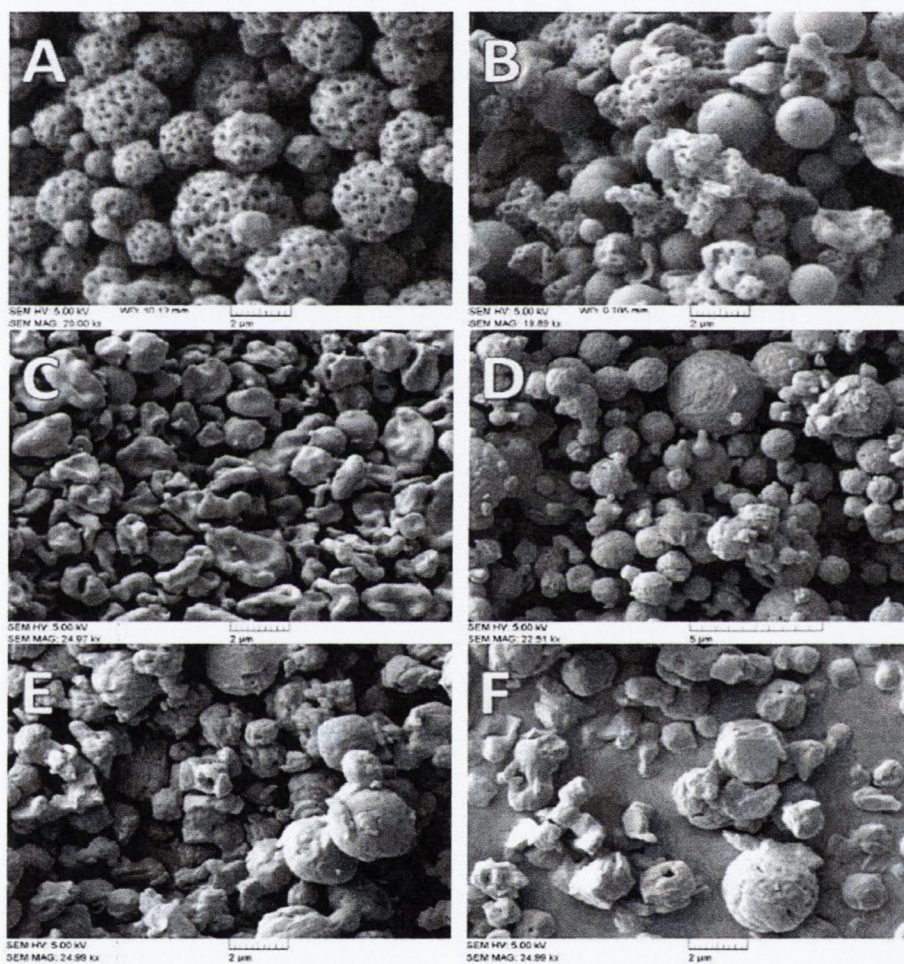


Figure 3.12 A) SD spray dried from ethanol:water 9:1 v/v; b) SD spray dried from ethanol:water 7:3 v/v; c) SD spray dried from water d) SD spray dried from acetone; e) SD spray dried from acetone:water 9:1 v/v; f) SD spray dried from acetone:water 7:3 v/v. (note different scale bars)

Porous spherical particles of SD were observed by SEM when spray dried from ethanol:water 9:1 v/v (Figure 3.12 A). With the increase of water content to 30% v/v the

Chapter 3 Amorphisation of sulfadimidine and sulfadimidine sodium upon spray drying

powder obtained was a combination of porous and non-porous particles (Figure 3.12 B). The spherical shape of SD particles spray dried from pure acetone (Figure 3.12 D) was not consistent and particles became much more irregular with increasing content of water in the solvent mix (Figure 3.12 E-F). The surface of the particles appeared to be rough. In contrast, when the drug was spray dried from water, the particles resembled deflated balloons with smooth surfaces (Figure 3.12 C).

3.8 Key findings on sulfadimidine

The key results related to the impact of spray drying on SD presented in this section of Chapter 3 can be summed up as follows:

- The physical state of sulfadimidine can be tuned by varying spray drying parameters. Spray drying SD from water or ethanol:water solutions in the OCM results in an amorphous material provided that the outlet temperature is kept below the glass transition temperature of amorphous SD found at approximately 80 °C.
- The use of acetic solutions in the CCM configuration produces partially crystalline materials. It is hypothesised that this is due to the increased water and acetone residual content present in the spray drier used with this type of configuration, causing a plasticising effect on the amorphous API.
- The use of different solvents has an impact on the morphology of the spray dried material. From a pharmaceutical development strategy this appears interesting because it is possible to select process parameters to obtain the morphology according to the intended use.

3.9 Sulfadimidine sodium (SDNa)

3.9.1 Introduction

Salt formation is a common strategy applied in the pharmaceutical sector to modify important physical properties of ionisable compounds. A drug molecule characterised by a low melting point for example is often not suitable for many processes which require high temperatures such as purification or drying. The ionic interactions involved between the counterion and the electrolyte drug in the crystal structure of a salt can have the effect of raising the melting point of the salt to a higher temperature compared to the unionised form. The selection of an appropriate counterion can also enhance the solubility in water of weakly acidic/basic compounds in the salt form. However, processing salts by different techniques such as milling, lyophilisation, precipitation from solution under reduced pressure and spray drying may introduce a degree of amorphous material in the compounds. Studies by Towler *et al.* (Towler *et al.*, 2008), Kumar *et al.* (Towler *et al.*, 2008), and Tong and Zografi (Tong and Zografi, 1999) analysed different properties of amorphous salts produced by the aforementioned pharmaceutical techniques. They found that amorphous salts generally have a higher T_g compared to that of the amorphous unionised compound. As the T_g reflects the stability of an amorphous material (Tajber *et al.*, 2005), the use of a salt form in its amorphous state can be an interesting strategy to stabilise these high energy forms. Therefore the impact of the spray drying process was investigated on the sodium salt form of sulfadimidine, with the objective of converting the crystal structure of the salt into an amorphous compound, thereby enabling comparisons to be made to the amorphous unionised form.

3.9.2 Sulfadimidine sodium spray dried from pure water and ethanol:water mixtures

The DSC thermogram (Figure 3.13) of crystalline SDNa starting material showed an endothermic event with onset at 309°C attributed to the melting of the drug. An additional endothermic event took place below 100°C due to the removal of residual solvent of a hydrated structure. This endotherm will be discussed in the section dedicated to dynamic vapour sorption analysis. The corresponding TGA thermogram presented mass loss of ~1% (w/w) from 25-100°C.

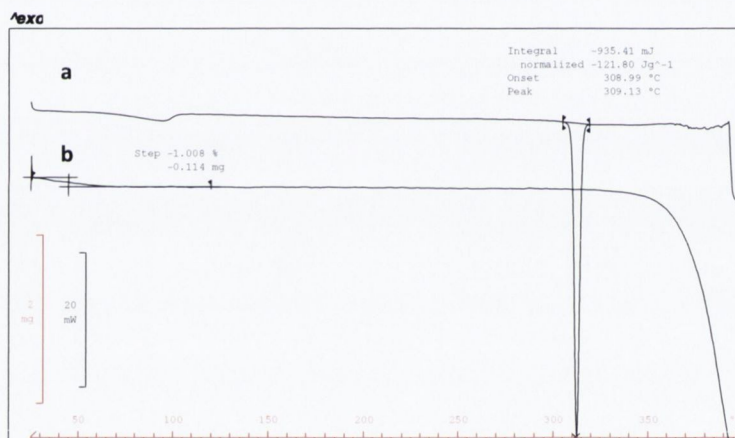


Figure 3.13: a) DSC & b) TGA thermograms of SDNa starting material.

3.9.3 SDNa spray dried from water

No information about spray drying of SDNa has been reported to date. Initially, for comparison purposes with the spray dried SD, the sodium salt form was processed from water starting with an inlet temperature of 120°C. No dry powder collection was possible at this particular inlet temperature as the material was sticky wet and adhered to the wall of the spray dryer. This outcome was in contrast to that previously observed for SD, which, at this

inlet temperature, was easily processed and resulted in the production of amorphous powders. A ten degree increase from 120 to 130°C for the inlet temperature when spray drying the salt form was sufficient to allow the recovery of a powder suitable for analysis. The salt solution was then spray dried at 140°C and finally at 160°C. The salt solution spray dried from water resulted in highly hygroscopic powders which converted to sticky materials soon after collection. Repeated experiments were performed and powders were immediately stored in humidity controlled chambers at low RH values (desiccated conditions). Physical characterisation was carried out with particular attention focused on minimising exposure of processed powders to environmental conditions prior to analysis. A broad endotherm was recorded on the DSC thermograms of the spray dried materials (Figure 3.14).

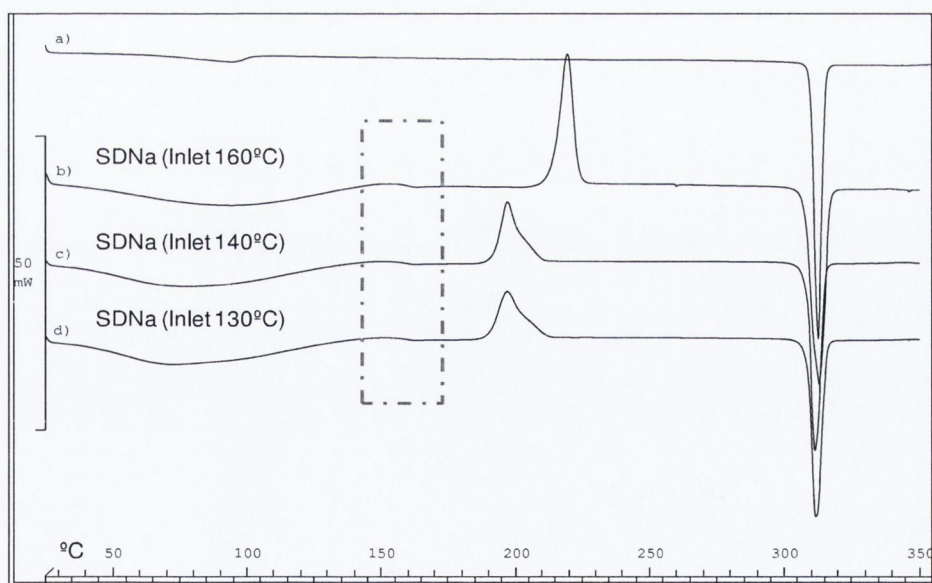


Figure 3.14 DSC curves of a) unprocessed SD Na; b) SD Na spray dried from water (inlet 160°C); c) SD Na spray dried from water (inlet 140°C); d) SD Na spray dried from water (inlet 130°C). Tg region highlighted.

Corresponding TGA analysis displayed mass loss between 5 and 7% (w/w). Regardless of the inlet drying temperature, thermal analysis by DSC of spray dried SDNa revealed a baseline deflection ranging between 155°C and 157°C, attributed to the glass transition temperature (T_g) of amorphous SDNa. This represents a significant increase in degrees centigrade compared to the T_g of SD detected at ~ 80 °C. An increase in the T_g value for a salt form compared to its unionised base was previously reported by Tong and Zografí (1999) for sodium indomethacin. The T_g for amorphous sodium indomethacin produced either via freeze drying, grinding or rota evaporation was 75°C higher than amorphous indomethacin. This temperature increase was attributed by the authors to strong ionic interaction between the sodium and indomethacin ions (Tong and Zografí, 1999). In contrast to the relatively constant T_g values, variability in crystallisation behaviour characterised SDNa spray dried from pure water using different inlet temperatures over the range of 130°C to 160°C. The highest onset of crystallisation (~210°C) was observed for the sample spray dried at the higher inlet temperature. This represented a 20 degree upward shift compared to SDNa spray dried at inlets of 130°C and 140°C, which crystallised at ~ 190°C. Finally all systems melted in the range of temperature between 305 and 308°C (Figure 3.14).

Chapter 3 Amorphisation of sulfadimidine and sulfadimidine sodium upon spray drying

Figures 3.15 and 3.16 show SE micrographs for unprocessed and spray dried SDNa from water respectively.

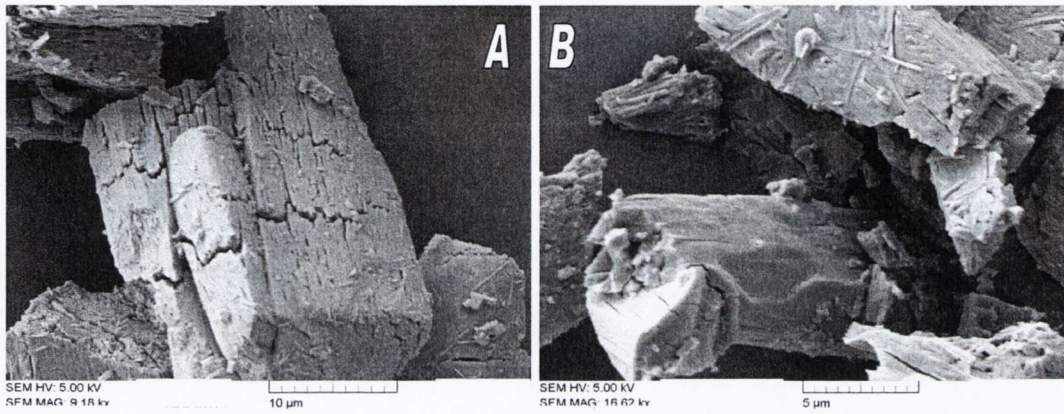


Figure 3.15 SE micrographs of unprocessed SDNa at different magnifications. (note different scale bars)

Changes in the particle morphology characterised the spray dried particles which were spherical, crumpled and with a smooth surface. The particles of the system spray dried at a lower inlet of 130°C was characterised by signs of fragmentation and collapse (Figure 3.16A). This morphology was different from that seen for SD spray dried from water described in section 3.7.

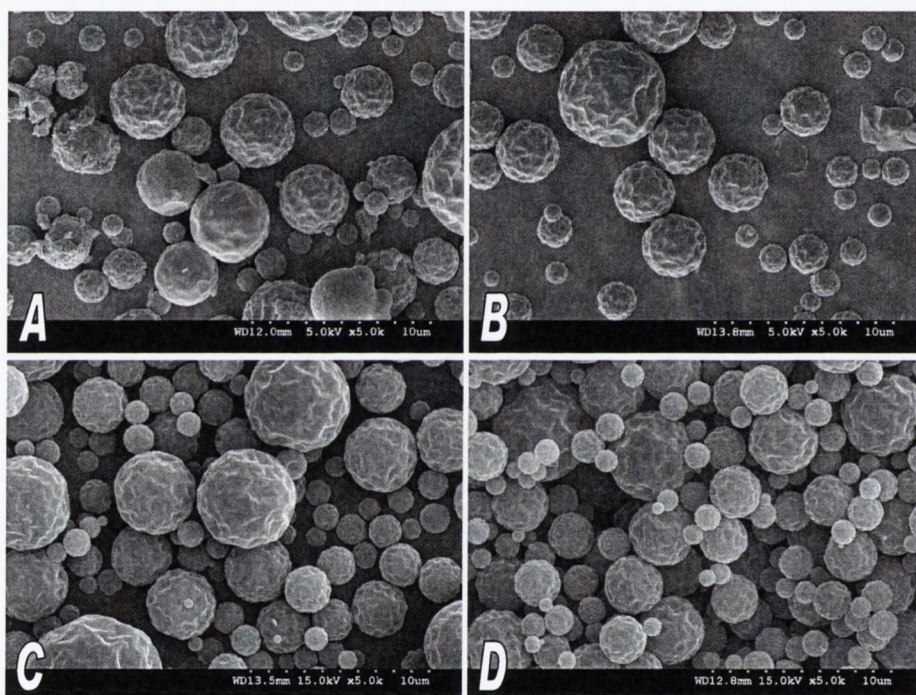


Figure 3.16 SE micrographs of SDNa spray dried from water at inlet temperature of: a) 130°C; b) 140°C; c) 160°C; d) 160°C and after 4 week storage under desiccated conditions at 5°C.

3.9.4 Sulfadimidine sodium spray dried from ethanol:water co-solvent systems.

In order to compare the behaviour of the salt form to sulfadimidine upon spray drying, an inlet temperature (78°C) and concentration (0.5% w/v) consistent with that employed previously for the non ionised form was used. The salt was spray dried from ethanol:water

solutions with ethanol content varying between 60-90% v/v. As indicated by the study of Delgado *et al.* the feed concentration used was below the maximum solubility of the salt in all four co-solvent systems (Delgado *et al.*, 2011). Systems spray dried from ethanolic solutions, at all compositions, did not show Bragg peaks on the PXRD patterns but diffuse halo patterns (Figure 3.17).

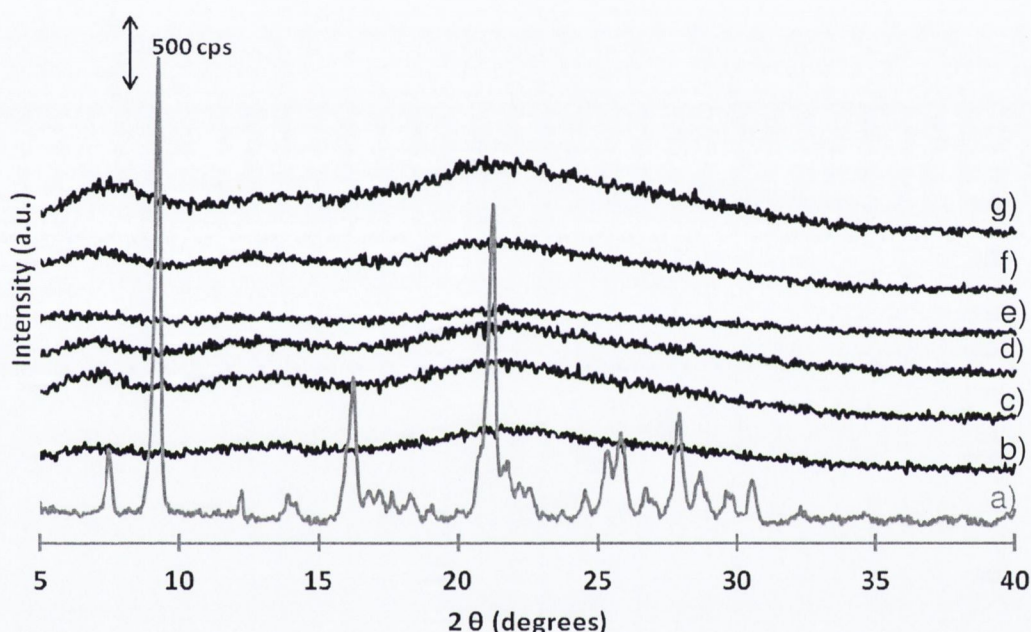


Figure 3.17 PXRD patterns of a) unprocessed SDNa; b) SDNa spray dried from ethanol:water 9:1 v/v; c) SDNa spray dried from ethanol:water 7:3 v/v; d) SDNa spray dried from ethanol:water 6:4 v/v; e) SDNa spray dried from water (Inlet 130°C); f) SDNa spray dried from water (Inlet 140°C); g) SDNa spray dried from water (Inlet 160°C).

DSC thermograms for the various systems were characterised by a broad endothermic event between 25 and 140°C. This event was due to the dehydration of the amorphous powder upon heating. Powders in fact were not completely dry as mass losses between ~7 and 9% were detected by TGA analysis when heated from 25 – 100°C. This contrasted to the 1% mass loss detected for the unprocessed material. A deflection of the baseline at ~154°C,

attributed to the glass transition of the salt was detected for all systems. At temperatures above the T_g of SDNa, all DSC thermograms of the processed powders presented an exotherm of crystallisation in the temperature range between 180-220°C (Figure 3.18). The onset temperature of the exotherm was comparable to SDNa spray dried from water at inlets of 130 and 140°C.

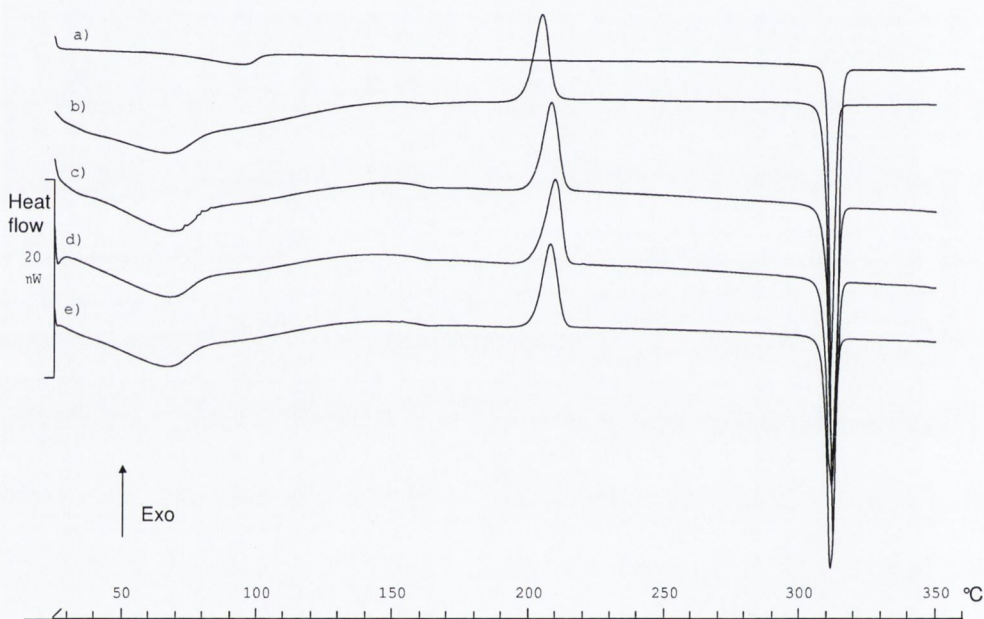


Figure 3.18 DSC curves of a) unprocessed SDNa; b) SDNa spray dried from ethanol:water 9:1 v/v c) SDNa spray dried from ethanol:water 8:2 v/v d) SD spray dried from ethanol:water 7:3 v/v e) SDNa spray dried from ethanol:water 6:4 v/v.

As previously reported for SDNa processed from water, spray dried samples were highly hygroscopic and tended to uptake moisture from the environment converting to sticky materials. SEM micrographs showed that minimal exposure of the sample to environmental conditions resulted in spherical particle with little degree of aggregation (Figure 3.19 A-B), while a more prolonged exposure resulted in agglomerated fused masses (Figure 3.19 C-D). The main application of the spray drying process is to achieve a suitable particle size

Chapter 3 Amorphisation of sulfadimidine and sulfadimidine sodium upon spray drying

(Vehring, 2008) and remove most of the solvent because water or other solvents retained in pharmaceutical formulation are known to be the cause of increased physical and chemical instability (Hancock and Shamblin, 1998).

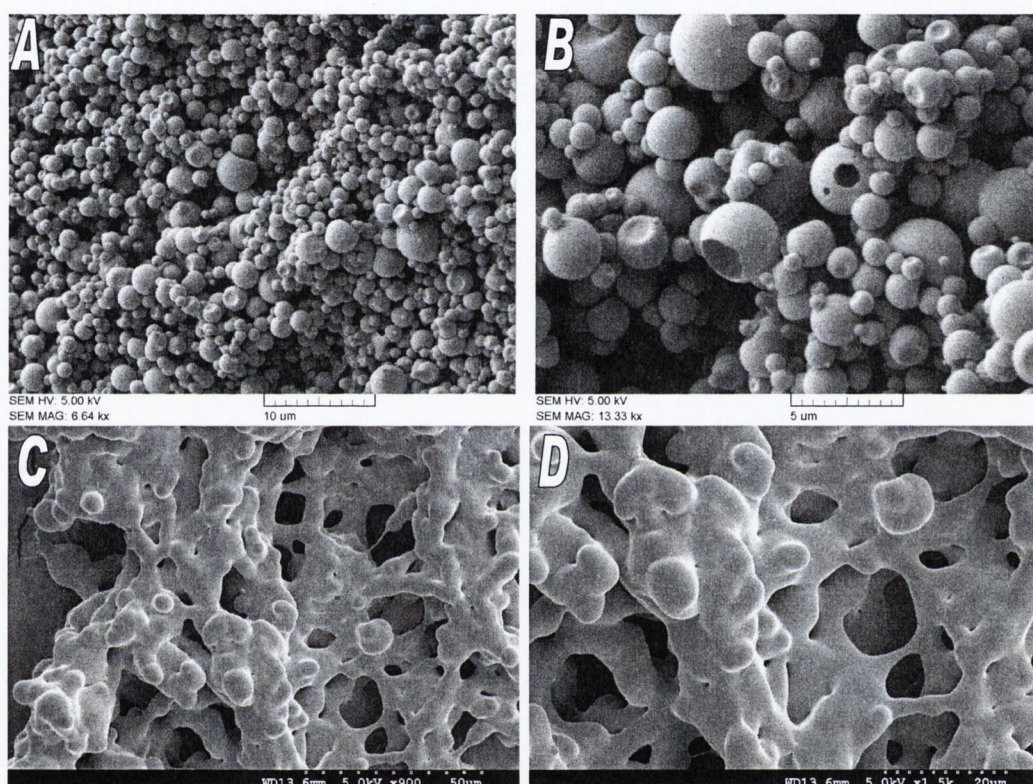


Figure 3.19 SE micrograph of SDNa spray dried from ethanol:water 9:1 v/v A-B) after storage in dry conditions; C-D) after exposure to environmental conditions of RH for 30 minutes. (note different scale bars)

It is well recognised and accepted that amorphous materials have a greater affinity for moisture, relative to their crystalline counterparts. Nevertheless, it was also anticipated that the nature of the solvent employed in the spray drying process might affect some properties, as a change in the morphology may influence the moisture sorption capabilities of the processed powders with associated implications for physical stability. SDNa was thus spray dried from a different solvent water/acetone combination and the resultant powders were investigated under a range of storage conditions.

3.9.5 SDNa spray dried from acetic solutions

The use of acetone:water co-solvent systems for spray drying unionised SD resulted in the production of partially crystalline materials. This was believed to be due to the high affinity of the organic solvent to the API which could plasticise the drug. However it was hypothesised that, as a consequence of the lower boiling point (58°C) and higher evaporation rate of acetone, compared to ethanol, spray drying the salt from acetic solutions might result in the production of distinct particles in contrast to the fused agglomerates seen for the API spray dried from the ethanolic systems. The salt was therefore spray dried from four different acetone:water co-solvent systems with the spray dryer operating in the closed cycle configuration, as previously carried out to process SD. PXRD analysis indicated that the spray dried samples converted to an amorphous phase (Figure 3.20).

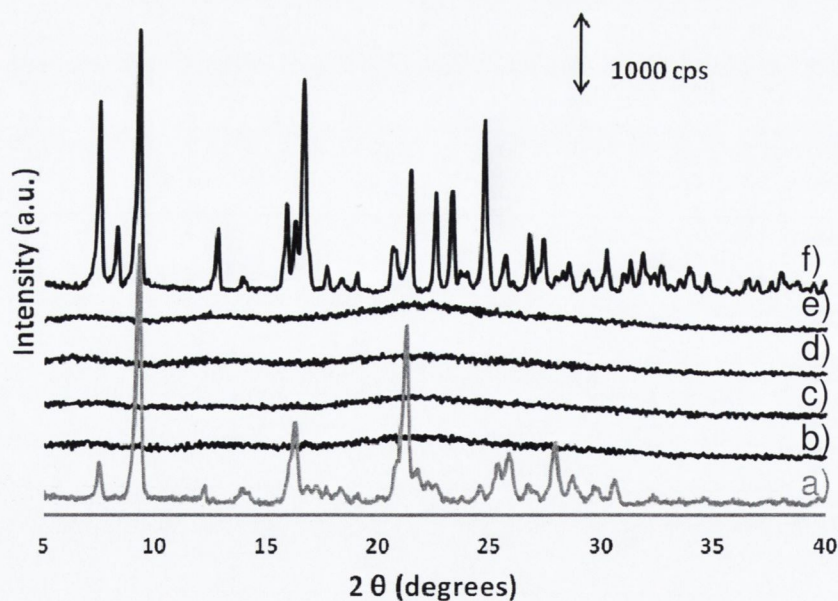


Figure 3.20 PXRD patterns of a) unprocessed SDNa; b) SDNa spray dried from acetone:water 6:4 v/v; c) SDNa spray dried from acetone:water 7:3 v/v; d) SDNa spray dried from acetone:water 8:2 v/v; e) SDNa spray dried from acetone:water 9:1 v/v; f) SDNa spray dried from acetone:water 9:1 v/v after storage at ambient conditions for 1hr.

The detection of Tgs ranging between 144-149°C and the presence of an exothermic peak of crystallisation on each thermogram confirmed that the salt subjected to the spray drying process was converted into an amorphous phase (Figure 3.21). However Tg values were lower compared to the systems spray dried from the corresponding ethanolic solution (detected at ~154°C).

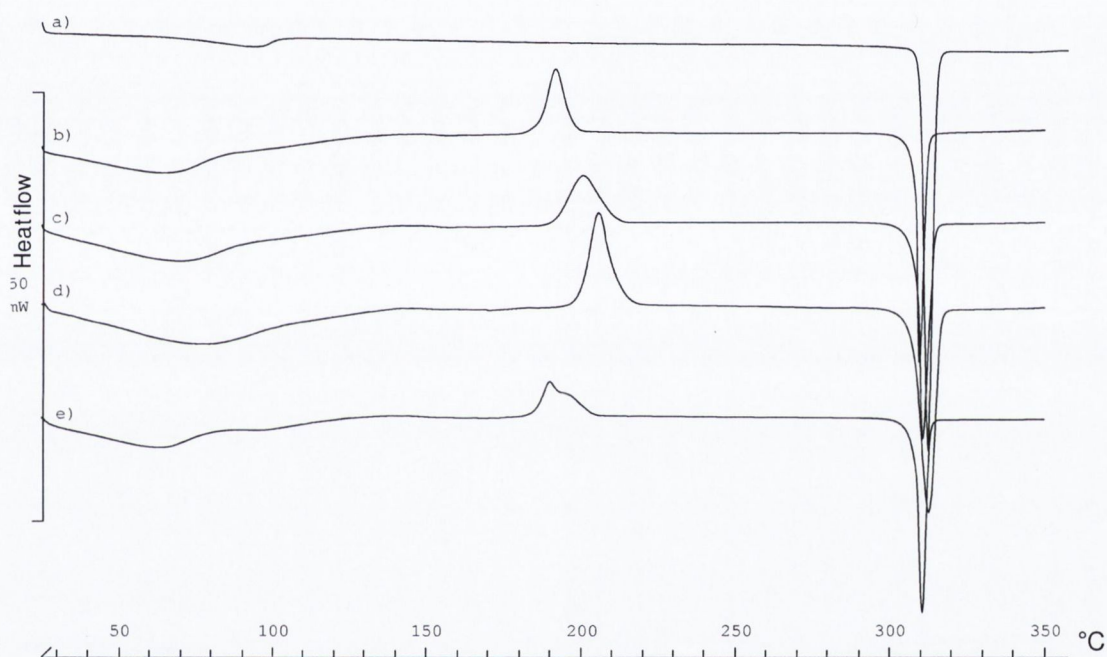


Figure 3.21 DSC thermograms of a) unprocessed SD Na; b) SDNa spray dried from acetone:water 9:1 v/v, c) SDNa spray dried from acetone:water 8:2 v/v d) SDNa spray dried from acetone:water 7:3 v/v e) SDNa spray dried from acetone:water 6:4 v/v

3.9.6 SEM analysis

The samples were analysed by SEM (Figure 3.22). Spherical particles obtained from the system acetone:water 6:4 v/v were fused together, while discreet particles with smooth surface were obtained from solutions with higher acetone content. This type of surface was

similar to that obtained by spray drying SDNa from ethanol and differed from the drug spray dried from water (Figure 3.16). As previously reported for the salt spray dried from water and ethanolic solutions, the spray dried drug samples were highly hygroscopic in nature and were therefore stored in controlled humidity chambers at ~0% RH.

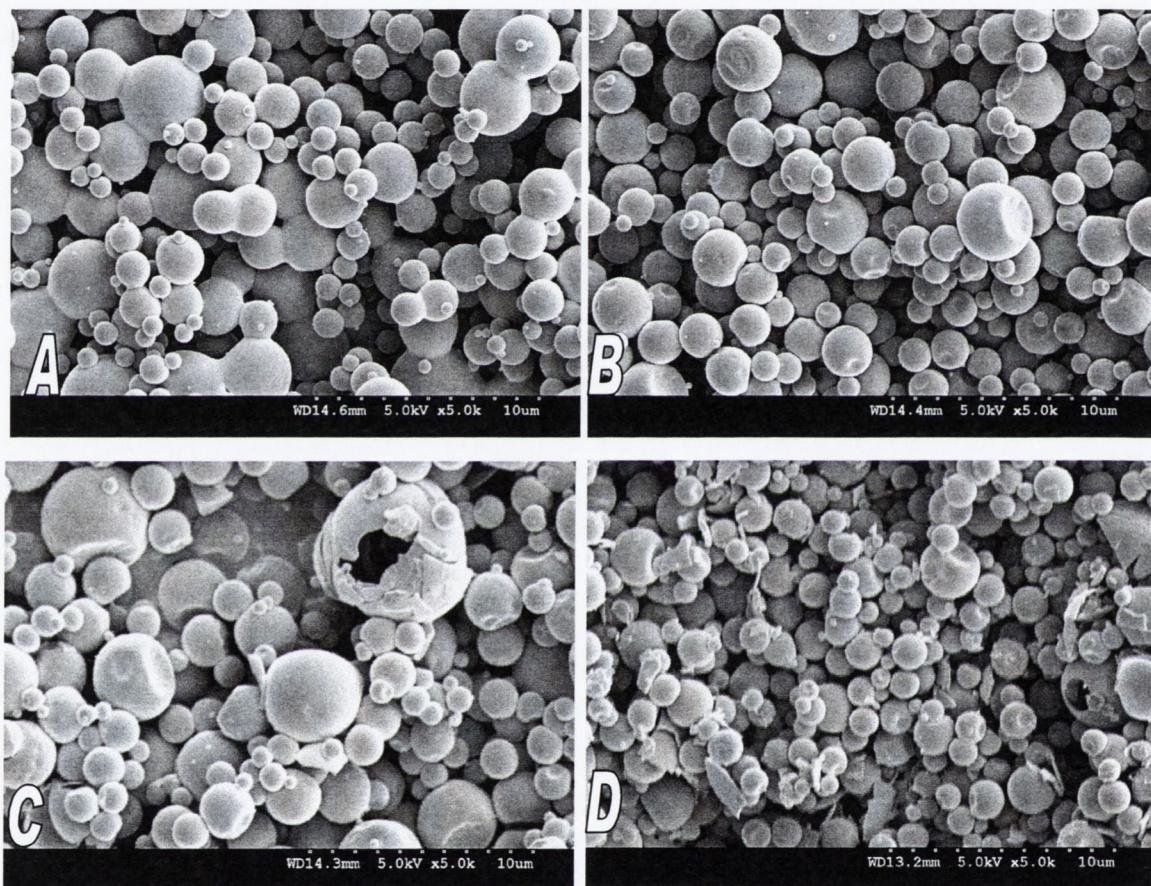


Figure 3.22 SEM micrographs of SDNa spray dried from a) acetone:water 6:4 v/v; b) acetone:water 7:3 v/v; c) acetone:water 8:2 v/v; d) acetone:water 9:1 v/v.

3.10 FTIR analysis of amorphous SDNa

Spray dried materials from all solvent systems were analysed by FTIR spectroscopy. Superimposable spectra characterised the amorphous materials except for the presence of an extra peak at $\sim 1700\text{ cm}^{-1}$ detected for the systems spray dried from acetonic solutions. This peak is due to the presence of residual acetone (Figure 3.23), as previously reported for the non ionised form and might explain the shift of the T_g to lower temperatures compared to the drug processed from water and ethanolic solutions at all compositions. Amorphous spectra were different to the spectrum of the crystalline unprocessed material because of the broadening of bands which was attributed to the disorder of the molecules in the amorphous state.

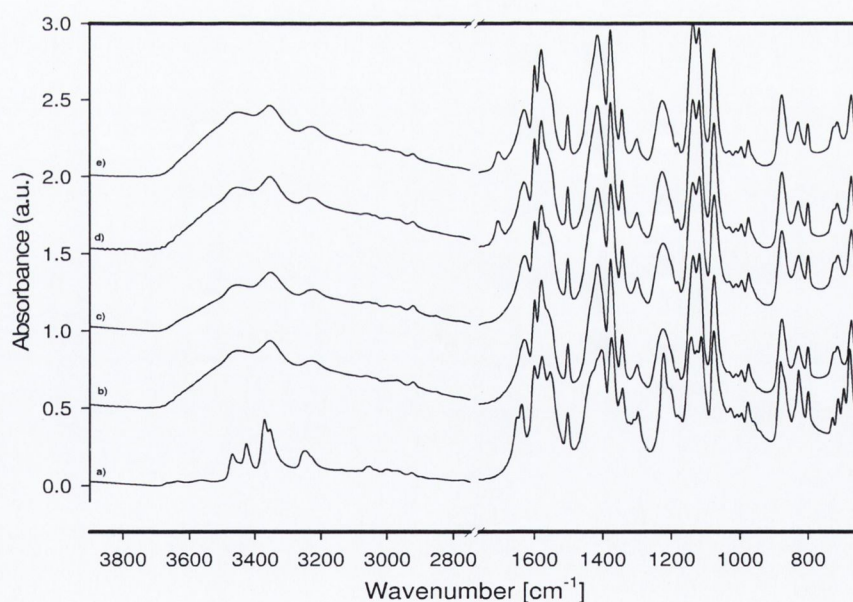


Figure 3.23 FTIR spectra of a) sulfadimidine sodium unprocessed material; b) spray dried SDNa from water; c) spray dried sulfadimidine from ethanol:water 9:1 v/v inlet 78°C ; d) spray dried sulfadimidine from acetone:water 9:1 v/v e) spray dried sulfadimidine from acetone:water 7:3 v/v.

3.11 DVS analysis

As previously reported, the exposure of the amorphous spray dried salt to environmental humidity conditions caused changes in the visual appearance and to the physical properties of the powders. The amorphous drug changed from a powder to a transient viscous mass and finally converted into a solid bulky structure. The state of hydration of a material may influence several physicochemical properties including physical and chemical stability (Airaksinen et al., 2005; Forbes, 1998). For example for many pharmaceutical materials, phase transitions can be influenced by the amount of water vapour surrounding the sample. Some crystalline sodium salts are known to be hygroscopic materials (Lee, 2002) and the possibility to investigate the impact of water vapour on a processed salt which might also be characterised by a certain degree of disorder subsequent to the spray drying process could provide fundamental guidelines on the storage conditions. Unprocessed and processed SDNa from ethanol:water 9:1 v:v were exposed to the following % of relative humidity profile: 0 to 90% in 10% steps and then the humidity was decreased in a similar fashion for the desorption phase. The moisture sorption-desorption isotherm (1st and 2nd cycle) for the crystalline raw original SDNa sample over the 0 to 90% RH range is displayed in Figure 3.24. The isotherm shows a wide hysteresis gap over the full RH range analysed. This is indicative of hydrate formation, where the sample desorbs the water molecules at a lower RH than it uptakes them (Hiatt et al., 2011). The continuous lines represent the sorption phases, while the dotted lines correspond to the de-sorption cycle. At 60% RH the sample sorbs approximately 6% of its dry weight in mass. For SDNa whose MW is 300.31 g/mol this mass increase would correspond to a stoichiometry of 1 molecule of water, associated with the formation of a monohydrate. This mass gain remained constant up to 80% RH. With a further increase in

RH to 90% the mass increase doubled to 12% of its dry weight corresponding to the formation of a dihydrate form.

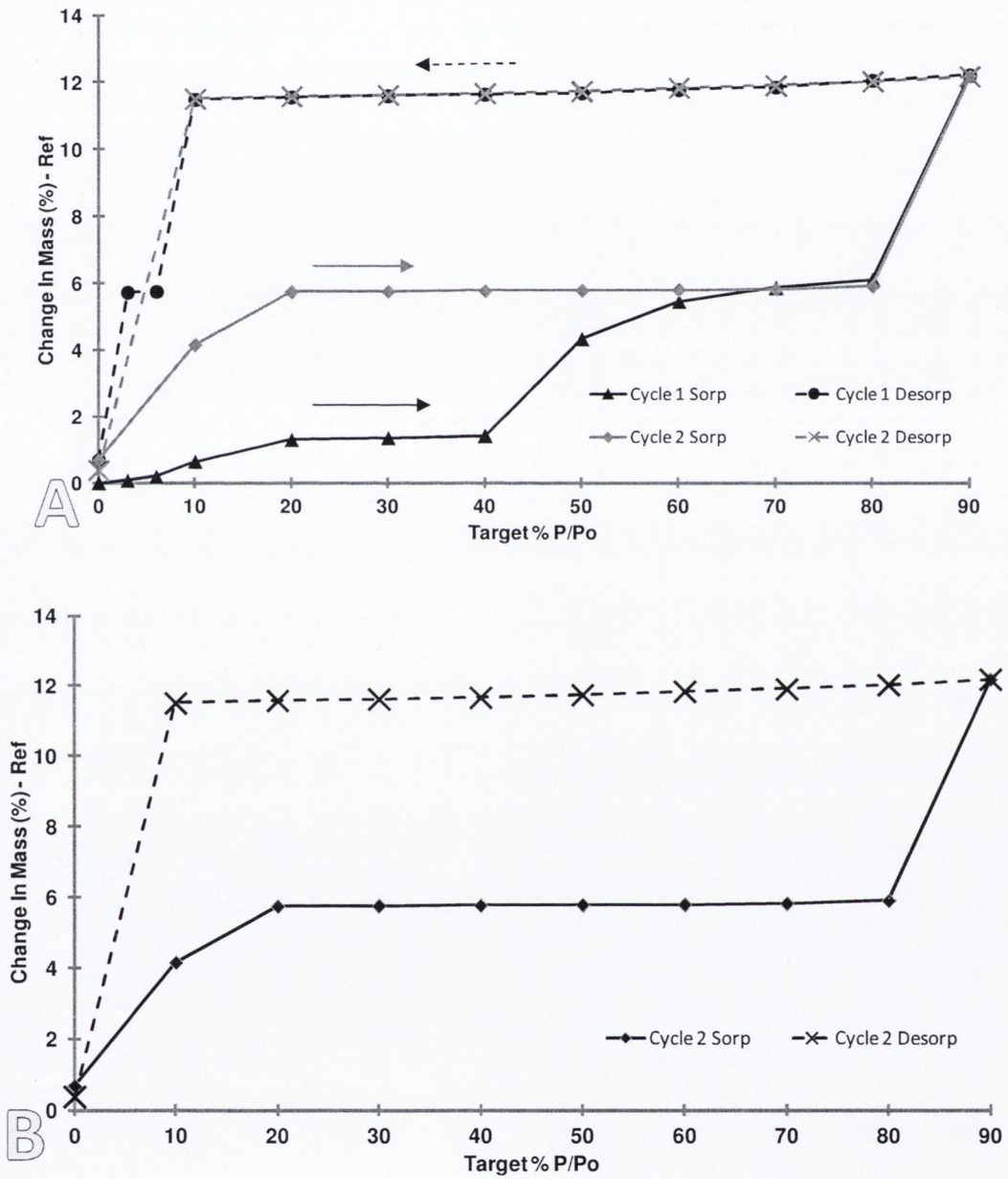


Figure 3.24 DVS sorption-desorption-isotherm of SDNa starting material A) 1st and 2nd cycle; B) 2nd cycle

During the desorption cycle there is little mass change as the humidity decreases to 10% RH, with the sample still retaining approximately 11.5% of its dry mass. During the final desorption step (10 to 0% RH), the sample loses all sorbed water and the mass returns to approximately the original value.

In contrast, in the 2nd sorption cycle (Figure 3.24 B) the salt converts into a monohydrate when the RH is increased to 20%. Differences in the water uptake capabilities between the first and second sorption cycle are hypothesised to be due to differences in the surface area of the salt before and after undergoing a first full DVS cycle. The amorphous form of SDNa (spray dried from ethanol:water 9:1 v/v) was subjected to the same humidity profile by DVS in order to investigate its behaviour and physical stability on exposure to changes in relative humidity. The moisture sorption kinetics for amorphous SDNa over the 0-90-0-90-0% RH range are displayed in Figure 3.25. The black continuous line traces the percentage change in mass (based on the dry value) as a function of time, while the grey dotted line traces the relative humidity as a function of time. The corresponding isotherms (2 sorption-desorption cycles) are shown in Figure 3.26, where the continuous lines represent the first and second cycle sorption while the dotted lines represent the corresponding first cycle and second cycle desorption phases respectively.

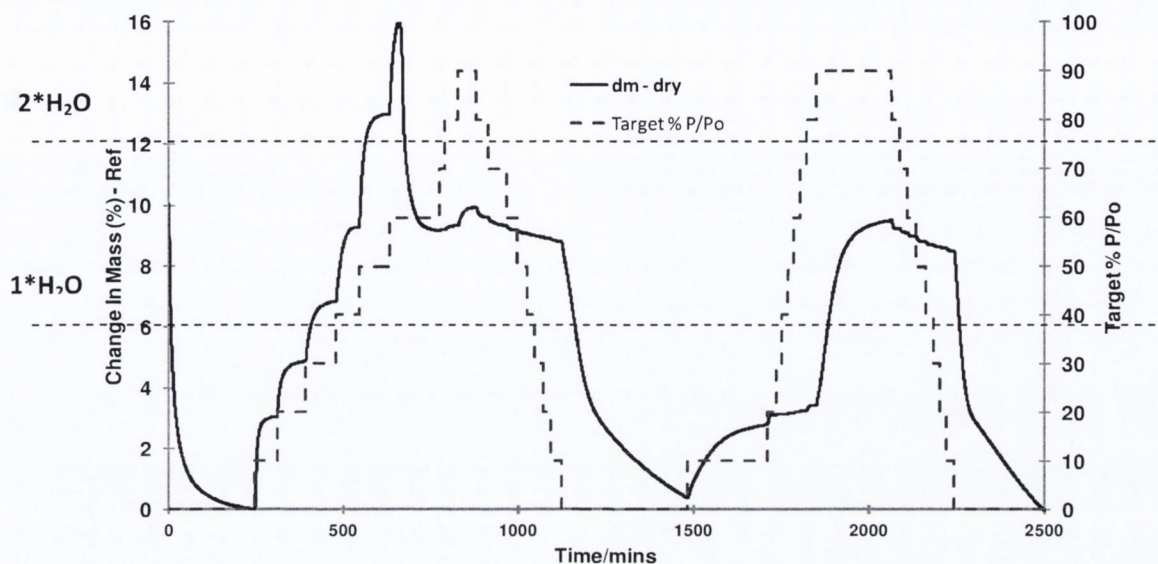


Figure 3.25 DVS sorption-desorption kinetics of amorphous SDNa

As the humidity is increased up to 50% RH, the sample uptakes significant amounts of water vapour and the weight approaches equilibrium at each step. In contrast, during the 60% RH step, the sample mass initially increases, but then steadily decreases before the mass finally reaches equilibrium. This phenomenon where there is a short, initial increase followed by a sharp decrease in mass is typical for a water-induced crystallisation event. Similar behaviour has been observed for amorphous lactose and salbutamol sulphate (Burnett et al., 2006; Grisedale et al., 2011). Absorbed water is a plasticising agent that lowers the glass transition of the compound thus inducing crystallisation. At higher RH values from 70 to 90 % almost no change in mass was recorded by the sample. During the desorption phase, a 1% decrease in mass from 90% to 10% RH was recorded which was probably due to slow surface desorption from the new crystalline material. During the 0% desorption step the sample mass returned to the initial dry value.

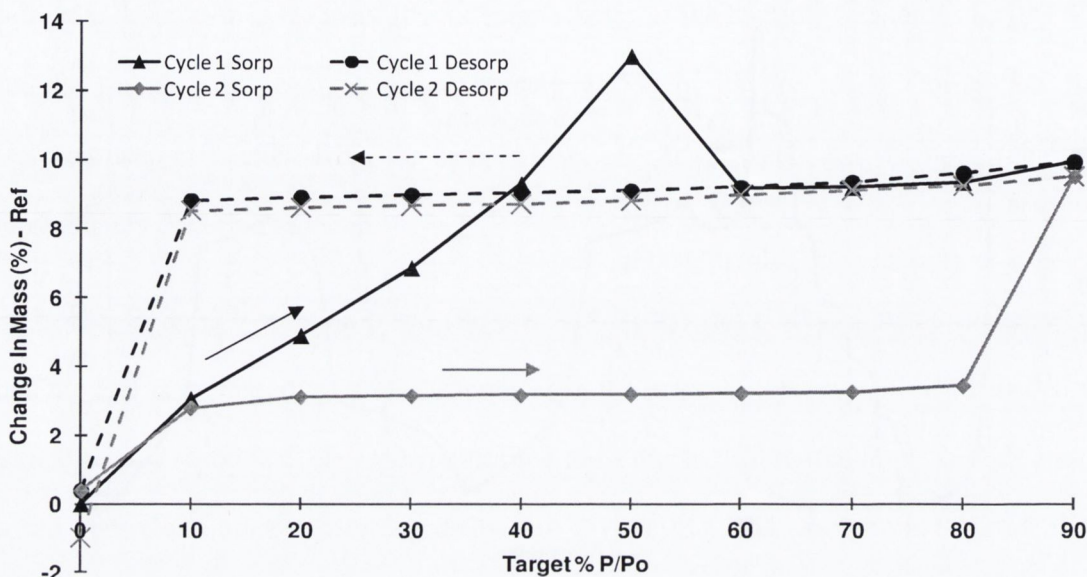


Figure 3.26 DVS sorption-desorption isotherms of amorphous SDNa

The second sorption-desorption cycle resembled the DVS behaviour of the unprocessed salt material except for the mass uptake % which was constantly 3% lower than that recorded by the unprocessed material. After DVS treatment, the PXRD patterns of both the processed salt samples and of unprocessed SDNa were identical. These patterns resembled the pattern of the original material (i.e. not subjected to DVS analysis), indicating that regardless of the initial physical state a full DVS cycle converted the drug into the original anhydrous crystal structure.

PXRD, DSC and TGA analyses were performed after equilibrating the materials in the DVS at different stages of RH. For example the PXRD patterns of unprocessed and spray dried SDNa from water (Figure 3.27b) or ethanol:water solutions, equilibrated at 90% RH, were identical. These patterns differed from the pattern of the original material (i.e. not subjected to DVS analysis), by the presence of extra peaks at the following 2θ values: 8.3, 12.8, 15.9, 16.7, 19.1, 23.3, indicating a change in the crystal structure (Figure 3.27b).

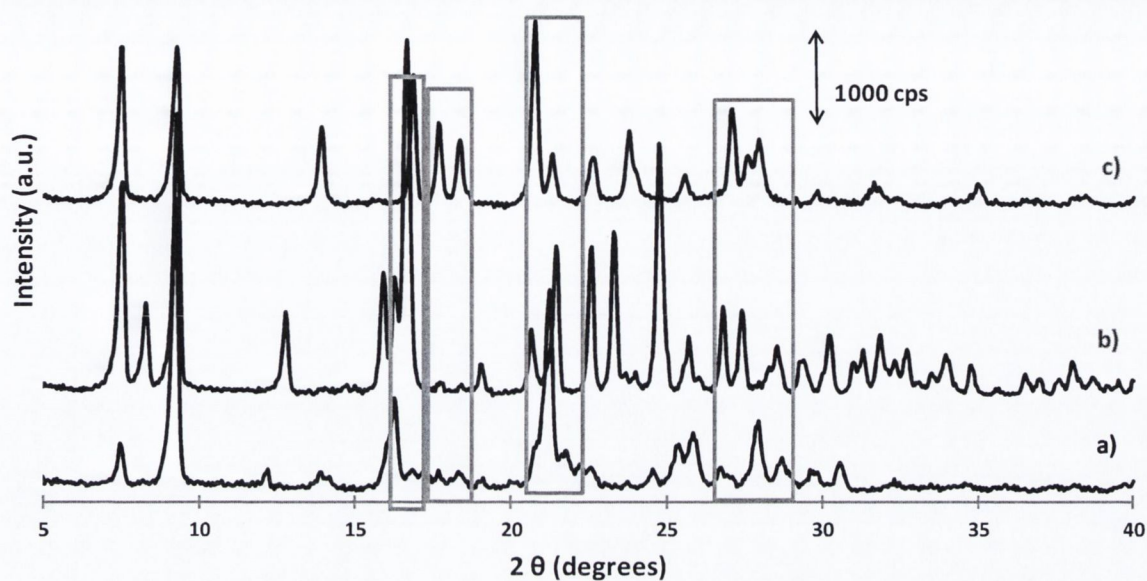


Figure 3.27 PXRD patterns of a) unprocessed SDNa; b) spray dried SDNa from ethanol:water 9:1v/v after equilibration at 90% RH in DVS cabinet; c) spray dried SDNa from water after equilibration at 50% RH (2nd sorption cycle) in DVS cabinet. Differences in characteristic peak positions highlighted.

An $11.4 \pm 0.0\%$ thermogravimetric mass loss between 25 and 140°C confirmed the stoichiometry of the spray dried material after DVS treatment (equilibration at 90% RH) to be a dihydrate (Figure 3.28a). The corresponding DSC thermogram (Figure 3.28b) showed a double endothermic peak of dehydration in the same temperature range of the mass loss recorded on the TGA thermogram, the material consequently reconverted into its anhydrous form and finally melted at 308°C consistent with the melting point of unprocessed SDNa. The shortfall in the mass gain percentage in the processed systems of $\sim 3\%$, compared to the final mass gain percentage of the original material subjected to DVS can be attributed to solvent retained in the amorphous form at the beginning of the experiment. This solvent does not separate from the powder during the pretreatment phase (drying at 0% RH in the DVS under N₂ flow). A single endotherm of dehydration (Figure 3.28d) characterised the

monohydrate obtained by subjecting both processed and unprocessed SDNa to a full DVS sorption-desorption cycle and then equilibrating the samples at 60% RH in the DVS cabinet. The corresponding TGA analysis recorded mass loss of $6.3 \pm 0.0\%$ consistent with a water content of 1 mole.

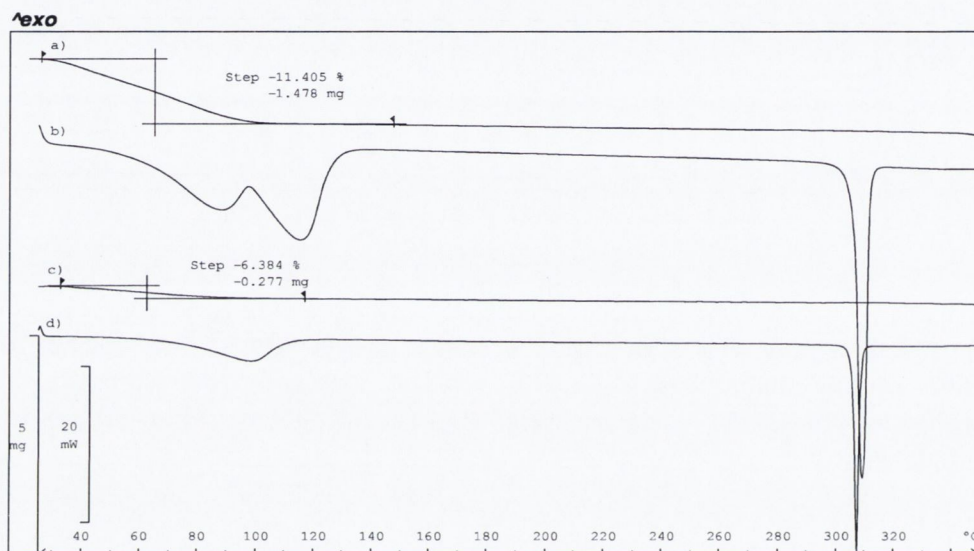


Figure 3.28 (a): TGA and (b): DSC thermograms of spray dried SDNA in OCM from ethanol:water 9:1 v/v after DVS analysis (equilibration at 90% RH); (c) TGA and (d) DSC thermograms of spray dried SDNA in OCM from ethanol:water 9:1 v/v after DVS analysis (equilibration at 60% RH after a full DVS sorption-desorption cycle)

3.12 Stability studies of spray dried SDNa at 4 and 25°C, under desiccated conditions / 60% RH / 70% RH

The physical stability of spray dried SDNa from all solvent composition upon storage at 4°C under desiccated conditions was monitored over a 3 year period. As indicated by PXRD analysis (data not shown), the amorphous drug did not crystallise when stored in these conditions. A similar outcome was found when the amorphous samples of the drug were

Chapter 3 Amorphisation of sulfadimidine and sulfadimidine sodium upon spray drying

stored at room temperature ($\sim 25^{\circ}\text{C}$) in humidity chambers at $<5\%$ RH. However it should be noted that these stability studies were performed over a shorter period of 4 months. In contrast, the exposure of the amorphous salt to higher humidity conditions caused changes in the visual appearance and on the physical properties of the powders. Regardless of the solvent used to spray dry SDNa, the amorphous drug stored at RH values of 60 and or 75% after 2 hrs crystallised into a crystal structure which was different from the original material. By comparing PXRD patterns it was found that these were identical to the pattern of the dihydrate obtained by subjecting the original and spray dried materials to DVS analysis (Figure 3.29).

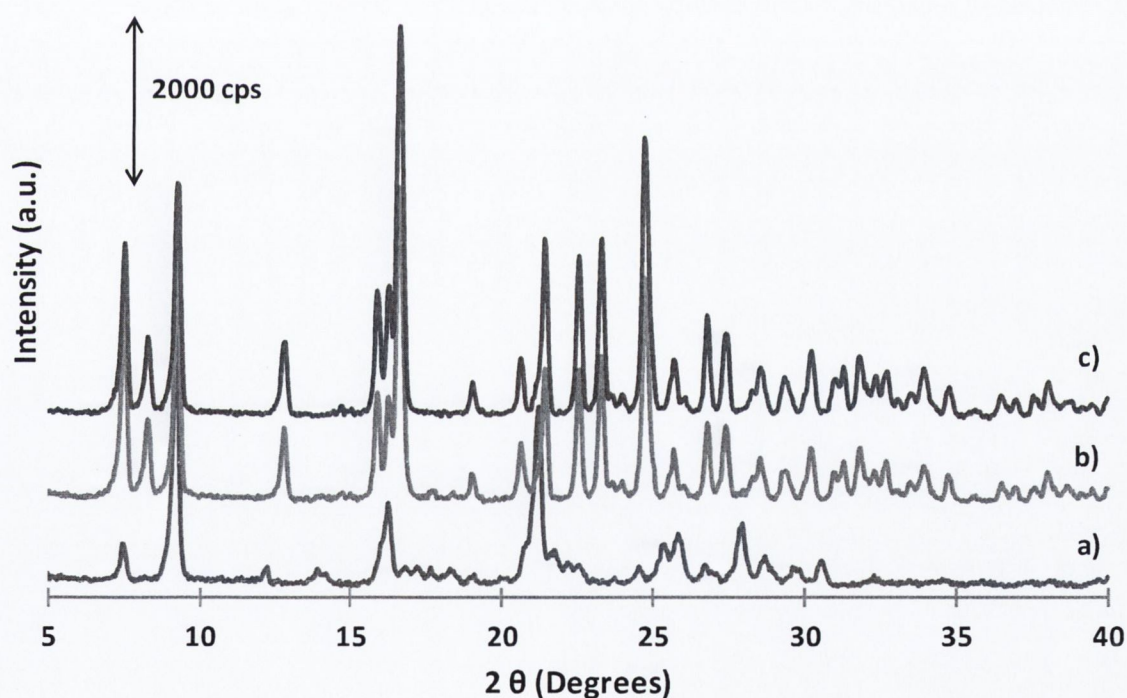


Figure 3.29 PXRD patterns of a) unprocessed SDNa; b) spray dried SDNa from ethanol:water 9:1v/v after equilibration at 90% RH in DVS cabinet; c) spray dried SDNa from ethanol:water 9:1 v/v after storage at 60% RH in humidity controlled devices.

3.13 Key findings on sulfadimidine sodium

The key results related to the impact of spray drying on SDNa presented in this section of Chapter 3 can be summed up as follows:

- The sodium salt of SD converted to an amorphous phase upon processing, regardless of the solvent employed and spray-dryer set up. It is characterised by a higher T_g (~155°C) with respect to the amorphous SD (~80°C).
- The higher T_g (~155°C) leads to an increased physical stability of the amorphous salt compared to amorphous SD but only in dry conditions.
- RH has a strong plasticising effect inducing phase transformation of the amorphous salt into a dihydrate when stored at RH above 60% in a time span of 2 hrs.

3.14 SD and SDNa co-spray dried systems

Processes involving solvent evaporation may lead to the transformation of crystalline substances into disorganised amorphous materials as described for SD and SDNa in the first part of this chapter. For amorphous solids, the temperature range in which properties of the material change from solid-like (glass) to liquid-like (super-cooled liquid) or vice versa is called the glass transition temperature (T_g) (Baird and Taylor, 2012). It is well recognised that below T_g , both chemical and physical stability is more pronounced compared to above T_g . Therefore basic strategies to stabilise the amorphous state require storage at temperature at least 50°C below the T_g (Hancock et al., 1995; Yu, 2001) and to reduce the exposure to water which can accelerate degradation, decrease the T_g and induce crystallisation (Airaksinen et al., 2005; Buckton and Darcy, 1995; Hancock and Shamblin, 1998). Another method to overcome stability issues is to produce drug-polymer amorphous solid dispersions (Caron et al., 2011; Qian et al., 2010; Tajber et al., 2005). These amorphous systems are usually characterised by improved physical stability generally related to the increase of the T_g which reduces the molecular mobility required for crystallisation at certain storage temperatures (Janssens and Van Den Mooter, 2009). However disadvantages such as the increase of hygroscopicity of the resulting systems or the increase in bulk volume of final dosage forms due to the poor miscibility of some drugs in the polymer can be limiting factors to the development of certain formulations (Löbmann et al., 2012). As an alternative approach to stabilise amorphous drugs, SD and SDNa were co spray-dried. The solid-state nature of SD-SDNa salt composite co-processed systems in comparison to each compound processed alone was then examined, to see if the composites (which are expected to become amorphous) might present a system of improved physical stability relative to each amorphous

API alone. In a study by Tong and Zografi, amorphous molecular dispersions of indomethacin and its sodium salt were produced by evaporation under reduced pressure. Interesting modified properties of the composites in comparison to each individual amorphous component were noted, such as an increased thermal stability (Tong and Zografi, 2001). The aim of this work was to try to improve the physical stability of the two APIs by synergistically exploiting, on one hand, the higher thermal stability of SDNa compared to SD, and on the other, the more hydrophobic character of the non ionised form compared to the salt.

3.15 Co-spray dried SD:SDNa

Four different composites were co-spray dried. The composites, indicated as SD 9:1, SD 3:1, SD 1:1 and SD 1:3 were produced by spray drying solutions of sulfadimidine and sulfadimidine sodium at weight ratios (w/w) of 9:1, 3:1, 1:1 and 1:3 w/w respectively. As expected SD-SDNa spray dried composites at all compositions presented a diffuse halo pattern, characteristic of XRD amorphous materials (Figure 3.30).

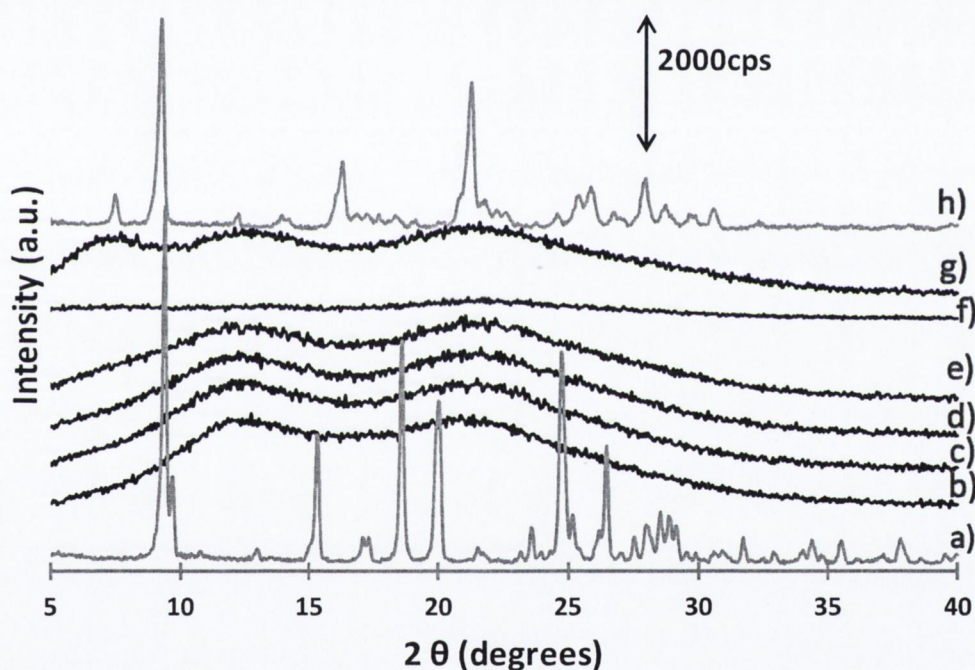


Figure 3.30 PXR D patterns of: (a) unprocessed SD; b) spray dried SD; c) spray dried SD 9:1; d) spray dried SD 3:1; e) spray dried SD 1:1; f) spray dried SD 1:3; g) spray dried SDNa; h) unprocessed SDNa.

Thermal analysis by DSC indicated that the increase in salt content resulted in a shift of the onsets of crystallisation of the amorphous materials towards higher temperature. The exothermic peaks of crystallisation ranged between those of the pure materials. Beyond

crystallisation a single melting endotherm was recorded for both SD 9:1 and SD 3:1. In contrast, the increase in salt content to systems SD 1:1 and SD 1:3 resulted in two endothermic events, the first of which ($\sim 200^{\circ}\text{C}$) is attributed to the melting of SD. These peaks were followed by broad endotherms with onset respectively at $\sim 240^{\circ}\text{C}$ and $\sim 260^{\circ}\text{C}$ for the thermograms of SD 1:1 and SD 1:3 (Figure 3.31).

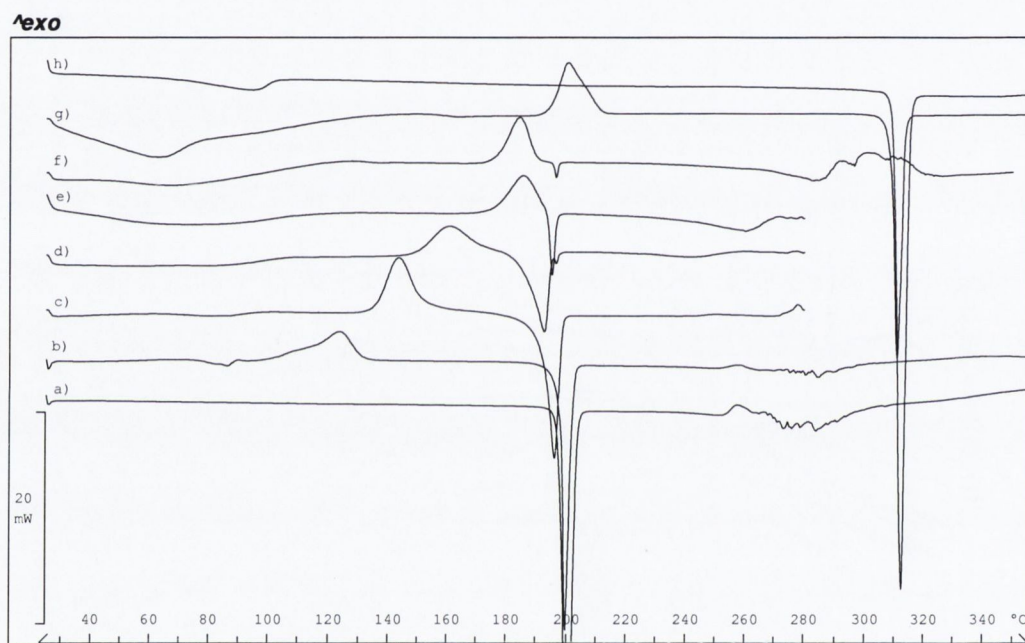


Figure 3.2 Heat flow thermograms of (a) unprocessed SD; b) spray dried SD; c) spray dried SD 9:1; d) spray dried SD 3:1; e) spray dried SD 1:1; f) spray dried SD 1:3; g) spray dried SDNa; h) unprocessed SDNa.

The glass transition temperatures (T_g) for pure SD and SDNa were previously detected by DSC analysis ($10^{\circ}\text{C}/\text{min}$) at $\sim 78^{\circ}\text{C}$ and at $\sim 154^{\circ}\text{C}$ respectively. To determine the T_g s of the various composites and differentiate between thermal events which could simultaneously happen upon heating, MTDSC was used in this work. All reversing heat flow thermograms recorded for the different spray dried systems showed a single T_g consistent with the production of homogeneous amorphous phases. The experimental T_g s were plotted together

with the T_g values calculated using the Gordon Taylor with Simha-Boyer rule (GT-SB) against the SDNa weight fraction (Figure 3.32). The GT-SB is an equation used by several authors for predicting the T_g of a two component mixed composite (Caron et al., 2011; Tajber et al., 2005). The true densities for the single amorphous components of 1.38 g/cm^3 and 1.45 g/cm^3 for SD and SDNa respectively, were used to obtain the K factor to calculate the GT-SB T_g theoretical values as described in Chapter 2, section 2.2.14. The co-spray dried systems were characterised by intermediate values of T_g which matched the predicted values and increased with the SDNa content. Therefore, having employed identical processing conditions, thermal analysis revealed that the salt had an antiplasticising effect in the mixtures by shifting the T_g s to higher temperatures.

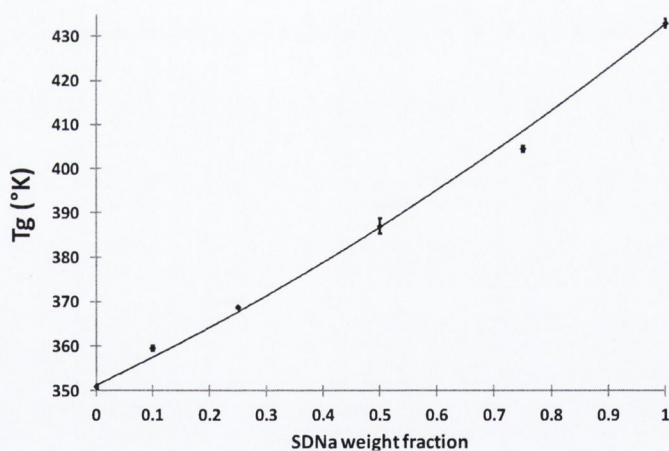


Figure 3.32 Glass transition temperatures of SD:SDNa systems as a function of SDNa content (squared markers). The solid line represents the T_g predictions based on the Gordon-Taylor with Simha-Boyer rule equation.

The T_g upward shift suggested the development of hydrogen bonding between the molecules although no significant shift in the peaks was detected by FTIR spectroscopy. The physical stability of the co-spray dried samples stored in desiccated conditions at 5°C was analysed over a period of 12 months. The co-spray dried systems remained amorphous as indicated by

PXRD analysis during the entire period. Therefore, it would appear that the introduction of ions into the systems developed interactions capable of increasing the T_g and protecting the amorphous material from crystallisation, as also indicated by the shift of onset of crystallisation to higher temperatures.

3.15.1 SEM analysis

No agglomeration was detected by SEM analysis for all composites. Distinct spherical particles characterised the samples with salt content at and above 25% w/w. In contrast inflated particles characterised the system SD 9:1 (Figure 3.33).

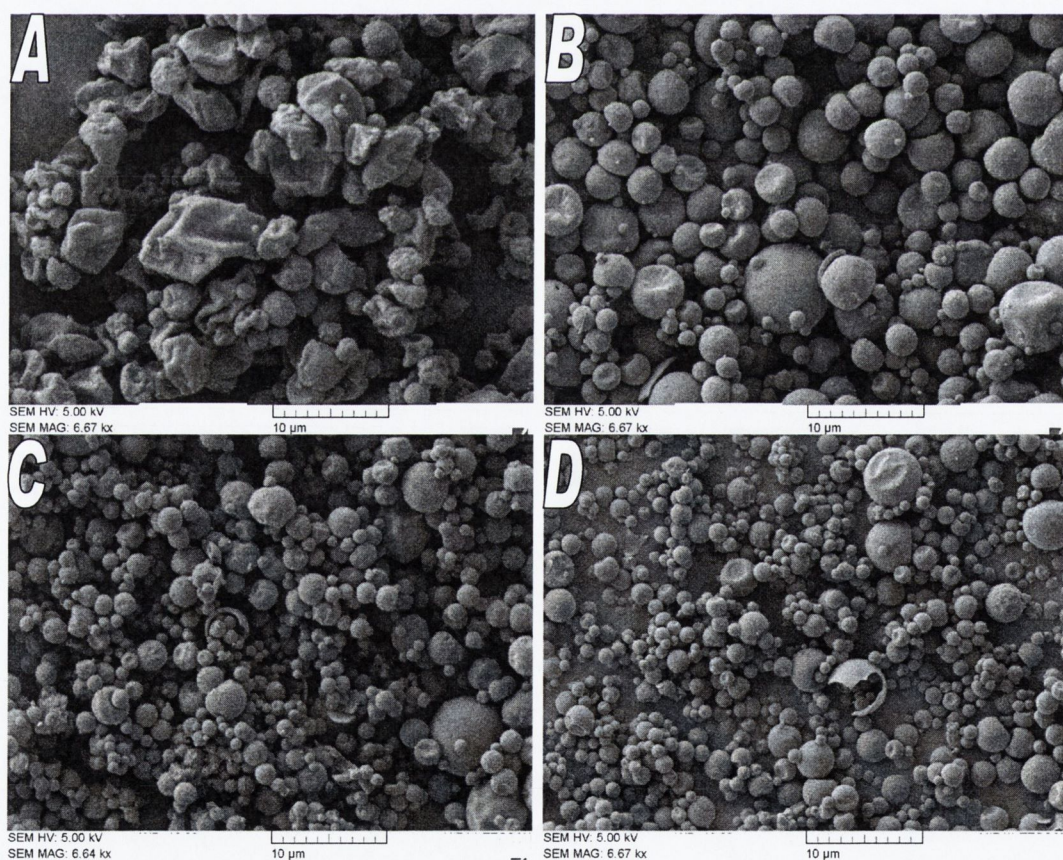


Figure 3.33 SEM micrographs of: a) spray dried SD 9:1; b) spray dried SD 3:1; c) spray dried SD1:1; d) spray dried SD 1:3.

3.15.2 DVS analysis

Accelerated stability studies by dynamic vapour sorption (DVS) were performed to investigate the crystallisation behaviour of two different composites (SD 3:1 and SD 1:1) when exposed to RH steps ranging between 0 and 90%.

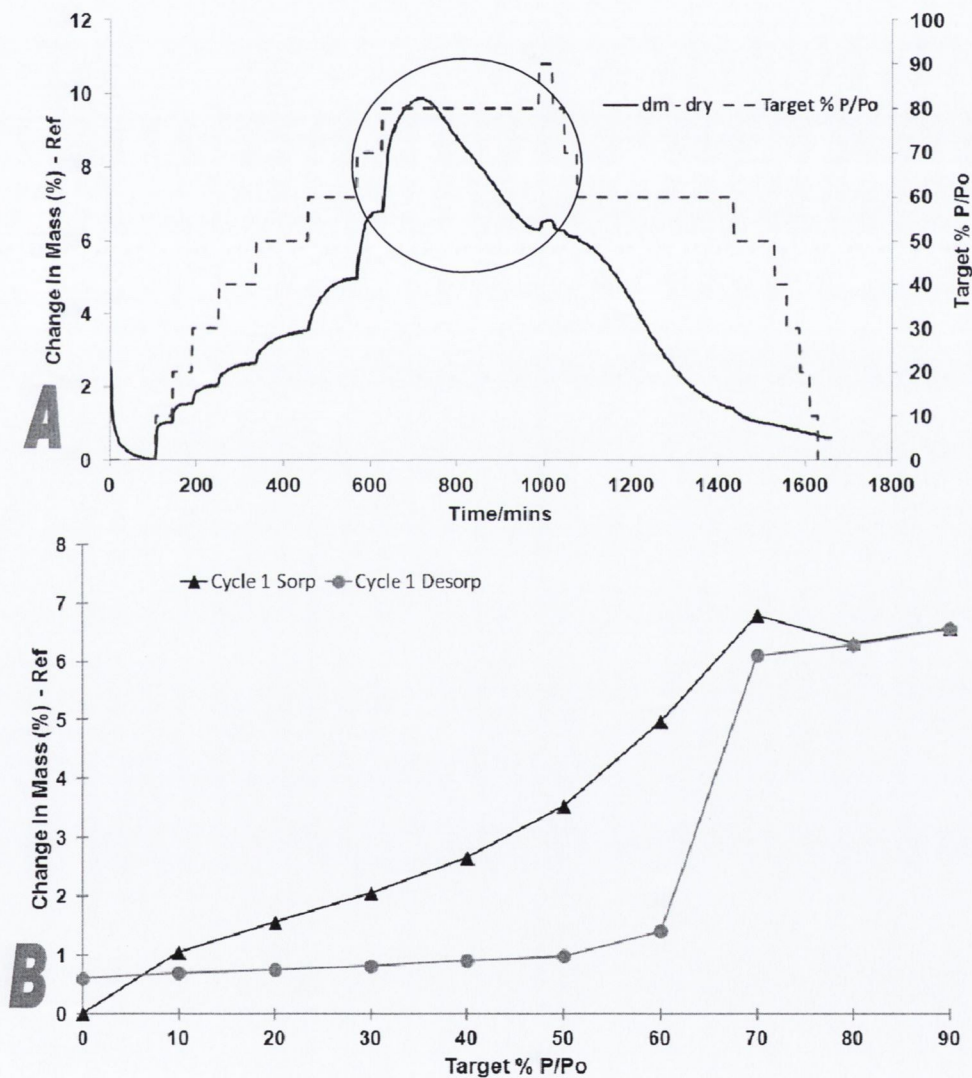


Figure 3.34 DVS kinetics (A) and isotherms (B) of spray dried SD 3:1

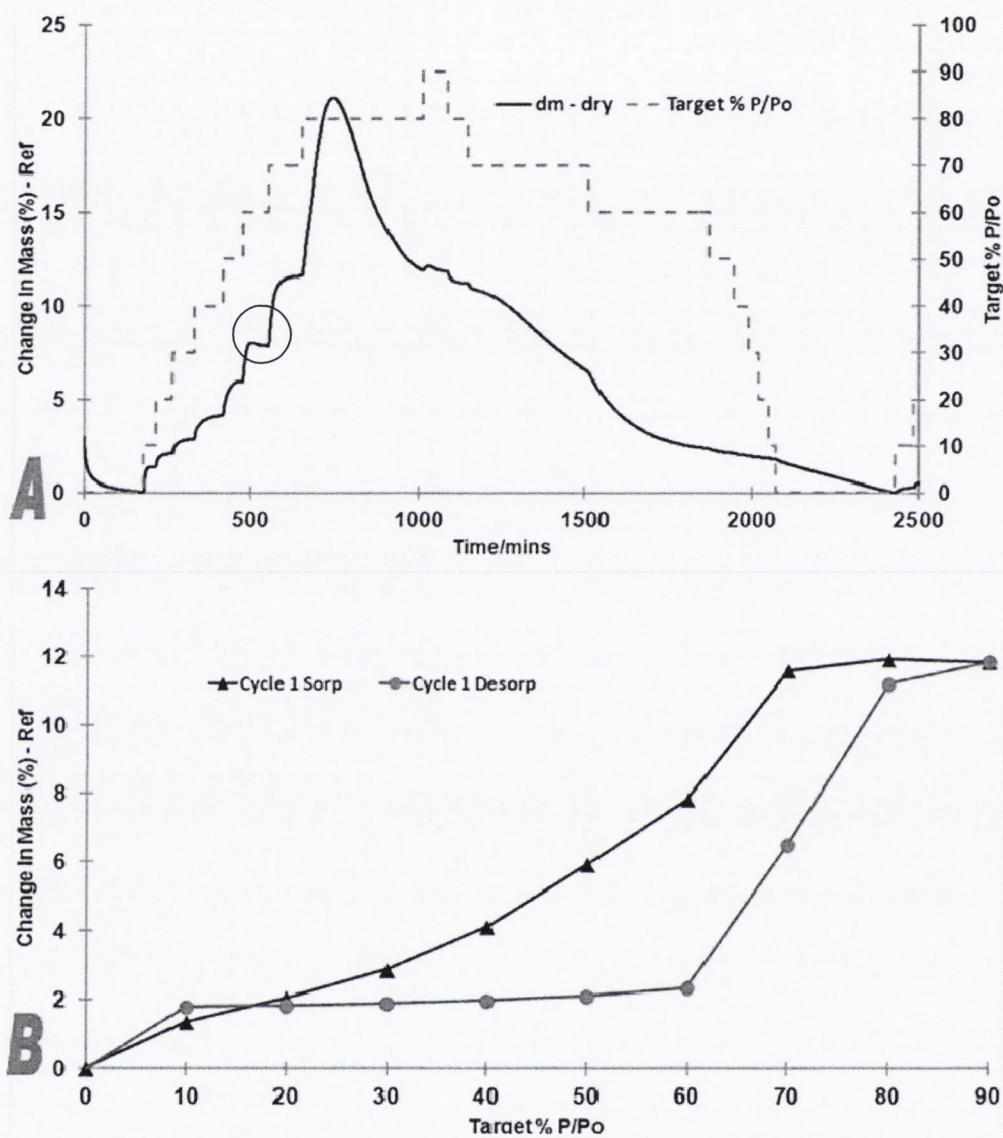


Figure 3.35 DVS kinetics (A) and isotherms (B) of spray dried SD 1:1

DVS kinetics and isotherms (Figure 3.34 and 3.35) showed that SD 3:1 and SD 1:1 collapsed to crystalline phases between 70-80% and 50-60% RH respectively. These findings indicated that amorphous SDNa was less stable compared to SD 3:1, as the salt was previously seen to crystallise at a RH between 50-60% (3.25 and 3.26). In contrast a higher stability

characterised amorphous SDNa compared to SD 1:1 which crystallised in the same RH range as seen for the salt alone despite a lower water uptake.

3.16 Conclusion

The work presented in this chapter showed that the physical state of sulfadimidine could be tuned by choosing specific spray drying parameters. Spray drying SD from water or ethanol:water solutions in the OCM resulted in an amorphous material. In contrast the use of acetone in the CCM configuration produced partially crystalline materials. Improving the physical stability of amorphous pharmaceutical systems is fundamental to exploit their favourable biopharmaceutical properties and developing a more stable amorphous drug by spray drying the corresponding sodium salt form of a drug appeared to be potentially advantageous. The sodium salt of SD converted to an amorphous phase upon processing, regardless of the solvent employed and spray-dryer set up. It was also characterised by an ~ two-fold increase of Tg with respect to the amorphous SD. The higher Tg (~155°C) led to an increased physical stability of the amorphous salt compared to amorphous SD but only in dry conditions. Storage at 4°C under desiccated conditions did not induce the crystallisation of the amorphous salt for over 3 years in contrast to SD which crystallised after 20 weeks. However the RH had a strong plasticising effect inducing phase transformation of the amorphous salt into a dihydrate when stored at RH above 60% in a time span of 2 hrs. Processing composites leads to materials with different properties compared to materials spray dried alone. Augmented amounts of salt in the mixtures shifted Tg and onsets of crystallisation towards higher temperatures indicating that the addition of salt to the non ionised drug is a viable strategy to increase the thermal stability. As a consequence the physical stability upon storage in desiccated conditions at 5°C for the composites was

enhanced compared to SD processed alone. The composites remained amorphous for a year while SD crystallised after 5 months. The ratio also influenced the physical stability following exposure to increasing RH. The amorphous salt crystallised at a lower RH (50%) compared to the system SD 3:1 (25% w/w salt content). In contrast, system SD 1:1 (50% w/w salt content) crystallised when exposed to the same RH, as for the salt, despite a lower water uptake.

Chapter 4

Modification of the solid state
nature of sulfathiazole and
sulfathiazole sodium via spray
drying

4 Introduction

Depending on the conditions of evaporation, solidification of a drug from solution may result in the generation of polymorphic or amorphous forms (Parmar et al., 2007; Tajber et al., 2005). These structural modifications are characterised by different energy states and therefore may undergo physico-chemical transformations further on in the drug formulation manufacture pathway (Huang and Tong, 2004). These changes can also occur during storage, as high energy solid states tend, over time, to reach a lower energy level which is characterised by an increased physical stability (Hancock and Zografi, 1997). Examples of modification of a solid state domain are the conversion of a compound into a different polymorphic or solvated structure, the transformation into its corresponding amorphous state (Tajber et al., 2005) or, vice versa, crystallisation from the amorphous state. The solid state nature of a compound determines its physico-chemical and biopharmaceutical properties such as its solubility, dissolution rate, bioavailability and stability (Huang and Tong, 2004). Spray drying is a multi-faceted process that may alter the solid state nature of a drug (Tajber et al., 2005) (Caron et al., 2011) (Master, 2002). Several parameters must be taken into consideration in the spray drying process, such as feed concentration, spray dryer configuration, settings and solvent selection. The composition of the feed liquid in spray drying can have a significant effect on the properties of spray dried products and can result in the production of powders with different degrees of crystallinity (Chidavaenzi et al., 1997). Chidavaenzi et al. (1997) for example demonstrated that an increase in lactose content in the liquid feed resulted in a decrease of amorphous lactose in the spray dried products.

Spray drying from non aqueous systems on an industrial scale most commonly involves the closed loop configuration. Nevertheless, there are numerous studies in the literature where

laboratory-scale spray drying based on similar solvent systems were performed in the open loop mode (Caron et al., 2011; Dontireddy and Crean, 2011; Janssens et al., 2009; Tajber et al., 2005). From this point of view, a comparison between the outcomes due to changes in the configuration is of interest, particularly in the context of scalability studies. Recently, Islam and Langrish (Islam and Langrish, 2010) studied the effect of different spray drier configurations and drying and atomising gases (N₂, CO₂ and air) on the physico-chemical properties of spray dried lactose. Under different conditions, lactose in solution solidified into powders characterised by different properties. Despite similarities in the thermal properties, differences in the sorption behaviour were found and attributed to three reasons: a different degree of crystallinity, different surface morphology and particle size differences. Furthermore it has been shown the ability of a solvent to determine the final polymorphic form of a drug after crystallisation from solution, process known as solution-mediated polymorphic transformations (Rodríguez-Hornedo and Murphy, 1999) (Crocker and Hodnett, 2010).

The aim of the current work is to analyse the impact of spray drying parameters on the physical state of the model compound sulfathiazole (ST), a sulphonamide drug known to present five different polymorphs (Hu et al., 2010) (Chan et al., 1999) and on its corresponding sodium salt form (STNa).

The wide variety of physical states in which sulfathiazole can exist including polymorphic, amorphous, salt and hydrate forms make this compound an ideal subject for theoretical pre-formulation studies. The ability to understand, conceptualise, and translate fundamental properties and behaviours from model compounds to current and newer systems has the potential to enhance our capabilities with the emergence of similar problematic API.

4.1 Sulfathiazole

4.2 Results

4.3 Solubility

The determined solubilities of unprocessed ST in ethanol, acetone, water, ethanol:water and acetone:water mixtures at different ratios (9:1, 8:2, 7:3 v/v) are listed in Table 4.1.

Table 4.1: Solubility data for sulfathiazole

A.P.I.	Solvent	Volume proportions (v/v)	Conc. (mg/mL)
Sulfathiazole	Ethanol	1/0	4.13 ± 0.15
Sulfathiazole	Ethanol:water	9/1	9.78 ± 0.28
Sulfathiazole	Ethanol:water	8/2	14.65 ± 0.50
Sulfathiazole	Ethanol:water	7/3	15.90 ± 0.62
Sulfathiazole	Water	1/0	0.26 ± 0.02
Sulfathiazole	Acetone	1/0	12.29 ± 0.88
Sulfathiazole	Acetone:water	9/1	60.38 ± 0.74
Sulfathiazole	Acetone:water	8/2	71.90 ± 1.32
Sulfathiazole	Acetone:water	7/3	64.59 ± 2.16

ST solubility in acetone was approximately three times higher than in ethanol. In contrast the solubility in water was close to zero. By adding water to the ethanol and to the acetone the properties of the solvents were modified. The solubility of the drug in the co-solvents mixtures increased up to three times and six times the solubility in pure ethanol and acetone respectively. The addition of an organic cosolvent to water makes the solvating environment less polar, resulting in a more favorable solvation of the hydrophobic ST in the liquid phase.

4.4 PXRD analysis

4.4.1 Open cycle mode (OCM)

The PXRD pattern of unprocessed ST (Figure 4.1k) was characterised by sharp Bragg peaks indicative of a crystalline structure, and it was found to be form III (Caron et al., 2011). ST spray dried from pure ethanol was partially crystalline and by comparing peak positions to theoretical patterns low intensity Bragg peaks of form I were detectable on the PXRD pattern as indicated by the arrows in figure 4.1d.

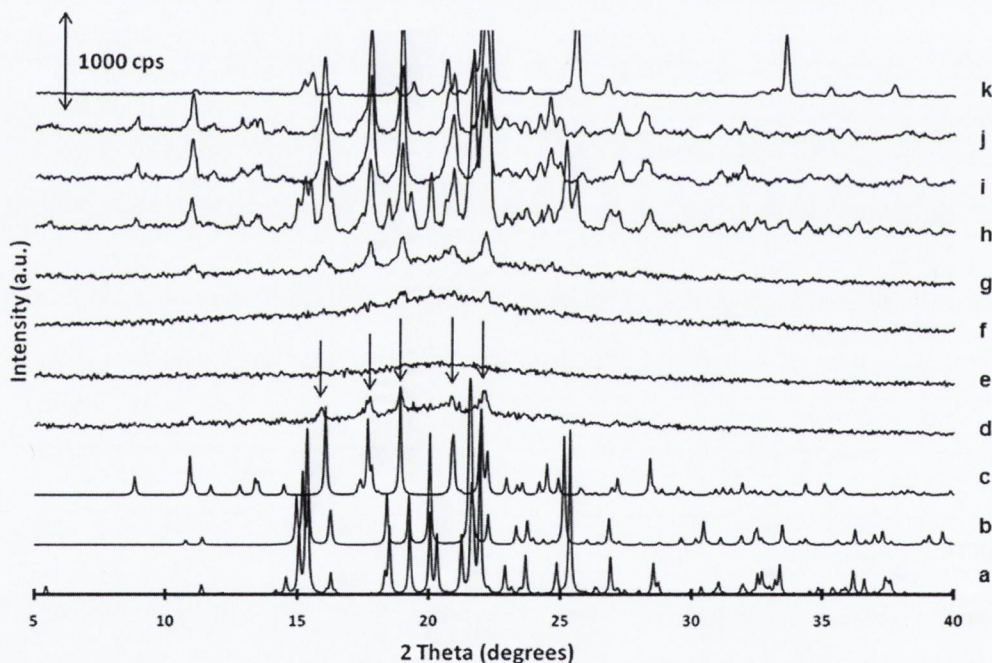


Figure 4.1: PXRD patterns of: (a) ST form III (CCDC normalised theoretical PXRD pattern); (b) ST form II (CCDC normalised theoretical PXRD pattern); (c) ST form I (CCDC normalised theoretical PXRD pattern); (d) spray dried ST in OCM from ethanol ($t=0$); (e) spray dried ST in OCM from ethanol:water 9:1 v/v ($t=0$); (f) spray dried ST in OCM from ethanol:water 9:1 v/v ($t=1/2$ hr); (g) spray dried ST in OCM from ethanol:water 9:1 v/v ($t=1$ hr); (h) spray dried ST in OCM from ethanol:water 9:1 v/v ($t=24$ hr); (i) spray dried ST in OCM from ethanol:water 9:1 v/v stored at 40°C and $<5\%$ RH; (j) spray dried ST in CCM from acetone:water 9:1 v/v. (k) unprocessed ST (Intensity divided by 3).

In contrast, ST powders spray dried from ethanol:water solutions at all compositions were amorphous with no diffraction peaks but a characteristic halo pattern in the diffractograms of the materials (Figure 4.1e). PXRD analysis on the processed materials was carried out immediately after the end of the spray drying process ($t=0$). Spray dried powders stored at ambient conditions (18-22°C and 45-80% RH) were subsequently analysed at different timescales following the end of the process: 30 minutes ($t=1/2$ hr), 1 hour ($t=1$ hr) and ~24 hours ($t=24$ hrs). The detection of Bragg peaks in the patterns of the materials spray dried from ethanolic solutions at all compositions was possible after 30 minutes from the end of the process (Figure 4.1f). Samples stored at ambient conditions up to 1 hr after processing presented Bragg peaks exclusively of form I (Figure 4.1g), a metastable polymorph of ST at room temperature, whilst the same samples analysed after 24 hrs were found to be a mixture of polymorphic forms. Extra diffraction peaks characteristic of form II and/or III (15.2, 15.5, 20.0, 21.6, scattering angle 2θ degrees) were visible together with those of form I (Figure 4.1h). Crystallisation occurred in a time span ranging from 1 to 24 hours. The influence of temperature and RH on the crystallisation of amorphous ST was investigated by characterising the samples after storage at various controlled temperatures and RH. Regardless of the spray drying parameters, the PXRD patterns of spray dried ST following storage at 40°C and 25°C and four different percentages of RH (5, 35, 55 and 60%) showed that amorphous ST converted to form I when the storage temperature was either at 25°C or 40°C and the RH was kept at or below 35% (Figure 4.1i and Figure 4.2 a-b). Peaks belonging to form II and/or III were detectable when the RH was increased to or above 55% (Figure 4.2 c-d). This demonstrated that the type of recrystallising polymorph was dependent on the

temperature and humidity of storage rather than on the solvent composition of the feed solution.

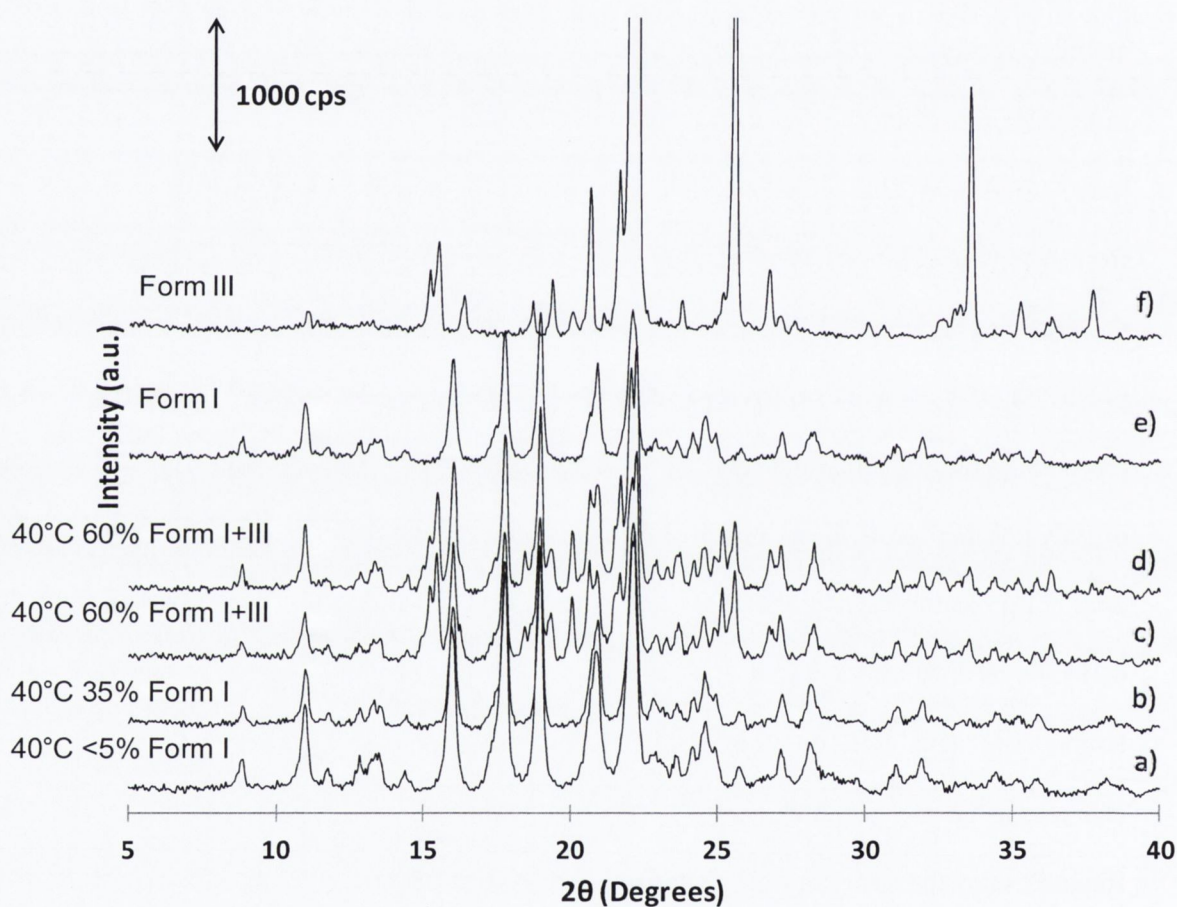


Figure 4.2 PXRD patterns of: (a) spray dried ST in OCM from ethanol:water 7:3 v/v stored at 40°C and <5% RH; (b) spray dried ST in OCM from ethanol:water 7:3 v/v stored at 40°C and 35% RH; (c) spray dried ST in OCM from ethanol:water 7:3 v/v stored at 40°C and 55% RH; (d) spray dried ST in OCM from ethanol:water 7:3 v/v stored at 40°C and 60% RH; (e) ST Form I; (f) unprocessed ST Form III (Intensity divided by 3).

4.4.2 Closed cycle mode (CCM)

Upon processing ST from both ethanolic and acetonic solutions, including pure ethanol and pure acetone, in a CCM configuration, the resulting powders subjected to XRD analysis immediately after the process ($t=0$) presented diffractograms characteristic of a crystalline material regardless of the organic solvent to water proportions or the feed concentration. ST powders processed in the CCM configuration from all solvent(s) systems presented PXRD patterns characteristic of form I (Figure 4.1j).

4.5 Thermal analysis

4.5.1 Open cycle mode (OCM)

The DSC thermogram of unprocessed ST was characterised by two endothermic events with onsets at $167 \pm 0.5^\circ\text{C}$ and $201 \pm 0.5^\circ\text{C}$, respectively (Figure 4.3f). The first endotherm was attributed to a solid state phase transition of form III into form I. The event with the higher temperature onset was consistent with melting of ST form I (Zeitler et al., 2006). Thermal analysis confirmed PXRD results that ST before being processed was form III. In contrast, DSC thermograms of spray dried ST at $t=0$ from ethanolic solutions at all composition including pure ethanol showed an exotherm with onset at $79 \pm 0.5^\circ\text{C}$ attributed to crystallisation of the amorphous material and a melting event at $200 \pm 0.5^\circ\text{C}$ characteristic of melting of form I (Figure 4.3e). The absence of thermal events between the endset temperature of the crystallisation peak and melting point indicated that thermal stress leads to the conversion of the amorphous material into pure form I, the polymorph which is stable at high temperature. A completely PXRD amorphous sample was characterised by a ΔH equal to $38.80 \pm 0.75 \text{ J/g}$. The glass transition temperature, T_g , was detected at $59 \pm 0.8^\circ\text{C}$ by

MTDSC. DSC analysis was carried out simultaneously to PXRD analysis 30 minutes, 1 hour and 24 hours after the end of the spray drying process for samples stored at ambient temperature and humidity. Crystallisation upon storage of ST powders, which was shown by the increase in intensity and number of Bragg peaks in PXRD patterns, was confirmed by the decrease of enthalpy of crystallisation in the thermograms of the spray dried powders.

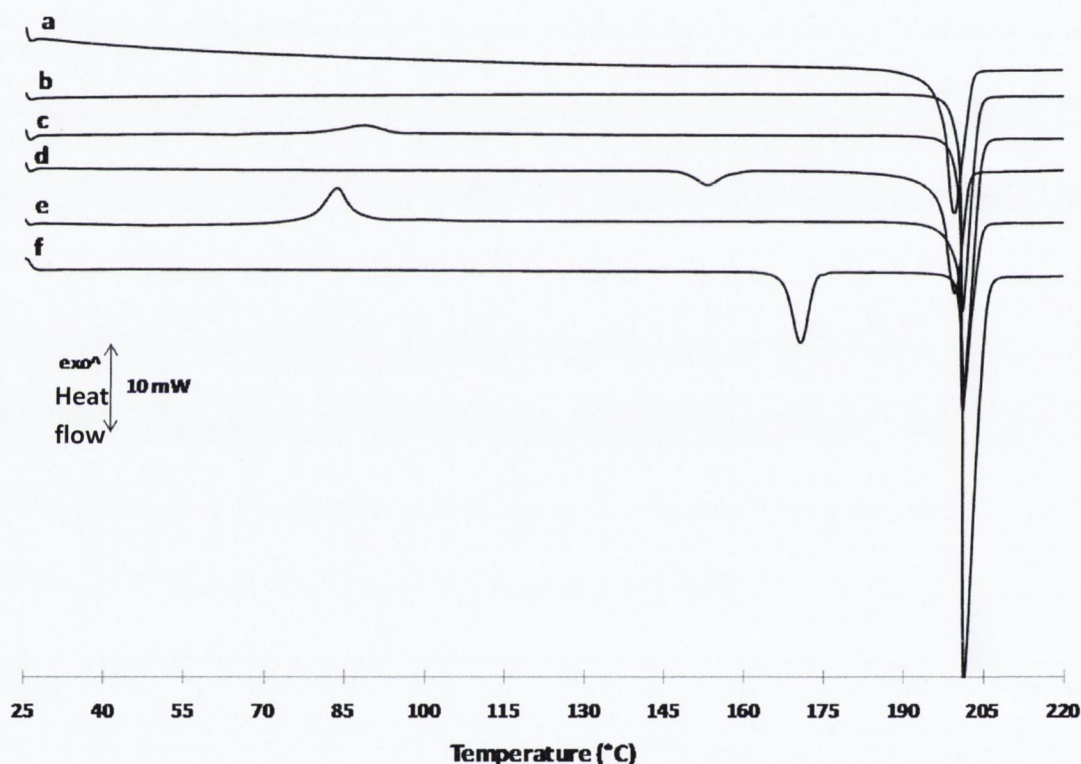


Figure 4.3 DSC thermograms of: (a) spray dried ST in CCM from acetone:water 9:1 v/v ; (b) spray dried ST in OCM from ethanol:water 9:1 v/v stored at 40°C and <5% RH after 72 hr; (c) spray dried ST in OCM from ethanol:water 9:1 v/v stored at 40°C and <5% RH after 24 hr; (d) spray dried ST in OCM from ethanol:water 9:1 v/v (t=24 hr); (e) spray dried ST in OCM from ethanol:water 9:1 v/v (t=0); (f) unprocessed ST (form III).

DSC thermograms of all spray dried ST samples stored at ambient temperature and humidity for 24 hrs presented two endothermic events (Figure 4.3d). The enthalpy (ΔH) and onset

temperature of the first event, attributed to the phase transition of form II and/or III to form I were not constant for different samples ranging from 3 to 12 J/g, indicating a variable amount of polymorphs in the completely crystallised products even for samples processed under the same spray drying conditions. Therefore, the influence of temperature and RH on the crystallisation of the samples spray dried from the different ethanol:water ratios was studied by subjecting the samples to DSC analysis after storage for 24 hours in different controlled conditions. Following storage at 25 and 40°C, DSC analysis carried out on spray dried ST confirmed that amorphous ST converted to pure form I when the RH was kept at or below 35%. A single endothermic event attributed to melting at ~200°C characterised the thermograms of the samples stored under these environmental conditions (Figure 4.3b). In contrast, the phase transition of form II and/or III to form I was detectable when the storage RH was increased to 55% or 60%. Under storage at <5% RH some residual amorphous material was still present within the material after 24 hours (Figure 4.3c). Full crystallisation at <5% RH occurred in a time span ranging from 24 to 72 hours from the end of the process.

4.5.2 Closed cycle mode (CCM)

DSC thermograms of ST spray dried in the CCM from all solvent systems were distinguished by a single endothermic event with onset at $197 \pm 0.5^\circ\text{C}$ and $199 \pm 0.5^\circ\text{C}$ for acetonic (Figure 4.3a) and ethanolic solutions respectively, attributable to the melting of form I. The increase in feed concentration for the acetonic systems did not affect the solid state nature of the API.

4.6 FTIR analysis

4.6.1 Open cycle mode (OCM)

FTIR analysis of unprocessed and spray dried ST from ethanolic solutions in the OCM are presented in Figure 4.4. The spectrum of unprocessed ST (form III) is similar to the spectrum of ST spray dried from ethanolic solutions after storage at 40°C and <5% RH (form I). However the position of the peaks is marked by a sharp shift. In particular the main differences can be observed in the region 3520-3150 cm^{-1} and by the presence of peaks at $\sim 1630 \text{ cm}^{-1}$ and $\sim 1200 \text{ cm}^{-1}$ for form I and 819 cm^{-1} for form III.

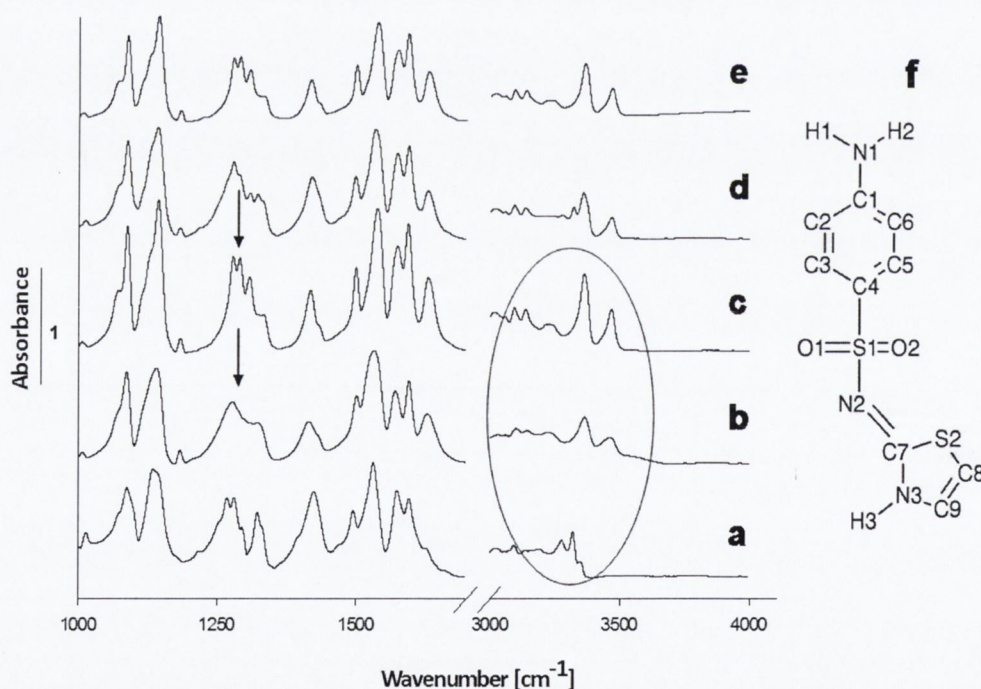


Figure 4.4 FTIR spectra of: (a) unprocessed ST form III; (b); spray dried ST in OCM from ethanol:water 7:3 v/v (amorphous); (c) spray dried ST in OCM from ethanol:water 7:3 v/v stored at 40°C and <5% RH (form I); (d) spray dried ST in OCM from ethanol:water 7:3 v/v stored at ambient conditions (form I and III); (e) spray dried ST in CCM from acetone:water 7:3 v/v (form I); (f) molecular structure of sulfathiazole (ref: Blagden et al. 1998).

Form I NH-stretch peaks at 3466 and 3361 cm^{-1} , are at higher wavenumbers compared to those of form III, visible at 3319 and 3276 cm^{-1} . The spectra of crystalline forms I and III are also compared to that of the amorphous form in Figure 4.4. The similarity between the spectra of the amorphous form and form I is evident, with the former characterised by a general broadening of the peaks. In the amorphous state the NH stretch peaks are broader than the corresponding peaks in form I and the NH-peak at the higher frequency appears at 3462 cm^{-1} in the spectrum of the amorphous form. The other NH peak, although broader, is found to be at roughly the same wavelength, $\sim 3363 \text{ cm}^{-1}$, compared to form I (Figure 4.4c). The fingerprint region of form I and of the amorphous phase did not show detectable differences except in the range 1290-1330 cm^{-1} . In this range, sulphonamides usually have a strong and broad adsorption band which generally consists of a number of peaks attributable to the asymmetric stretching vibration of the SO_2 group (Socrates, 2001). The further broadening and the disappearance of two of the three peaks that form this band (fusion of the 3 peaks in a broader single peak) observed upon amorphisation may indicate a different involvement of this group in hydrogen bonds in the amorphous phase compared to the crystalline phase. In contrast the symmetric SO_2 peak (1143 cm^{-1}) shifted by only 3 cm^{-1} towards lower frequencies from the crystalline to the amorphous state.

4.7 SEM analysis

4.7.1 Open cycle mode (OCM)

Figures 4.5a and 4.5c show SE micrographs for spray dried ST samples stored at 40°C and <5% RH and at ambient conditions, respectively. As can be observed in figure 4.3a spray dried ST samples after crystallisation into form I showed spherical particles with rough

surfaces. In contrast, smooth platelets together with spherical particles could be observed when spray dried ST crystallised into a mixture of polymorphs I and II/III (Figure 4.5c). These platelets are consistent with the morphology of both form III, characteristic of the starting material (Figure 4.5d) and of form II (Blagden et al., 1998).

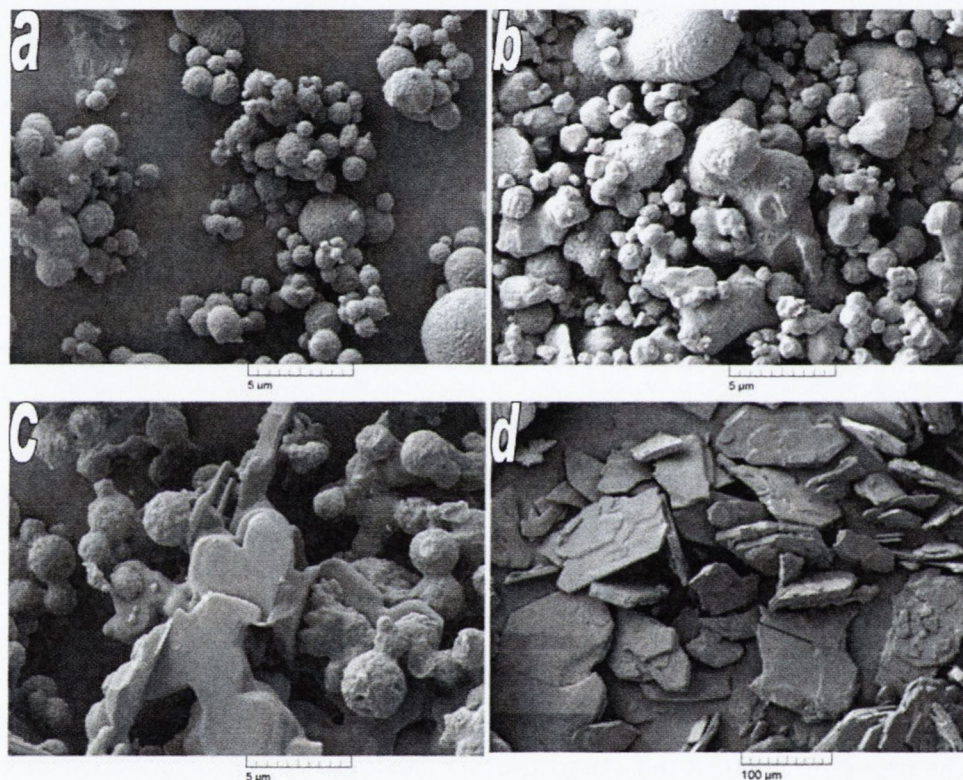


Figure 4.5 SEM micrographs of: (a) spray dried ST in OCM from ethanol:water 9:1 v/v stored at 40°C and <5% RH (form I); (b) spray dried ST in CCM from acetone:water 9:1 v/v (form I); (c) spray dried ST in OCM from ethanol:water 9:1 v/v stored at ambient conditions (form I and III); (d) unprocessed ST (form III). (Note different scale bars)

4.7.2 Closed cycle mode (CCM)

Figure 4.5b shows SE micrographs for ST samples spray dried in the CCM from acetone:water. The particles ranged from spherical to irregularly shaped with rough surfaces.

4.8 DVS analysis

Sorption-desorption isotherms showed that unprocessed crystalline ST (form III), when exposed to a series of 10% step changes of RH (0-90-0%), reached a maximum water uptake of ~0.1% at 90% RH (Figure 4.6a). The powder although subjected to drying pretreatment in the DVS apparatus, before the start of the experiment, lost a small amount of mass (~ 0.03%) at the end of the first sorption-desorption cycle indicating that the sample was not completely dry at the end of the pretreatment stage.

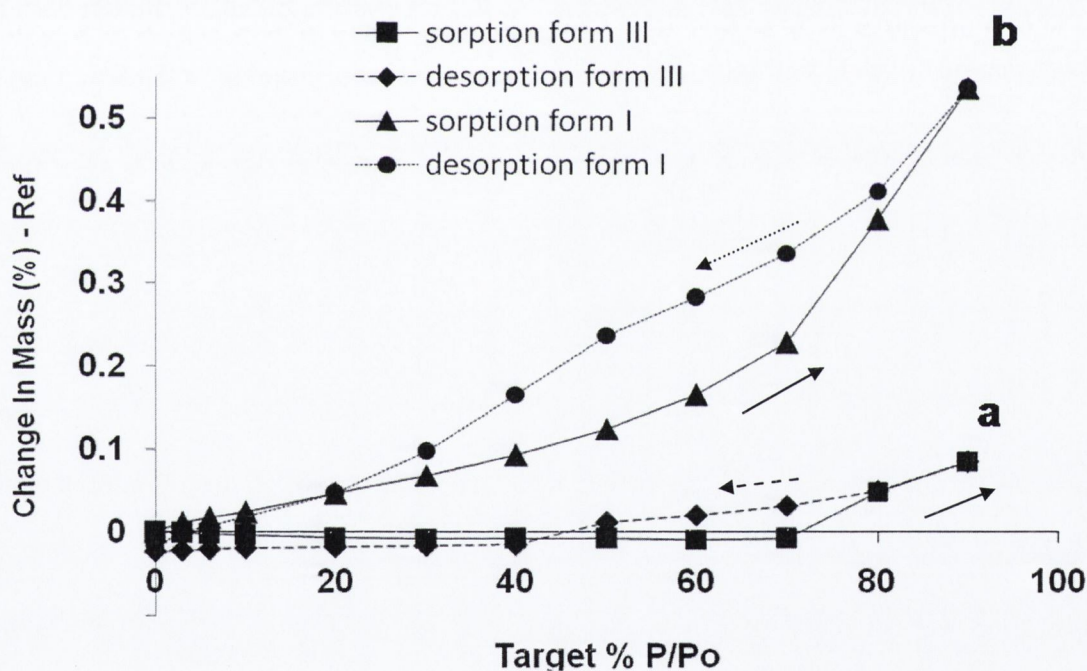


Figure 4.6 Sorption-desorption isotherms of: a) unprocessed ST (form III); b) spray dried ST in OCM from ethanol:water 9:1 v/v stored at 40°C and 5%RH (form I).

No polymorphic changes could be detected by PXRD after subjecting the powder to three full sorption-desorption cycles. In contrast, ST form I (Figure 4.6b) converted to a mixture of

form I and II and /or III at the end of the three sorption-desorption cycle experiment. Form I was also found to be more hygroscopic than the unprocessed material, with a maximum mass uptake of 0.54% at 90% RH (Figure 4.6b). The water uptake was progressively reduced to 0.50% and to 0.47% at 90% RH in the second and third cycle, respectively, probably due to the lower hygroscopicity of the polymorphic form(s) developing within the material. A series of experiments were carried out on ST form I to establish the critical RH at which this phase transition was favored. Different powder samples of ST form I were placed in a DVS cabinet at different % of RH for 1200 minutes. DSC and PXRD analysis showed the presence of the new form together with form I after subjecting ST Form I samples to the critical RH of 65%. In contrast, no phase transition was detected when the same experiment was carried out at RH values fixed at or below 60%.

4.9 Discussion on Sulfathiazole

As clearly shown from PXRD diffraction and confirmed by thermal analysis data, powders of metastable ST polymorph I were produced by using the CCM configuration of the lab scale spray drier using nitrogen as the drying gas while amorphous powders of ST were obtained from ethanolic solutions in the OCM configuration. These results agreed with the findings of Islam and Langrish (2010) who demonstrated how the selection of different spray drier configurations and drying gas could affect the properties of spray dried lactose. Different equipment configurations and use of different solvents will lead to different pressure, temperature and humidity environments inside the spray drier causing variations in the heat-mass transfer which could affect the properties of the spray dried materials. For example, it has been shown that the exposure of an amorphous system to vapours of a solvent in which the system is more soluble has a greater plasticising effect compared to a solvent in which the

solubility is lower (Yoshioka and Tashiro, 2004). The potential presence of a higher amount of ethanol vapour in the spray drier when operating in CCM compared to OCM is most likely the reason for the different outcomes obtained from changing the spray drier configuration. In theory, in the closed loop system the solvent contained in the gas stream is cooled and consequently condensed. The regenerated flow is then returned to the spray dryer. However, it is possible that a certain amount of the organic vapour contaminates the regenerated carrier gas. In contrast, in the open loop system, the ethanol vapour is diluted by the environmental air (which contains water vapour) and exhausted into the atmosphere thus affecting the crystallisation process to a lesser extent. Interestingly, only ST spray dried from pure ethanol in the OCM was partially crystalline. The residual crystallinity in the sulfathiazole spray dried from pure ethanol can be related to the use of an oversaturated solution. It is possible that the initial evaporation of solvent results in the sulfathiazole precipitating from the supersaturated solution, resulting in a suspension and subsequently a crystalline dried solid, in contrast to solvent evaporation from an undersaturated solution which results in amorphous solids. Unexpectedly solvent selection and feed concentration appeared not to affect the solid state nature of ST when the API was spray dried in the CCM. In contrast, numerous reports in the literature describe ST as a compound that can be isolated in at least five different polymorphic forms and that the solidification from solution into a specific polymorph or into mixtures of polymorphs can be determined by the choice of: solvent, type of crystallisation process and parameters used in the crystallisation process (Aaltonen et al., 2003; Anwar et al., 1989; Blagden et al., 1998; Khoshkhoo and Anwar, 1993; Parmar et al., 2007).

The differences between the results presented here and the aforementioned results of crystallisation studies can be attributed to the nature of the process employed in this study. Although based on the same principles of solvent removal and solidification of solute, spray drying and crystallisation by solvent evaporation are characterised by different kinetics. In the latter process, at supersaturation, form I starts to nucleate regardless of the solvent employed in the process, which implies that ST molecules are connected in α dimers, basic units of polymorph I (Blagden et al., 1998; Parmar et al., 2007). At a certain stage the metastable form I will start to dissolve, and β dimers, basic units of polymorphs II-V (Blagden et al., 1998; Chan et al., 1999; Parmar et al., 2007), if not thermodynamically inhibited, will subsequently develop, leading to a different crystalline polymorph (next most stable). In spray drying both the rupture of the α dimer bonds and the formation of β dimers are suppressed/inhibited due to the kinetics of the solvent evaporation process. Atomisation of the liquid feed and the drying step are extremely rapid, and the metastable form has to remain suspended in the solvent to favor its phase transition to the next more stable form. In this study it was found that spray dried powders obtained from ethanolic solutions in the OCM under air drying were amorphous and physically unstable. Solvent removal did not allow the nucleation of ST form I in the OCM, leading to an amorphous material. In contrast to the work of (Caron et al., 2011), who previously obtained ST form I upon spray drying in the OCM with an inlet temperature of 85°C, the use of an inlet temperature of 78 °C in the current study induced a reduction of the outlet temperature below the Tg of the drug (~59°C) resulting in ST being obtained in its amorphous state. In contrast to other studies this work investigates the amorphous ST obtained without employing the melt quench technique, a technique which is usually successful in the production of amorphous materials but often

characterised by degradation of the materials and considered not suitable for large scale manufacturing.

FTIR analysis of amorphous and crystalline ST forms (Figure 4.4b - 4.4c) suggests that the molecular arrangement of the amorphous form is closer to form I than to form III as evidenced by the peak position in particular in the NH stretching region. Previously Threlfall (Threlfall, 2003) compared the spectra of amorphous ST obtained by melt quench to the spectra of the crystalline forms of ST. Although melt quench ST presented a strong absorption band at 1518 cm^{-1} not visible in other polymorphs nor in the amorphous ST obtained in the current study via spray drying, it can be maintained in agreement with the author that the similarity between the spectra of form I and amorphous ST compared to the other polymorphs is due to the lack of β dimers constituting forms II, III and IV. In the current work the only differences noted between the spectra of the amorphous state and form I are a general broadening of the peaks in the former and a slight shift in the peaks, to a value not superior to 8 cm^{-1} . The close similarity of the FTIR spectra of the amorphous form to form I compared to form III, in particular in the NH stretching peak region, leads us to hypothesise that the short range molecular order of amorphous ST might be represented by α dimers. This hypothesis is supported by the recrystallisation of ST from the amorphous state upon different storage conditions and upon heating in a DSC oven. Amorphous ST powders tend to crystallise rapidly and at even low relative humidity. An analogy between the crystallisation of ST from solution and from its amorphous state is evident. In both cases the first form to nucleate is form I. The amorphous material was seen to partially crystallise into form I up to 1 hour from the end of the spray drying process (Figure 4.1) regardless of the environmental conditions, consistent with Ostwald's rule of stages. Keeping the material in

dry conditions below 35% of RH led to a full transformation into pure form I while keeping it at RH above 35% led to crystallisation towards a mixture of forms I, III and/or II (the close similarity between the PXRD patterns of form II and III (Figure 4.1) does not allow the identification of which ST polymorph or mixtures of polymorphs are developing together with form I upon different storage conditions). The low humidity conditions prevent the formation of β dimers, which necessitate ST molecules to be solvated, and it is hypothesised that the α dimers already present in the amorphous structure are the reason why form I rapidly develops within the material under dry conditions of storage. In contrast, high RH provided the environmental conditions necessary to favour the formation of β dimers and consequently the crystallisation of the amorphous material into a mixture of polymorphs.

Another important observation from the current work is that spray drying allowed spherical particles of ST form I with rough surfaces to be generated, which is in contrast to the typical morphology reported in the literature for form I following conventional crystallisation processes. According to the literature, the morphological representation of ST form I and typical of several metastable polymorphs is needle-like (Parmar et al., 2007) (Blagden et al., 1998; McArdle et al., 2010), a morphology which is usually considered adverse for pharmaceutical development (Cuppen et al., 2004).

4.10 Sulfathiazole sodium

4.10.1 PXRD analysis

4.10.1.1 Open cycle mode (OCM)

Unprocessed STNa presented a PXRD pattern typical of a crystalline substance (Figure 4.7a), while diffractograms of all the processed material patterns regardless of the solvent composition and ratio employed in the process appeared as amorphous halos (Figure 4.7 b-c). For all amorphous salt powders, crystallisation of the materials was not observed over 12 months when stored in a desiccator at 4°C.

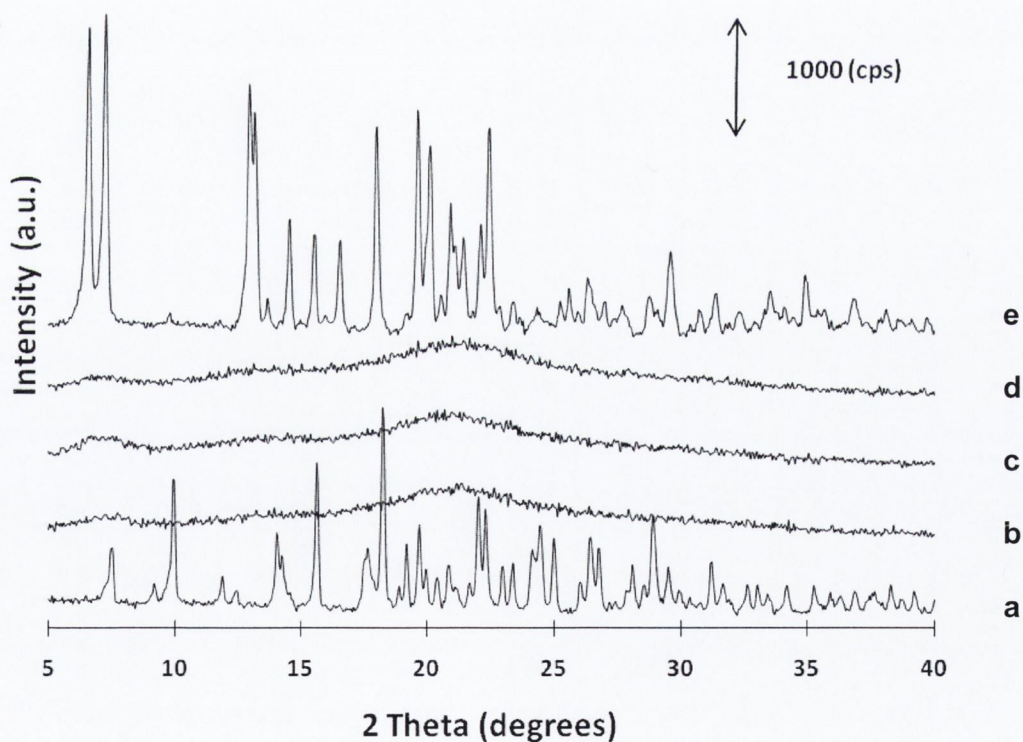


Figure 4.7 PXRD patterns of: (a) unprocessed STNa; (b) spray dried STNa in OCM from ethanol:water 9:1 v/v; (c) spray dried STNa in OCM from water; (d) spray dried STNa in CCM from acetone:water 9:1 v/v; (e) unprocessed STNa after DVS.

4.10.1.2 Closed cycle mode (CCM)

The powders collected after spray drying from acetone:water 9:1 v/v (Figure 4.7d) and from ethanolic solutions at all compositions presented an amorphous PXRD pattern and were immediately placed in controlled humidity devices at < 5% RH due to their physical instability. Under this storage RH the powders did not recrystallise over 12 months. Concerning the other acetonic systems spray dried in the CCM (water content in the feed above 10% v/v), the spray dried powders converted in a few minutes to a sticky mass during sample collection and therefore were not analysed.

4.11 Thermal analysis

4.11.1 Open cycle mode (OCM)

The DSC scan of unprocessed STNa and the DSC and TGA thermograms of the material spray dried from different solvents are shown in Figure 4.8A. Unprocessed STNa presented an endothermic event attributable to the melting point at $268 \pm 0.2^\circ\text{C}$. It was preceded by a small endotherm appearing between 70 and 100°C attributed to solvent removal. TGA presented a mass loss of $\sim 0.4\%$ between 25 and 100°C and indicated that melting was accompanied by decomposition. DSC thermograms of the processed powders presented an exotherm of crystallisation in the temperature range between $150\text{-}180^\circ\text{C}$ (Figure 4.8A). The onset temperature of the exotherm was variable depending on the solvent composition of the feed solutions employed in the process. Higher onset temperatures were recorded when the materials were spray dried from pure water, pure ethanol and ethanolic solutions with a water content at or below 20% v/v compared to the systems spray dried from ethanol:water 7:3 v/v. A second exothermic peak, albeit of lower intensity, was observed above 175°C on the

thermograms of all the materials spray dried in the OCM (Figure 4.8A). The DSC thermograms were also characterised by a broad endotherm between 25 and 100°C, attributable to weakly bonded or adsorbed solvent. A deflection of the baseline at ~ 120°C was observed and attributed to the glass transition (T_g).

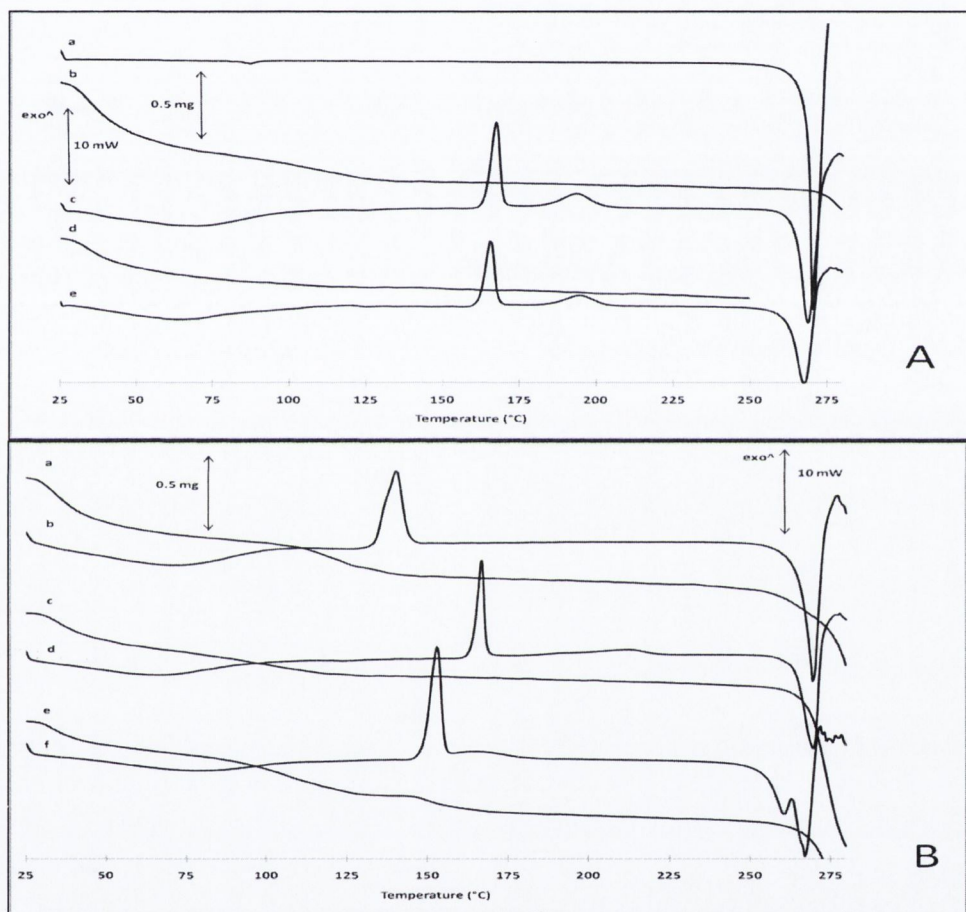


Figure 4.8 A: (a) DSC analysis of unprocessed STNA; (b) TGA of spray dried STNA in OCM from ethanol:water 9:1 v/v; (c) DSC analysis of spray dried STNA in OCM from ethanol:water 9:1 v/v; (d) TGA of spray dried STNA in OCM from water; (e) DSC analysis of spray dried STNA in OCM from water. **Figure 4.8B:** (a) TGA of spray dried STNA in CCM from ethanol:water 9:1 v/v; (b) DSC analysis of spray dried STNA in CCM from ethanol:water 9:1 v/v; (c) TGA of spray dried STNA in CCM from ethanol:water 7:3 v/v; (d) DSC analysis of spray dried STNA in CCM from ethanol:water 7:3 v/v; (e) TGA of spray dried STNA in CCM from acetone:water 9:1 v/v; (f) DSC analysis of spray dried STNA in CCM from acetone:water 9:1 v/v.

Spray dried STNa from ethanol:water 9:1 v/v was subjected to modulated calorimetry and the reversing heat flow thermogram showed a deflection of the baseline at $\sim 122^{\circ}\text{C}$, confirming the detection of Tg. Corresponding TGA thermograms of the spray dried samples showed mass loss ranging from ~ 4.2 to 6.5% between 25 and 130°C . The solid state changes of the processed drug during heating were studied combining both DSC and PXRD techniques.

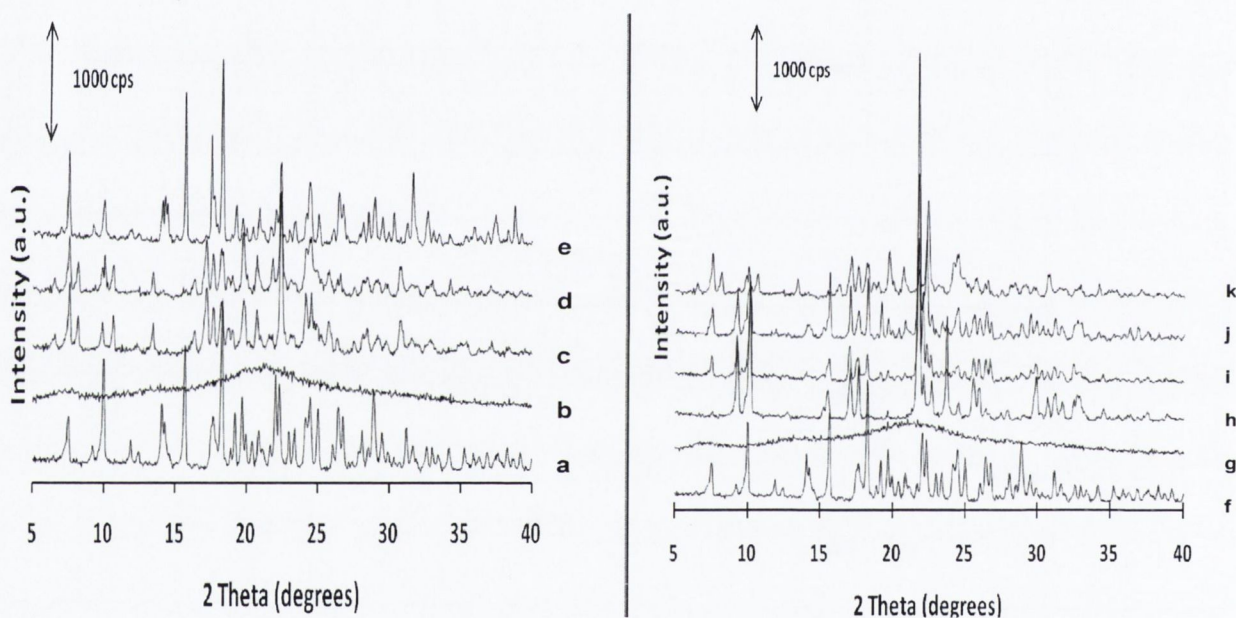


Figure 4.9 XRD patterns of: (a) unprocessed STNa; (b) spray dried STNa in OCM from ethanol:water 9:1 v/v; (c) spray dried STNa in OCM from water heated up to 180°C ; (d) spray dried STNa in OCM from ethanol:water 9:1 v/v heated up to 180°C ; (e) spray dried STNa in OCM from ethanol:water 9:1 v/v heated up to 210°C ; (f) unprocessed STNa; (g) spray dried STNa in CCM from acetone:water 9:1 v/v; (h) spray dried STNa in CCM from acetone:water 9:1 v/v; heated up to 155°C ; (i) spray dried STNa in CCM from acetone:water 9:1 v/v heated up to 170°C ; (j) spray dried STNa in CCM from acetone:water 9:1 v/v heated up to 230°C ; (k) spray dried STNa in OCM from ethanol:water 9:1 v/v heated up to 180°C .

The PXRD patterns of STNa spray dried from water, ethanol and ethanol:water solutions (Figure 4.9 c-d) heated up to 180°C , above the endset of the first exotherm peak, at a heating

rate of 10°C per minute, were all similar and differed from the pattern of the crystalline unprocessed material (Figure 4.9a) by the presence of extra peaks at the following 2θ values: 6.57, 8.13, 10.61, 13.39, 16.36, 17.15. The PXRD pattern of the materials heated at the same rate above the endset of the second exothermic peak ($\sim 200^\circ\text{C}$), was the same as the diffraction pattern of the unprocessed material (Figure 4.9e).

4.11.2 Closed cycle mode (CCM)

The DSC thermograms of STNa samples spray dried from acetone:water showed tailing of the exothermic peak (two peaks fused together) with onset at $\sim 150^\circ\text{C}$ (Figure 4.8B). The material presented two melting peaks. The first peak was reported at 255°C . The second peak was recorded in the melting range of the powders obtained from pure water and ethanolic systems at $\sim 262^\circ\text{C}$. A $\sim 4.7\%$ mass loss was determined by TGA between 25 and 130°C . An additional mass loss of about 1.1% in the acetonic system was detected in the same temperature range where the corresponding DSC exotherm was recorded. When subjected to modulated calorimetry, the reversing heat flow thermogram for STNa from acetone:water 9:1 v/v showed a deflection of the baseline in two steps at $\sim 113^\circ\text{C}$. The thermal behavior of STNa spray dried from ethanolic solution was dependent on the solvent ratio employed to produce the feed solution. The systems spray dried from pure ethanol and ethanol:water 9:1 v/v were characterised by a single exothermic peak (Figure 4.8B). These crystallisation peaks were recorded at the lowest temperatures for all spray dried systems either in the OCM or CCM. The corresponding TGA thermograms were characterised by mass loss in two steps, between 25 and 90°C and between 95 and 150°C . In contrast, the systems spray dried from

ethanol:water with ethanol content at or below 80% v/v were characterised by two exothermic peaks, as previously seen for the systems spray dried in the OCM and corresponding TGA thermograms presented mass loss in a single step (Figure 4.8B). The PXRD patterns of the material spray dried from acetone:water 9:1 v/v heated up to different temperatures 155, 175 and 230°C at a heating rate of 10°C per minute, differed from the pattern of the crystalline unprocessed material (Figure 4.9). New Bragg peaks together with those of the unprocessed material were evident in the pattern of the material heated up to a temperature of 230°C, above which no thermal events were observed apart from melting.

4.12 DVS analysis

In Figure 4.10 A, B and C DVS isotherms of sorption-desorption (2 full cycles) of the original material and of the spray dried material obtained from ethanol:water 9:1 v/v in the OCM and acetone:water 9:1 v/v in the CCM are shown. The isotherms showed that unprocessed STNa when exposed to a series of 10% step changes of RH from 0 to 90% and back to 0% was characterised by water-uptake. The mass gain percentage was equal to $9.5 \pm 0.1\%$ (Figure 4.10 A). In contrast, STNa spray dried in the OCM from ethanol:water 9:1 v/v at the end of the same experiment was characterised by a mass gain of $\sim 7.7\%$ (Figure 4.10B). A lower mass gain by the end of the analysis, of $\sim 5.7\%$, characterised the salt spray dried in the CCM from acetone:water 9:1 v/v (Figure 4.10 C). In the first sorption cycle no mass loss was detected from the ethanolic system at any stage (Figure 4.10 B). In contrast, the acetic system showed a $\sim 2.7\%$ mass loss in the 40-50% RH step as indicated by the arrow in Figure 4.10 C. All the materials analysed after DVS presented an identical PXRD pattern, which differed from the original material pattern (Figure 4.7 e).

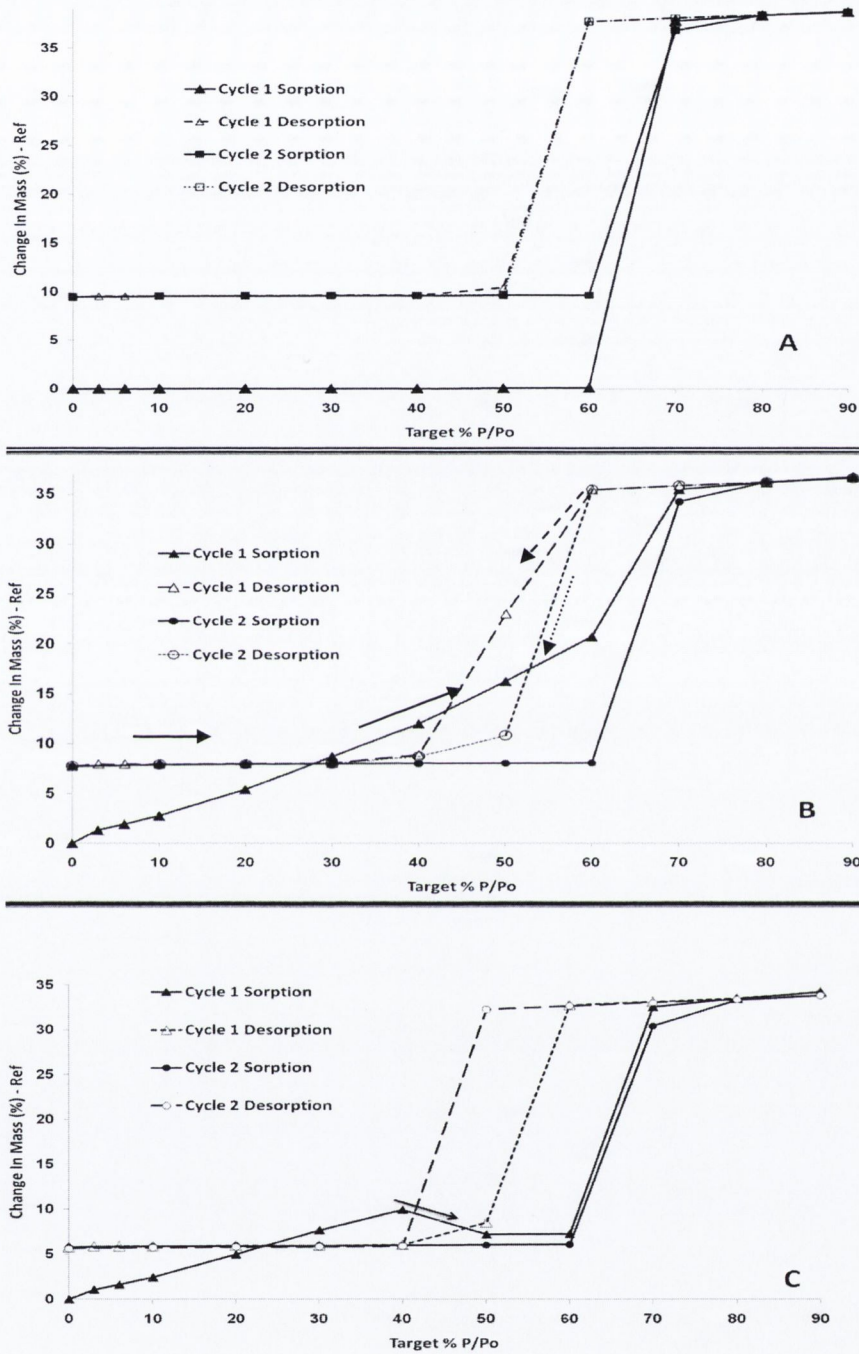


Figure 4.10: DVS Sorption-desorption isotherms of (A) unprocessed STNA; (B) spray dried STNA in OCM from ethanol:water 9:1 v/v; (C) spray dried STNA in CCM from acetone:water 9:1 v/v

A $9.8 \pm 0.4\%$ thermogravimetric mass loss between 30 and 120°C confirmed the stoichiometry of the spray dried material after DVS treatment to be a sesquihydrate (STNa* 1.5 H₂O) (Figure 4.11). The corresponding DSC thermogram showed a sharp endotherm in the same temperature range, the material consequently reconverted into its anhydrous form and finally melted at 268°C consistent with the melting point of unprocessed STNa.

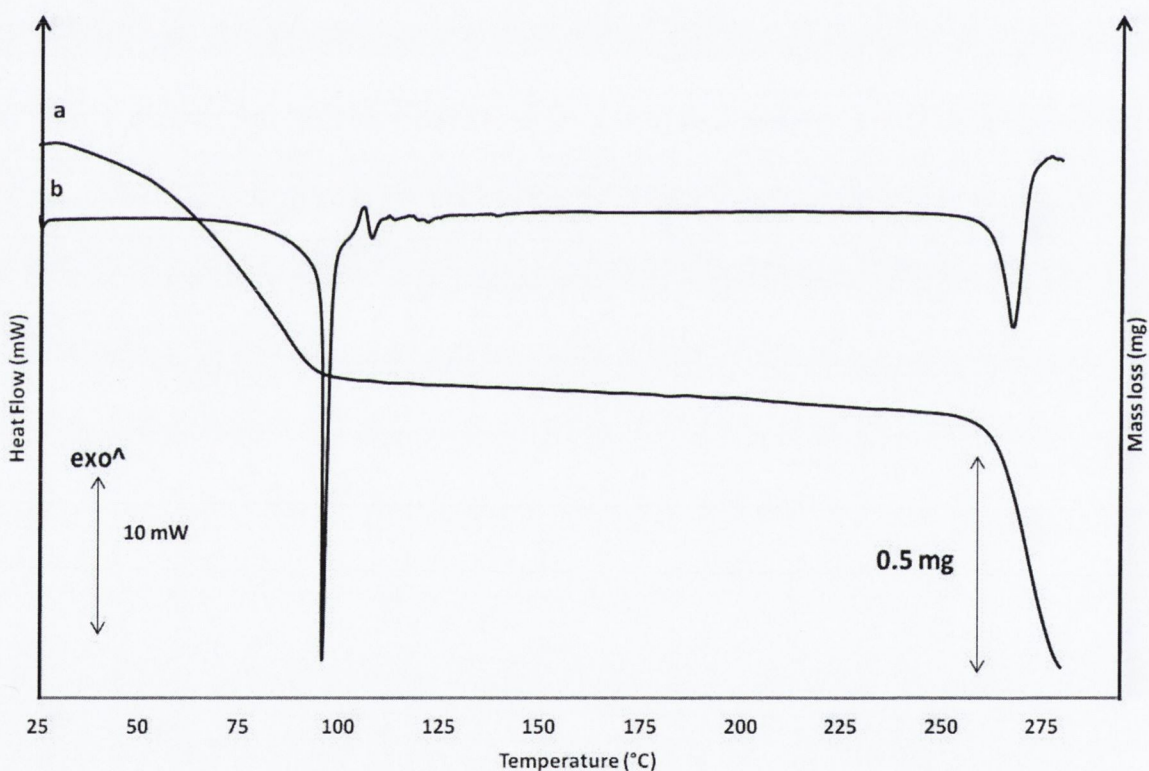


Figure 4.11 (a): DSC and (b): TGA thermograms of spray dried STNA in OCM from ethanol:water 9:1 v/v after DVS analysis.

4.13 Discussion on Sulfathiazole sodium

Ensuring the physical stability of amorphous systems is essential to exploit their likely favourable properties. As a strategy to succeed in the development of a more stable amorphous form the spray drying process was tested on the sodium salt of ST. The remarkable rise in melting point ($\sim 268^{\circ}\text{C}$) with respect to the corresponding non-salt form ($\sim 201^{\circ}\text{C}$) is attributed to an increased stability due to the introduction of ionic interactions within the crystalline structure (Tong and Zografı, 1999). The sodium salt of ST converted to an amorphous phase upon processing, but in this case regardless of the solvent employed and spray-drier set up. A significant increase of T_g in the amorphous salt with respect to the amorphous ST confirmed the influence of the counterion on the thermal properties of the amorphous material as was previously reported by Tong and Zografı for indomethacin sodium (Tong and Zografı, 1999).

However, spray drier set up, solvent selection and ratio affected the thermal features of the processed salt. For example, STNa spray dried from pure ethanol and ethanol:water 9:1 v/v in the CCM crystallised at a lower temperature compared to the same systems spray dried in the OCM. Corresponding TGA analysis showed that the two samples spray dried in the CCM were characterised by mass loss up to 150°C . In contrast, the same samples spray dried in the OCM presented mass loss between 25 and 130°C . Thus solvent molecules appear to be more strongly retained in the amorphous samples spray dried in CCM, causing a decrease in the onset of crystallisation. Likewise, the deflection of the baseline attributed to the T_g of the material spray dried from acetone:water 9:1 v/v in the CCM was recorded at a lower temperature compared to the systems spray dried in the OCM. MTDSC analysis showed that the glass transition deflection in the acetonic system was in two steps. A double T_g might

explain this result from MTDSC analysis, the first T_g would represent the change in heat capacity for a certain proportion of amorphous material exposed to acetone, the second T_g represented by the remaining dry material. The FTIR spectra of amorphous STNa processed from acetone:water presented a peak at $\sim 1700\text{ cm}^{-1}$. This peak is typical of the CO stretching vibration of ketones. It was not found in the spectra of neither the original material nor the processed materials from water and ethanol:water solvent systems and therefore attributed to the acetone retained in the amorphous salt. In addition, TGA analysis recorded a $\sim 1\%$ mass loss from the material spray dried from acetone:water 9:1 v/v in the CCM at a temperature corresponding to the crystallisation of the material from the amorphous state. This mass loss may be attributed to release of solvent upon crystallisation, confirming the presence of solvent retained in the amorphous material.

Complementary methods (DSC and PXRD) were useful to demonstrate the ability of STNa to give rise to polymorphism when subjected to thermal stress. All amorphous samples spray dried in the OCM and the samples spray dried from ethanol:water in the CCM, when the water content in the solvent was 20% v/v or more, crystallised into a different crystal structure compared to the starting material. This new polymorph then reconverted to the original material with a further rise in temperature. In contrast, amorphous STNa spray dried from acetone:water in the CCM after complete crystallisation was found to be a mixture of the two polymorphic forms. Only amorphous STNa spray dried from ethanol and ethanol:water 9:1 v/v in the CCM crystallised directly into the original structure at a temperature ~ 20 degrees lower than the other systems. Solvent retained in the amorphous structure seems to play an important role in the crystallisation from the amorphous state upon heating.

Higher T_g ($\sim 120^\circ\text{C}$) and onset of crystallisation led to an increased physical stability of the amorphous salt compared to amorphous ST in dry conditions. The recommended storage temperature for amorphous materials has to be at least 50 degrees lower than the T_g in order to reduce the molecular mobility close to zero (Hancock et al., 1995). Hence the storage temperature of 4°C did not induce the crystallisation of the amorphous salt. Though the T_g of amorphous STNa was higher than that of amorphous ST, RH was found to have a strong plasticising effect inducing the phase transformation of the salt into a hydrate form when exposed to a full cycle (0-90-0%) of step changes in RH. After DVS treatment, the PXRD patterns of both the processed salt samples and of unprocessed STNa were identical. These patterns differed from the pattern of the original material (i.e. not subjected to DVS analysis), indicating a change in the crystal structure. The shortfall in the mass gain percentage in the amorphous systems of $\sim 1.7\%$ and $\sim 3.7\%$ for the ethanolic and acetonic systems respectively, compared to the final mass gain percentage of the original material subjected to DVS can be attributed to solvent retained in the amorphous form at the beginning of the experiment. This solvent does not separate from the powder during the pretreatment phase (drying at 0% RH in the DVS apparatus until constant mass). Several hydrates of STNa are reported in the literature (Rubino, 1989). A mass uptake % of 9.5 ± 0.1 at the end of a full DVS cycle experiment for unprocessed STNa is consistent with the theoretical stoichiometric water content for a sesquihydrate. Interestingly the DVS sorption profiles were different for different spray dried samples. No loss of mass was detected in the first sorption isotherm for STNa spray dried from either water or ethanol:water 9:1 v/v. Therefore, it would appear that the amorphous material converts directly to a hydrated crystal form with the increase of RH. In contrast, the amorphous salt spray dried from acetone:water 9:1 v/v showed mass loss in

the RH step between 40-50%. Mass loss is hypothesised to be due to loss of acetone. The acetone retained in the amorphous powder is released from the material during the crystallisation stage, indicating a higher affinity of the solvent for the amorphous structure of the drug compared to ethanol.

4.14 Conclusion

The solid state characteristics of a drug can be controlled by careful adjustment of processing and/or storage parameters. This study demonstrated that accelerating the kinetics of solvent evaporation in a solidification process can induce a drug to solidify in its metastable polymorph or its amorphous form. Therefore spray drying can be used as an alternative technique for isolating a metastable form. Its advantage lies in producing pure metastable polymorphs with no needle-like morphology which traditionally, may be hard to achieve with slow evaporation techniques. In the case of form I, production of spherical particles by spray drying is a clear advantage compared to the needle-like shape observed with other methods. Control of spray drying adjustable parameters is essential to ensure consistent solid state characteristics of the spray dried product. The configuration of the spray drier employed in the spray drying process was seen to have a significant impact on the solid state nature of a drug as was seen for CCS and OCS configurations which led to crystalline and amorphous sulfathiazole, respectively. Intermolecular forces and structural similarities between a metastable crystalline polymorph and its corresponding amorphous counterpart in highly polymorphic systems can explain the recrystallisation of the amorphous state into a specific form rather than another polymorph. Nevertheless it was seen that the amorphous system can be guided to recrystallise into a specific polymorphic form by providing ideal environmental storage condition. The basis behind the recrystallisation of ST from the amorphous state is

analogous to its solvent mediated recrystallisation from solution and both processes follow Ostwald's rule of stages.

Under dry condition full recrystallisation to form I can be achieved while high RH conditions favour the development of form III. Spray drying a salt form appears to be promising to stabilise amorphous drugs. The transformation of STNa into the corresponding amorphous state can be easily achieved, most likely due to a significantly high T_g value compared to the non ionised form. However its hygroscopicity affects its physical stability. High water absorption exerts a plasticising effect inducing recrystallisation to a hydrate form. Nevertheless, the spray drying of a salt form is potentially a positive approach to stabilise the amorphous form of a drug, if the salt employed is characterised by favourable hygroscopic properties.

Chapter 5

Bulk, surface properties and water uptake mechanisms of salt/acid amorphous composite systems

5.1 Introduction

The requirement to improve the bioavailability of poorly soluble active pharmaceutical ingredients (API) has resulted in a growing use of processes such as milling and spray drying, which reduce particle dimensions and increase specific surface area. It is well established that partial or full amorphisation of an API can occur as a result of these processes and that changes in the solid state nature can alter their physicochemical and biopharmaceutical properties (Caron et al., 2011; Tajber et al., 2005; Yu, 2001). Amorphous materials are structurally disorganised and have different bulk and surface properties compared to the corresponding crystalline materials. They typically display higher surface free energy (Newell et al., 2001b), higher hygroscopicity (Newman et al., 2008), greater solubility and a higher dissolution rate (Tajber et al., 2005). Although these properties are relevant from a pharmaceutical development perspective, the full exploitation of amorphous drugs and formulations can not always be achieved mainly due to low physical and chemical stability (Caron et al., 2011; Yu, 2001). Therefore a thorough understanding of the properties of the amorphous state is required to develop new strategies to physico-chemically stabilise amorphous compounds.

Previously, as described in Chapter 4, we studied several physicochemical properties of sulfathiazole (ST) and sulfathiazole sodium (STNa) which solidify into unstable amorphous materials after spray drying. The acid rapidly crystallised regardless of the relative humidity (RH) conditions. The crystallisation of amorphous solids can be promoted by heat and therefore these materials usually require storage at temperatures well below their glass transition temperature (T_g) (Caron et al., 2011; Hancock et al., 1995; Yu, 2001). Considerable effort has been made to address this problem, either by co-processing heat labile amorphous drugs with high T_g excipients (Caron et al., 2011)

or by using amorphous salt forms of these compounds (Tong et al., 2002; Tong and Zografi, 1999). In many cases a shift of the T_g to higher temperature has been achieved, which is potentially a good strategy to stabilise amorphous formulations. However this is not always sufficient and other influential factors affecting stability must also be considered. For instance, amorphous STNa was characterised by a 60°C increase in T_g compared to ST and was physically stable when stored under desiccated conditions. Nevertheless, it deliquesced when exposed to ambient RH conditions.

Deliquescence together with adsorption, capillary condensation, hydrate formation and absorption, is one of the known mechanisms of solid-water interactions (Airaksinen et al., 2005; Hiatt et al., 2011). It is a first order phase transition that happens when a water soluble solid generates a saturated solution by dissolving into the water sorbed from the environment at a specific relative humidity (RH_0) characteristic for that solid. Due to high void space and enlarged free volume relative to the crystalline state, amorphous substances absorb water below RH_0 and undergo deliquescence at a lower RH compared to their crystalline counterparts (Mikhailov et al., 2009). The amount of water absorbed into amorphous materials is proportional to the volume/weight of the amorphous solid and high absorption and retention of water can enhance chemical reactions which may lead to product degradation (Hancock and Shamblin, 1998). Furthermore, sorbed water as well as heat can promote the crystallisation of amorphous materials (Baird and Taylor, 2012; Burnett et al., 2006).

Therefore strategies to stabilise amorphous materials should aim at both increasing the T_g and protecting the amorphous system from water uptake. Co-formulation of a deliquescent salt form (sodium ascorbate) with excipients (maltodextrins) was seen to reduce the moisture sorption and enhance the physical stability of this salt (Hiatt et al.,

2011). It was also observed that the production of molecular dispersions of indomethacin and indomethacin sodium via evaporation under vacuum influenced the physicochemical characteristics of each species (Tong and Zografi, 2001). The aim of the current research was to improve the physical stability of amorphous ST/STNa mix in terms of crystallisation and deliquescence by adjusting the salt/acid ratio in the composite systems.

5.2 Results and discussion

Previous experiments (Chapter 4) showed that ST and STNa solidified into amorphous materials on spray drying. However, both spray dried substances were physically unstable. Amorphous ST started to crystallise to polymorph I ~30 minutes after the end of the spray drying process regardless of the temperature and RH of storage. In contrast spray dried STNa remained amorphous when stored for over a year in desiccated condition at $5 \pm 1^\circ\text{C}$. Nevertheless, amorphous STNa rapidly deliquesced at ambient conditions (18-25°C and 40-80% RH).

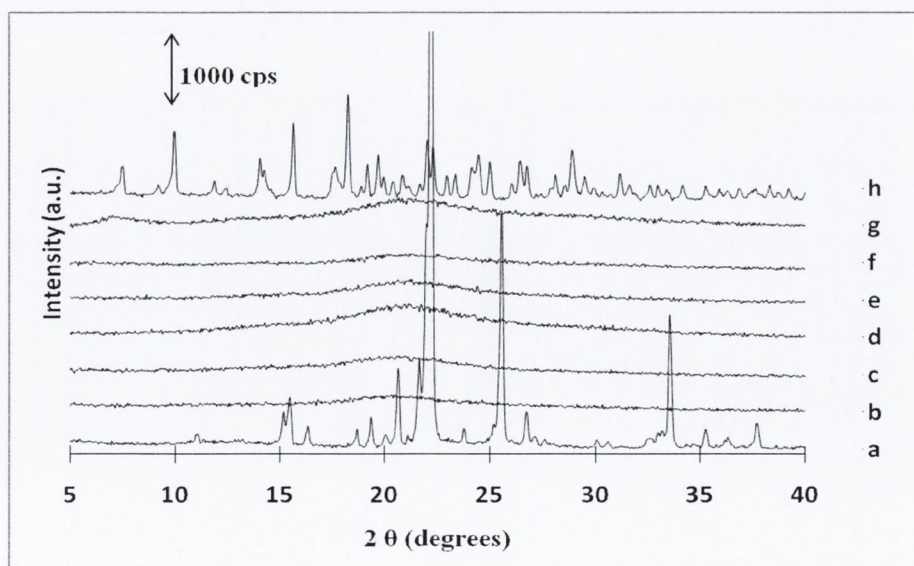


Figure 5.1: PXRD patterns of: (a) unprocessed ST (form III); b) spray dried ST; c) spray dried ST 9:1; d) spray dried ST 3:1; e) spray dried ST 1:1; f) spray dried ST 1:3; g) spray dried STNa; h) unprocessed STNa.

All ST:STNa spray dried composites presented a diffuse halo pattern, characteristic of XRD amorphous materials (Figure 5.1). The ST:STNa ratio employed and the storage conditions influenced the physical stability of the processed powders. For example in desiccated conditions at 5°C, by adding just 10% w/w of the salt form, the resulting composite remained amorphous for ~2 months as observed by PXRD. Higher amounts of salt in the composites increased the stability by up to 5 months for ST 3:1 and by six months for ST 1:1 and ST 1:3. SEM images showed that ST:STNa composite samples were homogeneous and consisted of spherical smooth particles with surface indentations for systems comprising up to 50% w/w STNa (Figure 5.2a-b-c).

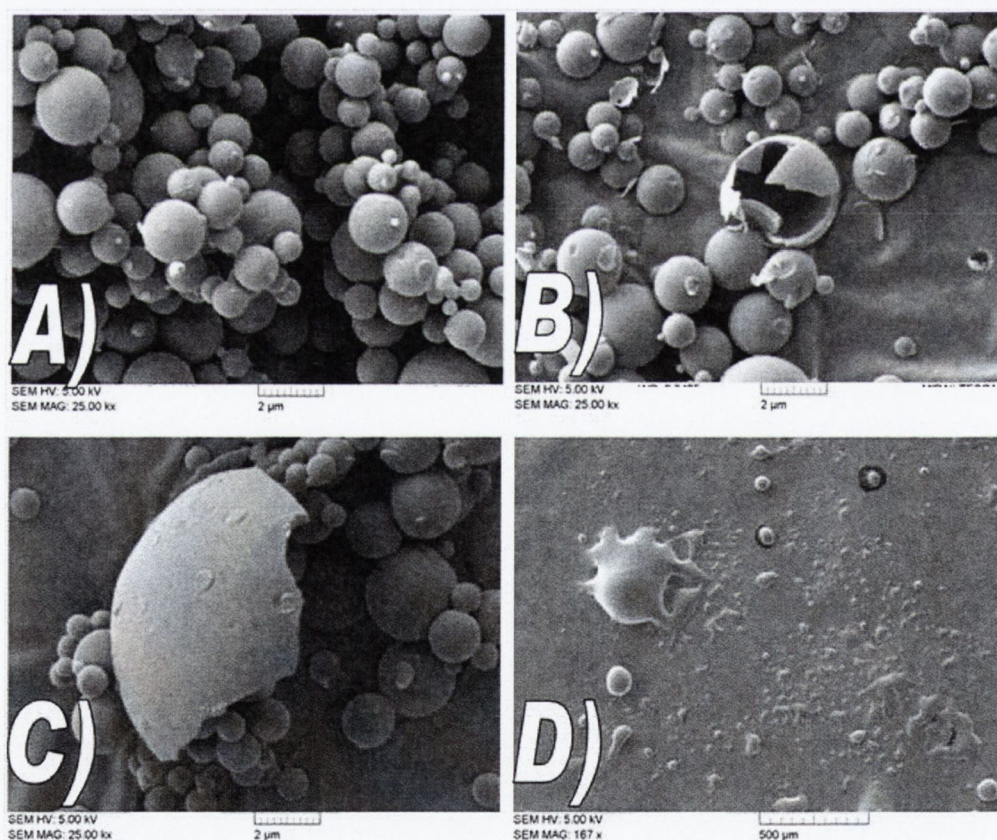


Figure 5.2: SEM micrographs of: a) spray dried ST 9:1; b) spray dried ST 3:1; c) spray dried ST1:1; d) spray dried ST1:3.

In contrast, no discrete particles were detected by SEM for a higher STNa content. Both ST 1:3 (Figure 5.2d) and STNa deliquesced, indicating a higher affinity of these two samples for water compared to the other systems. Previously reported thermal analysis of pure spray dried ST showed an exotherm of crystallization at $79 \pm 0.5^\circ\text{C}$ followed by an endotherm of melting at $201 \pm 0.5^\circ\text{C}$ while the amorphous salt crystallised above 160°C and melted at $268 \pm 0.2^\circ\text{C}$ (Chapter 4).

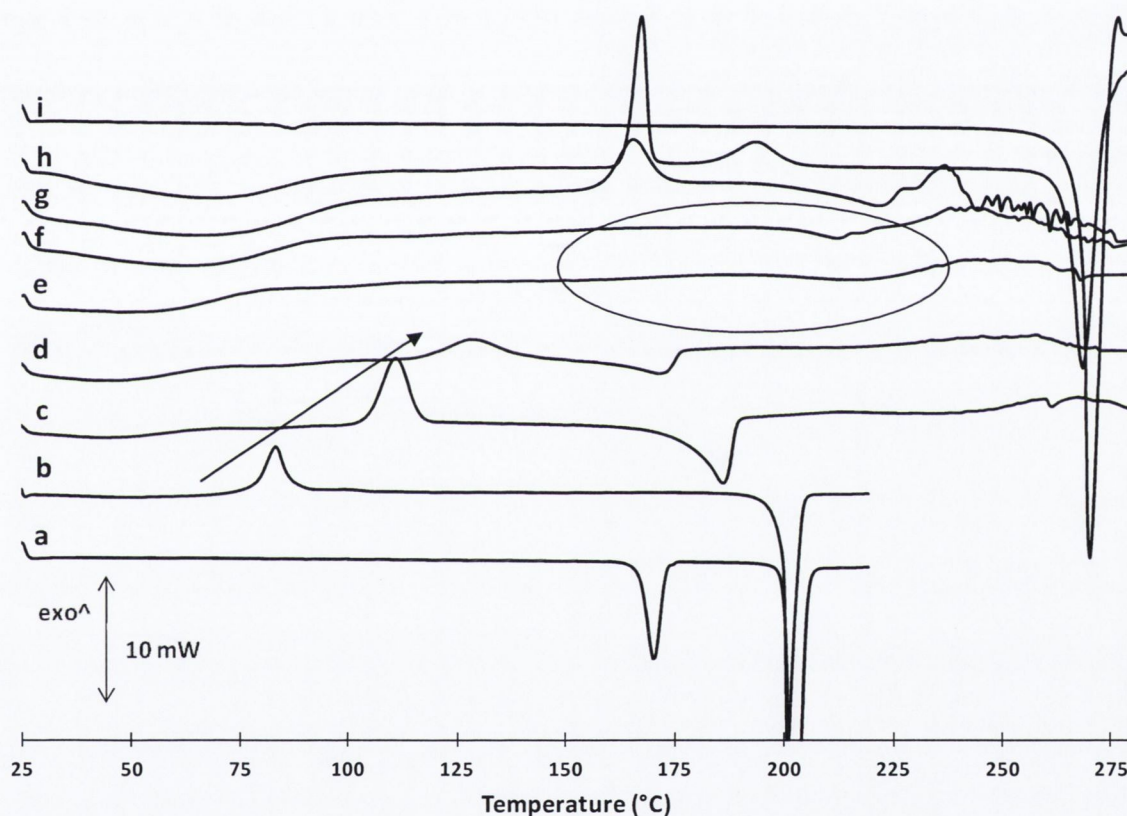


Figure 5.3 Heat flow thermograms of: (a) unprocessed ST (form III); b) spray dried ST; c) spray dried ST 9:1; d) spray dried ST 3:1; e) spray dried ST 1:1; f) spray dried ST 1:3; g) spray dried ST 15:85 h) spray dried STNa; i) unprocessed STNa. (Shift of exothermic peak indicated by the arrow while inhibition of crystallisation is indicated by the circled region)

Spray dried ST 9:1, ST 8:2, ST 3:1 and ST 15:85 (Figure 5.3) presented one endothermic event of melting. These composites also showed one exotherm of crystallisation (indicated by the arrow in figure 5.3) with onset ranging between those of the pure

materials. In contrast ST 6:4, ST 1:1, ST 4:6 and ST 1:3 did not show either exothermic or melting peaks on the thermograms. The inhibition of crystallisation upon heating (at 1 or 10°C/min) for these mixtures (within the circle in figure 5.3) could be due to the development of molecular interactions between ST:STNa for these specific ST:STNa ratios (Tong and Zografi, 2001).

The glass transition temperature (T_g) for pure ST and STNa were previously found to be $\sim 59^\circ\text{C}$ and $\sim 120^\circ\text{C}$ respectively. To determine the T_g s of the various composites and distinguish between thermal events which could happen simultaneously upon heating, MTDSC was employed in this work.

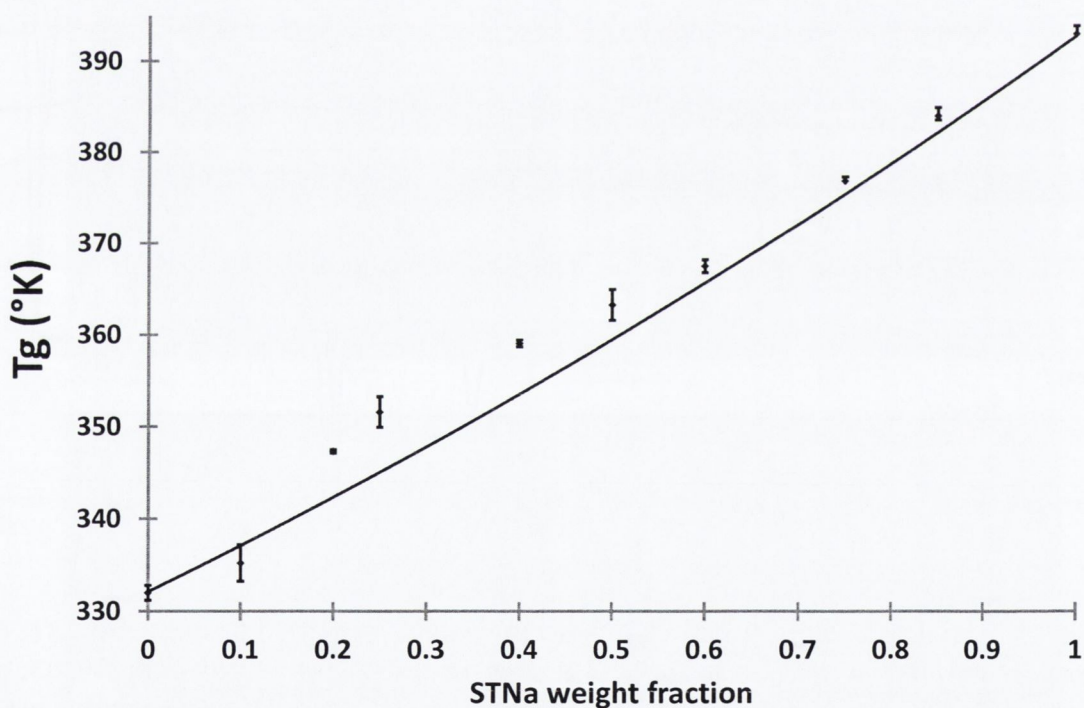


Figure 5.4: Glass transition temperatures of ST:STNa systems as a function of STNa content (squared markers). The solid line represents the T_g predictions based on the Gordon-Taylor with Simha-Boyer rule equation.

All reversing heat flow thermograms recorded for the different spray dried systems showed a single T_g , with values between those of the pure materials and increasing with

the STNa content. According to several authors (Bosma et al., 1988; Caron et al., 2011; Tong and Zograf, 2001) the detection of a single T_g is indicative of homogeneous amorphous phases (molecular dispersions). Therefore, thermal analysis revealed that the increase of physical stability was due to the introduction of STNa in the mixture which shifted the T_gs to higher temperatures. Measured T_gs and T_g values calculated using the Gordon Taylor with Simha-Boyer rule (GT) (Caron et al., 2011; Tajber et al., 2005) were plotted versus STNa weight fraction (Figure 5.4). The true densities for the single amorphous components of 1.52 g/cm³ and 1.57 g/cm³ for ST and STNa respectively, were used to obtain the K factor to calculate the GT-SB T_g theoretical values as described in Chapter 2, section 2.2.14. The T_gs of the composites deviated positively from the GT predicted values. The Gordon-Taylor equation is widely accepted to predict the T_g of mixtures. The theory affirms that in the ideal mix free volumes are additive and no interaction between the components takes place during mixing (Caron et al., 2011). However, because of the presence of interacting groups in either species, the ST-STNa mixture could in theory result in the formation of intermolecular bonds, such as hydrogen or ion-dipole bonding, which should cause an increase in T_gs compared to the predicted values. For example Tong and Zograf showed positive deviations of T_g from GT predicted values when indomethacin was co-processed with its corresponding sodium salt, suggesting a stronger acid-salt interaction in the amorphous state than that between acid-acid and salt-salt (Tong and Zograf, 2001).

5.3 FTIR analysis

FTIR spectroscopy has been used to investigate molecular interaction between species, included in composites (Caron et al., 2011; Tong and Zograf, 2001). FTIR spectra (1800-1000 cm⁻¹) of spray dried ST, STNa and ST mixed in different proportions with STNa are

shown in Figure 5.5A. Peaks shifts of different magnitude were recorded depending on the STNa content, indicative of interactions between the two species (Caron et al., 2011; Tong and Zograf, 2001).

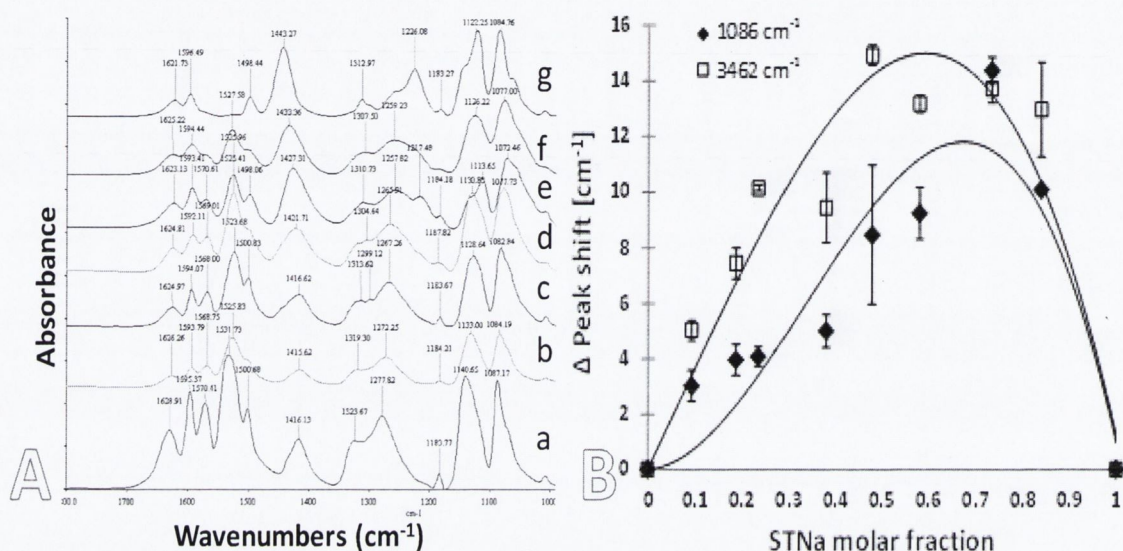


Figure 5.5A: FTIR spectrum of a) spray dried ST; b) spray dried ST 9:1; c) spray dried ST 3:1; d) spray dried ST 1:1; e) spray dried ST 1:3; f) spray dried ST15:85 and g) FTIR spectrum of spray dried STNa. **5.5B:** Job plot representation

For example, in the 3000-3500 cm^{-1} region, the N-H₂ asymmetric stretch peak, which in the spectrum of pure ST appears at $\sim 3462 \text{ cm}^{-1}$, shifted to lower wavenumbers. The shift to lower wavenumbers can be due to weakening of the N-H bond as a result of a stronger involvement in H-bondings (Kaushal et al., 2008; Tang et al., 2002). The simultaneous shift to higher wavenumbers of the C-NH₂ stretching peak ($\sim 1417 \text{ cm}^{-1}$ on the spectrum of ST), confirmed the NH₂ group being increasingly involved in H-bonds (Figure 5.5A). In contrast the stretching peaks recorded at 3363 and 3221 cm^{-1} remained relatively at the same positions in the spectra of all the composites. In the 1000-1600 cm^{-1} region, shifts to lower wavenumbers were seen for the peaks at 1140 and 1084 cm^{-1} characteristic of the stretching of both symmetric SO₂ and C-S peaks (Hu et al., 2010). These shifts to lower

wavenumbers suggested the SO_2 group as the H-bond acceptor and the development of $\text{N-H}\cdots\text{O}$ bondings. This type of interaction was previously described to link the dimers of ST in the polymorph I (Parmar et al., 2007).

The stretching peak shifts of N-H_2 and C-S for the different composites were plotted against the mole fraction of STNa to create a Job plot representation (Fig 5B) in order to determine the stoichiometry of the interaction involving $-\text{NH}_2$ and $-\text{SO}_2$ groups (Likussar and Boltz, 1971). The STNa molar fraction associated to the maximum of the Job plots, obtained at two wavenumbers, were between 0.6 and 0.7. The ST:STNa molar ratio of 1:2 lies between these two molar fractions. Therefore from the plot it appears that one molecule of ST interacted with two molecules of STNa. This interaction between ST and STNa could be responsible for the lack of thermal events observed on the DSC thermograms obtained for the ST 4:6 and ST 1:3 as the ST: STNa molar ratio of 1:2, which is estimated to correspond to the system ST 35:65, falls between these two composites.

5.4 iGC analysis

iGC was used to more fully investigate the surface of the systems and to assess the possibility of interactions between ST and STNa at the surface of the particles. Several phenomena of pharmaceutical importance start at the surface, and are critically affected by the surface properties of the substances involved (Buckton and Gill, 2007; Puri et al., 2010). Surface solid-liquid interactions for example, besides affecting processes such as dissolution, can have a deep impact on the stability of the solid, powder flow etc., and are, above all, governed by solid surface free energy (γ_s^T) (Puri et al., 2010). Generally a substance in its amorphous form has a higher γ_s^T than the corresponding crystalline form

because of a more random orientation of molecules exposing higher surface energy groups at the particle surface (Brum and Burnett, 2011; Newell et al., 2001a). This γ_s^T difference can have a significant impact on the behaviour of the two solid states upon processing. Differences in the γ_s^T can also be displayed by amorphous samples of the same material obtained with different processing techniques and changes with time due to relaxation can affect the γ_s^T of amorphous material upon storage (Buckton and Gill, 2007).

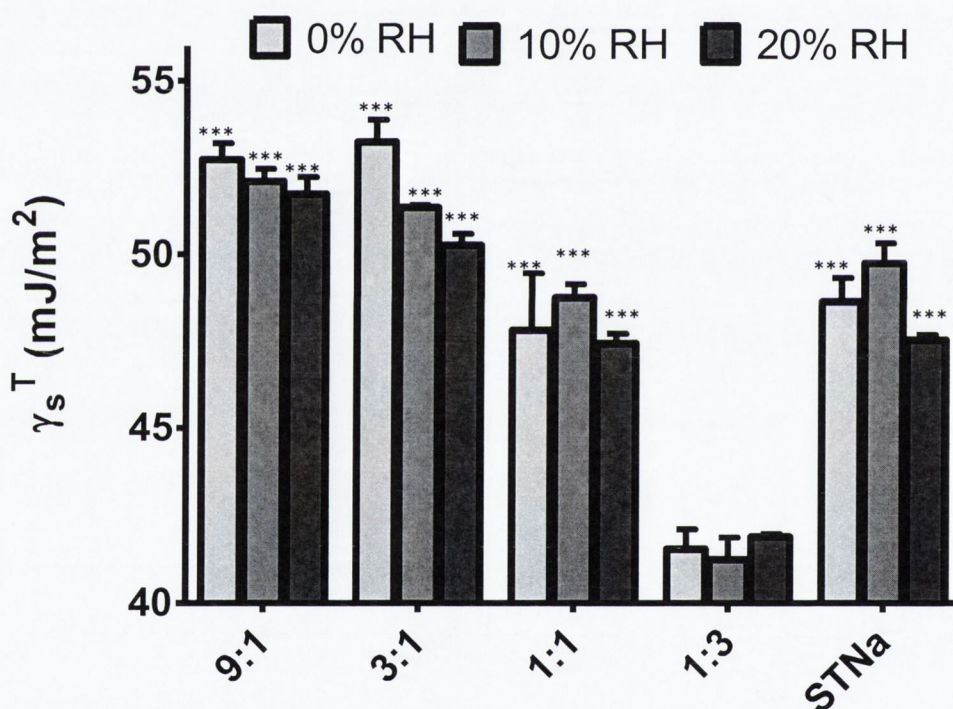


Figure 5.6: Total surface free energy for the different weight ratios (ST:STNa) at different %RH. Statistical analysis compares data obtained at the same RH value. System ST 1:3 was taken as reference of comparison for statistical post-hoc analysis. *** P<0.001

As a consequence of the development of interaction between the species included in the processed mixtures variations of the γ_s^T among the various systems would be expected.

STNa and four different composites were analysed by iGC. The γ_s^T values measured for ST 9:1 and ST 3:1 were not significantly different and found to be the highest among all systems at $\sim 53 \text{ mJ/m}^2$ (Figure 5.6). The increase in STNa content to ST 1:3 decreased significantly the γ_s^T values down to $\sim 41 \text{ mJ/m}^2$ ($P < 0.001$). Then γ_s^T rose up again for the pure amorphous salt reaching $\sim 48 \text{ mJ/m}^2$ (Figure 5.6). The minimum of γ_s^T obtained for ST 1:3 could be due to a different organisation and/or to the development of interactions between the molecules at the surface of the particles, decreasing the number of chemical groups available to interact with external molecules such as the probe molecules. Moreover, changes in ST:STNa ratio also influenced the polarity of the powder surfaces

as shown by the variation in the polarity index (γ_s^d) in Figure 5.7A.

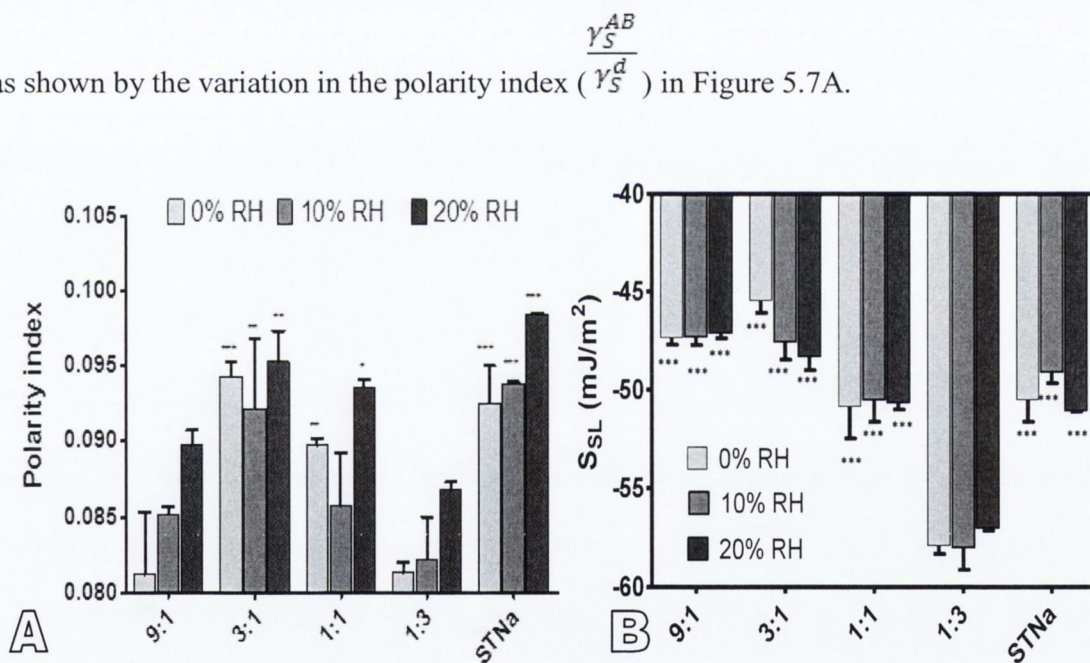


Figure 5.7: Polarity index (A) and spreading coefficient (B) changes for different weight ratios and %RH. Statistical analysis compares data obtained at the same RH value. System ST 1:3 was taken as reference of comparison for statistical post-hoc analysis *** $P < 0.001$, ** $P < 0.01$, * $P < 0.05$.

An increase in salt content from ST 9:1 to ST 3:1 raised the polarity index, reaching a value similar to that obtained for pure amorphous STNa. However, a further increase (in salt content) to ST 1:1 and ST 1:3 reduced the surface polarity. The ST:STNa molar ratio

1:2 falls between that of these two systems (i.e. ST 1:1 and ST 1:3) which supports the concept of the development of the 1:2 interactions, as previously suggested by FTIR spectroscopy. Therefore, ST-STNa interaction should involve polar bonding, decreasing the amount of polar chemical groups available at the surface to interact with the probe molecules.

Water adsorption is strongly influenced by surface polarity (Bradley et al., 2010). In particular, water vapor molecules can interact with solids through specific hydrogen-bonding with surface polar groups. Furthermore, when the solid is ionic, water molecules can interact with the components of the solid through ion-dipole interaction. For amorphous solids, the wettability and interaction with water are fundamental aspects to be studied because they can affect both dissolution properties (Puri et al., 2010) and physical stability (Hancock and Zografis, 1994; Puri et al., 2010). Both STNa and ST 1:3 deliquesced when exposed to ambient humidity conditions. Hence, the interaction of the composites with water was investigated by calculating the powder wettability and analysing the water vapor sorption isotherms. The wettability of a powder by water depends on both the work of adhesion of the water onto the powder surface (W_A) and on the water work of cohesion (W_C). Complete spreading of the water over a powder is possible if the work of adhesion onto the surface is equal to or higher than the work of cohesion among the water molecules (Zdziennicka and Jańczuk, 2010). This difference equals the spreading coefficient (S_{SL}).

The S_{SL} of water over the composites, for various %RH, is reported in Figure 5.7B. For all systems the S_{SL} was negative, indicating that the spreading of water on the powder surface is not favoured and requires work. For each system, S_{SL} was not affected by a change in the %RH from 0% to 20% but changed depending on the ST:STNa ratio. Mainly, an

increase in salt content from ST 3:1 to ST 1:3 decreased the S_{SL} , indicating a decrease in water affinity to the powder surfaces.

5.5 DVS analysis

The overlaid DVS 1st sorption isotherm plots of the systems indicated that the whole/entire water uptake increased with the increase of salt content over the entire RH range (Figure 5.8).

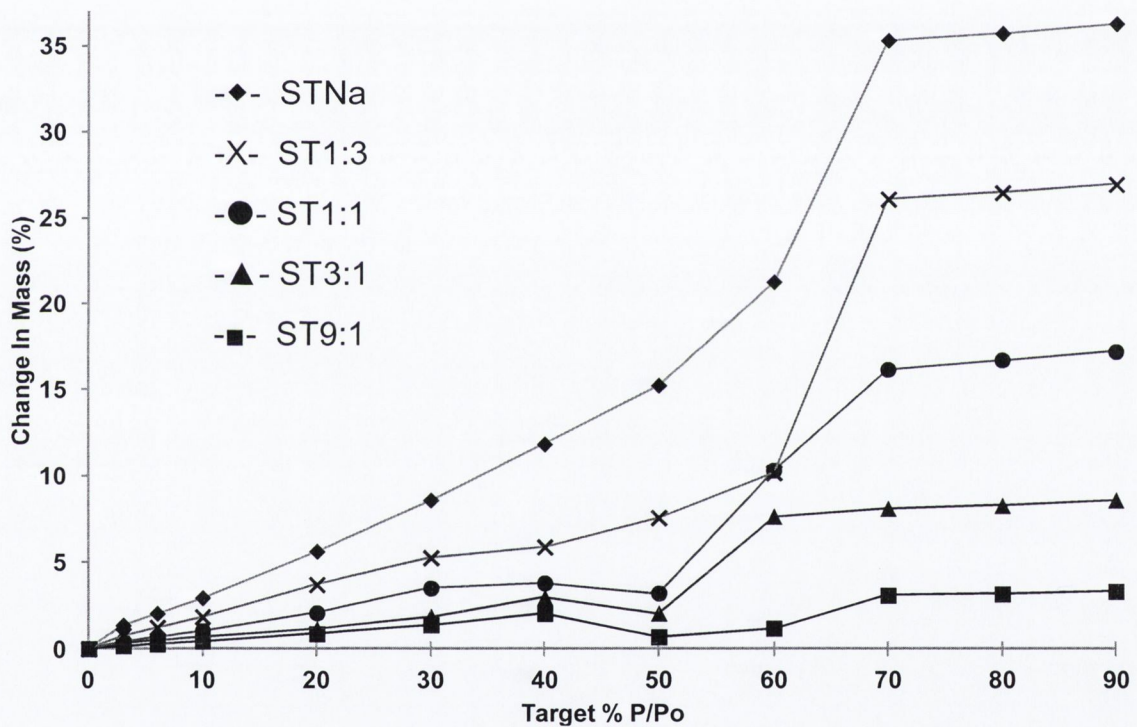


Figure 5.8 Water sorption isotherms for different ST:STNa weight ratios.

The mass gain recorded at 90% RH was linearly proportional to the STNa content in the composites. For instance, spray dried STNa mass uptake was 36% w/w of the dry mass and decreased to 3.6% w/w for ST 9:1. The coefficient of determination (r^2) of the linear fit was 0.99. As previous studies (Chapter 4 section 4.8) on the hygroscopicity of ST after

spray drying indicated that the API had a maximum water uptake of only 0.5% at 90% RH, the water uptake for the blends is primarily due to the salt.

The kinetic profiles obtained for systems ST 9:1 (Figure 5.9A), ST 3:1 and ST 1:1 showed continuous water uptake versus time before reaching equilibrium for each % RH steps up to 40% RH. For these systems during the 50% RH step an initial mass increase was followed by a decrease in mass (indicated within the circle in Figure 5.9A). A similar behaviour was also seen for ST 1:3 but the decrease in mass was lower, recorded at a lower RH and in the two following steps at 30% and 40% RH (Figure 5.9B). A decrease in mass versus time with increasing RH for amorphous substances corresponds to the crystallisation of the material (Burnett et al., 2006). The mass loss is attributed to water loss due to the reduced hygroscopicity of a new crystalline phase compared to the amorphous form. Therefore the content of salt in the mixtures influenced the RH at which crystallisation took place by promoting the water uptake which acts as a plasticiser for the mixture. In contrast the kinetics for the pure amorphous STNa did not show any mass loss but a continuous increase in mass with increasing RH (Figure 5.9C).

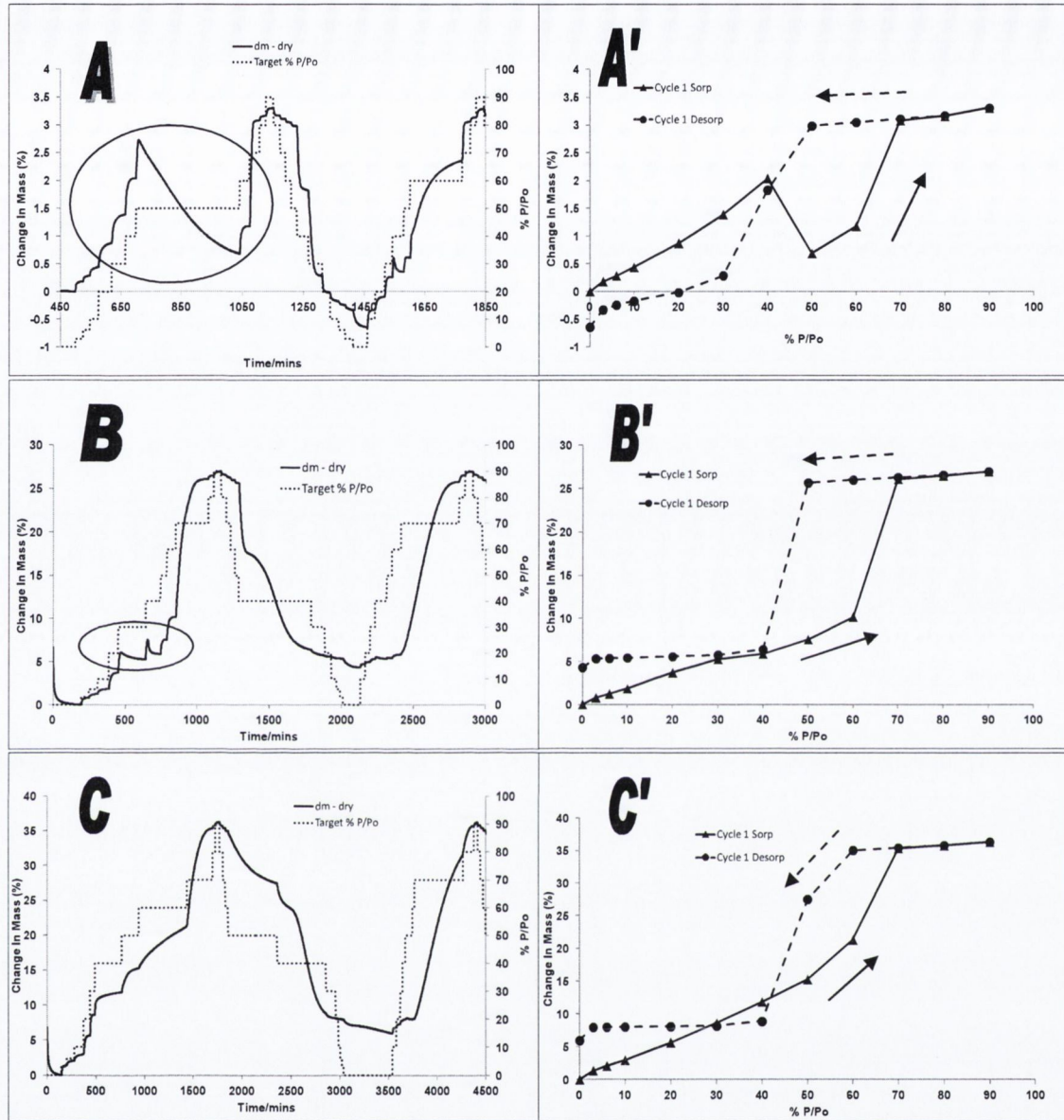


Figure 5.9 DVS kinetics (A, B, C) and isotherms (A', B', C') of: A-A') spray dried ST 9:1; B-B') spray dried ST 1:3; C-C') spray dried STNa. (Water induced crystallisation is indicated within the circled region)

Generally, crystalline solids with high solubility such as salts may deliquesce at a RH value lower than 100%, defined as RH_0 , which is characteristic of the material and related to its solubility (Van Campen et al., 1980). RH_0 of a crystalline compound can be determined from the moisture sorption isotherm as a sharp break due to a sudden change in water uptake which takes place at deliquescence (Hiatt et al., 2011). In contrast, when dealing with amorphous solids, deliquescence can be regarded as a non-equilibrium phase

transition because water uptake by amorphous substances proceeds in a gradual way and their transformation from solid to liquid state may involve intermediate semi-solid stages (Mikhailov et al., 2009). It was not possible to determine the RH of deliquescence for amorphous STNa either from the water sorption isotherm (Figure 5.9C) or the corresponding kinetics (Figure 5.9C'). Therefore two experiments were carried out to investigate at which RH deliquescence of amorphous STNa would be favoured. PXRD analysis on the amorphous salt after equilibration at 20% RH in the DVS cabinet indicated that the powder remained amorphous. However, when the amorphous STNa was stored in humidity controlled devices (Amebis), it was seen to transform into a viscous liquid solution when exposed to RH conditions at and above 35%, indicating that the range of RH of deliquescence was between 20 and 35%.

Both ST 1:3 and STNa recorded mass uptake of respectively ~4.3% and 7% at the end of the first cycle. The water uptake for amorphous STNa, as previously described in Chapter 4, was attributed to the crystallisation of the amorphous salt to a sesquihydrate (Chapter 4 section 4.12). PXRD analysis performed at the end of the water sorption isotherm confirmed that ST 1:3 converted to the same hydrate. In contrast at the end of the first cycle ST 9:1 ST 3:1 and ST 1:1 lost ~ 0.6, 0.7 and 0.7% of mass respectively. The mass losses for ST 9:1 ST 3:1 and ST 1:1 suggested that the composites did not completely dry at the end of the pre-treatment stage (drying under nitrogen flow). However after a second full sorption desorption cycle all samples were characterised by mass uptake, except ST 9:1. As for STNa and ST 1:3, PXRD measurement performed at the end of the water sorption isotherm confirmed that both ST 3:1 and ST 1:1 had converted to the same hydrate.

Additional mass losses of lower magnitude compared to the ones in the first cycle in the 2nd sorption cycle (Figure 5.9) were detected in the kinetics for all composites. These

mass losses indicated a not complete (partial) crystallisation of the amorphous systems at the end of the first sorption cycle. Full crystallisation following exposure to a first full 0-90% RH cycle was not achieved, this may be attributed to water not completely penetrating the bulk of the composites.

If we consider the adsorption process as the only mechanism of interaction between water and the powders, the higher the surface energy, surface polarity and spreading coefficient the greater the expected water uptake. However the surface properties measured for the different composites did not correlate with the whole water uptake isotherms. The γ_s^T of ST 9:1 and ST 3:1 were greater than those of STNa, ST 1:1 and ST 1:3, respectively. Nonetheless, ST 9:1 and ST 3:1 were characterised by lower water uptake compared to the other systems. Despite the lowest γ_s^T profile (Figure 5.6) among all systems the water uptake of ST 1:3 was the second highest, lower only than STNa. According to the spreading profile ST 9:1 and ST 3:1 would be expected to better interact with water molecules than ST 1:3 which had the lowest spreading coefficient followed by STNa, in contrast to DVS analysis. However amorphous materials can either adsorb water, or absorb it in the bulk of the material (Agrawal et al., 2004; Alvarez-Lorenzo et al., 2000; Bravo-Osuna et al., 2005). Hence, the distribution of water in the different systems was determined by establishing quantitative correlations between equilibrium moisture content and the %RH using the Young and Nelson equations (Agrawal et al., 2004; Alvarez-Lorenzo et al., 2000; Bravo-Osuna et al., 2005; Tewes et al., 2010). Fitting DVS data with the Young–Nelson equations indicated that the water distribution within the different systems was dependent on the ST:STNa ratio. For ST 9:1, adsorption was the main process of water uptake, as can be confirmed by the high value of the A parameter, compared to the B parameter of the Young-Nelson equations (Figure 5.10).

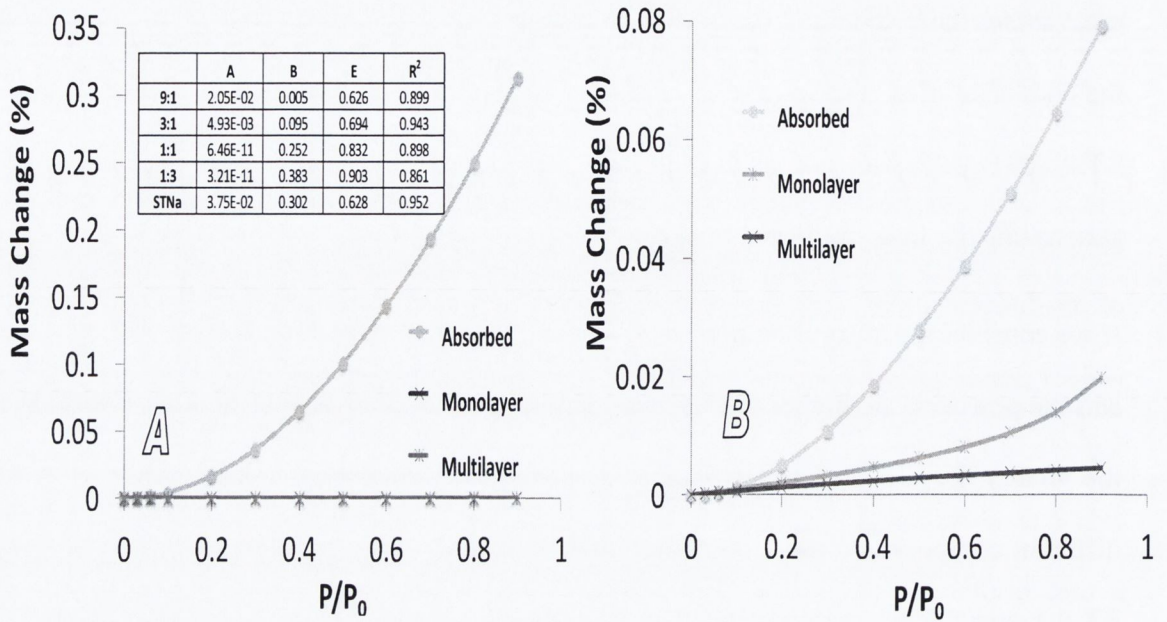


Figure 5.10: Moisture distribution patterns for 1:3 (A) and 3:1 (B) samples obtained by fitting experimental DVS results with the Young and Nelson equations. Estimated A, B, E Young and Nelson parameters and fit correlation coefficient for all the composites investigated are inserted in the chart (A).

It was found that an increase in STNa content increased the proportion of water absorbed, and water sorption for ST 1:1 and ST 1:3 was mainly by absorption. Figure 5.10 shows a comparison of the Young and Nelson distribution patterns of water obtained by fitting DVS results for two systems (A) ST 1:3 and (B) ST 3:1 which are characterised respectively by low and high surface free energy. Most of the water uptake by ST 1:3 was absorbed in the bulk while only a minute amount was adsorbed on the surface. In contrast the water uptake for the higher γ_s^T system ST 3:1 was due to both adsorption and absorption. The higher amount of water adsorbed by ST 3:1 compared to ST 1:3 is consistent with the surface profiles for the two different systems. (Differences between the amounts of water adsorbed and absorbed also is consistent with the composites having additional mass losses in the 2nd DVS cycle). Therefore the ratio ST:STNa influenced not

only the total hygroscopicity but also the water distribution in the different systems and this may have an important impact on the physical stability of the powders. Several authors have attributed the water uptake by amorphous materials mainly to absorption processes (Alvarez-Lorenzo et al., 2000; Bravo-Osuna et al., 2005; Hancock and Shamblin, 1998). However, according to this study the main water sorption mechanism for the system ST 9:1 was by adsorption with a minimal amount of water absorbed.

Among the various ST:STNa co-spray dried systems produced and analysed, ST 1:1 and ST 1:3 resulted the most physically stable when stored in desiccated conditions. However, on exposure to environmental humidity ST 1:3 deliquesced while ST 1:1 remained stable in its powder state. This indicates ST 1:1 as the most favourable w/w ratio overall.

5.6 Conclusions

This study showed that an extremely unstable amorphous API like sulfathiazole can be protected from crystallisation by co-spray drying it with its corresponding sodium salt form. In particular the addition of just 10% w/w salt was enough to delay the crystallisation of the resulting powder from 1 hour to 60 days of storage under desiccated conditions. Increasing the proportion of salt in the composite further improved the storage stability; however this was opposed to an increased hygroscopicity. The increased physical stability is attributed to interactions between the species which cause the shift of T_g to higher temperature. FTIR spectroscopy, iGC and thermal analysis suggested interactions between the species with a stoichiometry of 1 molecule of acid for 2 molecules of salt. For the systems investigated, by analysing the hygroscopic properties it has also emerged that water uptake by an amorphous material could either be mainly by adsorption or by absorption depending on the chemical nature of the material, with the salt facilitating water absorption. Therefore controlling the physico-chemical properties of the composites by varying the ratio of the components can be beneficial to stabilise amorphous formulations. For example among the ST:STNa composites an optimum mixture which provided the best compromise between hygroscopicity and stability was the 1:1 w:w system. In this ratio the amorphous powder was characterised by good physical stability, intermediate water uptake and low surface free energy.

Chapter 6

General discussion

6.1 Introduction

The research presented in this thesis focuses on the impact that the spray drying process has on two sulphonamide compounds and their sodium salts. In particular, it examines the potential of tuning their physical state to produce (metastable) crystalline and amorphous powders. The physico-chemical stability of the resulting powders is also investigated as well as eventual strategies to apply in order to improve the performance of such metastable systems. The model drugs selected were sulfadimidine and sulfathiazole. The selection criteria were based on several factors. The initial focus was to investigate the impact of processing on compounds which provided an adequate balance of chemical similarity, in terms of an identical core structure, and chemical diversity manifested by substitution of the pyrimidine ring in sulfamethazine with a thiazole ring in sulfathiazole. Moreover both weakly acidic drugs are able to be obtained as sodium salt forms.

Spray drying, together with milling and micronisation, is a common pharmaceutical technique employed to reduce the particle size of a pharmaceutical substance. It is well known that these techniques often induce polymorphism and/or produce materials characterised by variable degrees of disorder, which alters their physicochemical properties and may be the cause of problems in manufacturing processes. Therefore, for many years, amorphisation and polymorphism were viewed as problematic and were avoided where possible. Nowadays the use of metastable forms is becoming part of the product development strategies in many pharmaceutical and food industries. Thus, the purpose of the present study was to utilise spray drying intentionally as a technique to produce metastable forms, and to characterise, understand and finally, attempt to exploit them. Therefore, an in-depth study of the physicochemical characteristics of the spray dried materials was undertaken and

comparisons made with the unprocessed equivalent systems. The study then proceeded to analyse the main problematic issues affecting the spray dried materials in terms of physical stability of the solid state obtained, the behaviour on storage at different temperature and RH values, and the hygroscopicity of the materials. Throughout this work, particular focus was directed at how to increase product shelf life, a crucial factor in determining the development of metastable formulations on the market. Therefore a potential strategy to enhance the stability of metastable forms was explored by co-spray drying the non ionised and salt form together at various w/w compositions.

6.2 Spray drying of sulfadimidine (SD) and sulfathiazole (ST)

An important aspect of amorphous drug development via spray drying is drug solubilisation. The first step in producing a drug in a metastable form via spray drying consists of making a solution of the compound of interest. For poorly soluble water compounds, the selection of appropriate solvents is fundamental. The solvents chosen in this thesis were based primarily on their low toxicity, combined with the suitability of the solvents to dissolve both APIs. Two organic solvents were selected: ethanol and acetone. Both solvents are reported as belonging to Class 3 (ICH Topic Q3C R4, 2009). Class 3 includes solvents which do not present a human health hazard at levels normally accepted in pharmaceuticals and may be regarded having low toxicity and being of low risk to human health. Solubility studies on SD and ST were previously carried out by Nolan (2008). The author measured the solubility of both SD and ST in water, ethanol and ethanol:water co-solvent combinations (Figure 6.1).

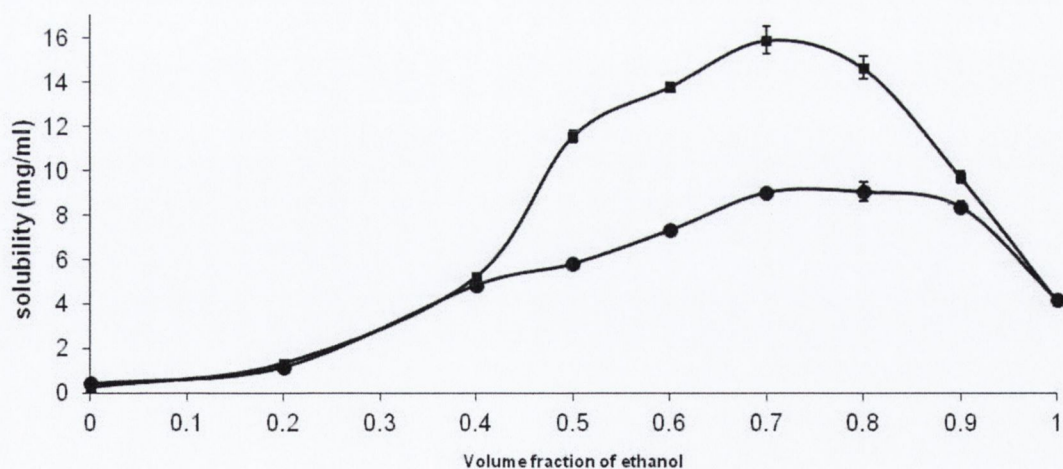


Figure 6.1 Ethanol:water solubility profile for sulfadimidine (—●—) and sulfathiazole (—■—) compounds at 25°C, the solubility of the solute plotted against the volume fraction of the mixed system (ethanol:water). Adapted from Nolan (2008).

The solubility in water was estimated to be 0.45 and 0.25 mg/ml for sulfadimidine and sulfathiazole respectively (Nolan, 2008). Ethanol was found to be a better solvent and the solubility for both APIs in ethanol was reported to be approximately 4 mg/ml (Nolan, 2008). The use of co-solvents is an effective means of solubilising hydrophobic drugs (Miyako et al., 2010) and combining ethanol with water proved effective at dissolving both sulphonamides at higher concentrations. The ethanol:water solvent fractions selected to perform spray drying in this project were those between 0.6 and 0.9 v/v so that the maximum solubility for these two systems could be obtained in such solvent systems (Figure 6.1).

Experimental work started with spray drying of SD. The background on spray drying of SD was set by the work of Nolan (2008). The author processed the API from several combinations of ethanol and water (80:20, 90:10, 95:5 v/v) and successfully produced amorphous systems. In this project following on the work of Nolan, some parameters were varied such as the feed concentration, inlet temperature, solvent and solvent ratio, to see if, by modifying the same alterations would result in the solid state nature of the API. ST was spray dried in identical conditions to those used for sulfadimidine, so as to allow for comparisons. For both APIs, the outlet temperature and the equipment configuration of open loop versus the closed loop mode were key factors impacting on the solid state nature of the materials. While the open mode always resulted in the amorphisation of the drug, provided that the outlet temperature was kept below the glass transition of the drug, the closed loop favoured the crystallisation of the APIs. A similar outcome was observed in the work of Paluch (2011). On spray drying chlorothiazide, different spray drying configurations resulted in differences in the physical state of the API, with processing in the open mode favouring amorphisation of the drug. It should be noted that in most pharmaceutical companies, open

loop is not recommended when spray drying from organic solvents and only nitrogen via closed loop is utilised due to safety concerns (Master, K., 2002; Buchi-B-290, 2007). Despite achieving more satisfactory results in obtaining amorphous substances and formulations from using the open mode technique in this work, as mentioned above, in the wider context at industry scale, there is still much reluctance to exploit this methodology. Health and safety criteria are the main reason underlying this bottleneck. The issue at stake however, is that a large number of drugs under development have poor bioavailability due to low aqueous solubility. This percentage is likely to increase in the future with the greater use of combinatorial chemistry in drug discovery targeting lipophilic receptors. Poor bioavailability results in increased development times, decreased efficacy, increased inter- and intra-patient variability and side-effects, and higher dosages that reduce patient compliance and increase cost. Thus the ability to improve drug solubility and, hence, bioavailability through the use of amorphous formulations has enormous implications. Pharmaceutical process technology, critical to improving drug product efficacy, and reducing cost is fundamental in terms of this new challenge. As concerns spray drying on a small scale, many reports in the literature present results based on open-loop systems only, even when spray drying from non-aqueous solvents. In the light of the above however, focus should also be addressed to scaling up open mode spray drying techniques to industry level. The impact of different equipment set-ups on the processed materials as well as the applicability of both configurations, open loop versus closed loop is discussed in more depth in Chapters 3 and 4.

6.3 Comparing differences in the tendency to crystallisation of SD and ST from the amorphous state

Prior to undergoing the spray drying process, both sulfadimidine (SD) and sulfathiazole (ST) were dissolved in suitable solvents in order to produce liquid solutions. A solution is defined as a mixture of two or more components which form a single phase, homogeneous at the molecular level (Aulton, 2002). This implies that the API molecules are randomly dispersed among the solvent molecules and therefore in a disordered state. After spray drying both drugs solidified as amorphous phases, in other words in a disorganised state. Following the spray drying process, the non crystalline nature of the processed materials were assessed by subjecting the two APIs to PXRD which provided patterns characterised by the absence of Bragg peaks. Although XRD is used to study the molecular arrangement in crystalline solids, it can be used to indirectly assess the absence of organisation associated with amorphous materials. However, when dealing with amorphous substances, XRD has to be/should be supported by complementary analytical techniques, such as thermal analysis, in order to assess the physical state of the substance. For instance, thermal analysis provided useful information on the characteristics of both spray dried APIs. DSC analysis of amorphous SD and ST enabled the identification of their glass transition temperatures, and it was found that the T_g of SD (~80°C) was nearly 20°C higher than that of ST (~ 60°C). Moreover the onset of crystallisation of SD was recorded at ~100°C, almost 20°C higher than that of ST, which took place at 80°C, indicating that the two amorphous phases were distinguished by a different degree of thermal stability, with SD the more stable. This characteristic was reflected also in the physical stability of the two amorphous APIs. When stored under identical conditions of RH and temperature, a greater tendency to crystallise was noted for

ST compared to SD. Spray dried amorphous ST was extremely physically unstable and started to recrystallise after less than one hour from the completion of the spray drying process, regardless of the temperature and RH of storage selected. In contrast, the recrystallisation tendency of SD was dependent on the storage conditions employed. However, in identical conditions of storage (5°C/ desiccated, 25°C/ desiccated or 25°C/ 60%RH), the findings regularly showed that SD was more physically stable than ST.

In a study by Caron et al. (2011), the author spray dried both SD and ST, which solidified respectively as an amorphous phase and the metastable polymorph I. Caron determined the thermodynamic driving force for crystallisation (i.e. free energy difference of a system in super-cooled liquid and crystalline state) and the relaxation function, a parameter of the molecular mobility of amorphous systems below T_g for both amorphous SD and amorphous ST (produced by melt quench). The authors found that amorphous SD was characterised by a greater driving force for crystallisation than amorphous ST but also that at a specific temperature below T_g , the molecular mobility of amorphous ST was greater than that of SD. They suggested that the solidification of SD as an amorphous phase and ST as polymorph I in the spray dryer environment was due to the fact that this process was mainly controlled by the kinetics of the amorphous state and less by the thermodynamic driving force of crystallisation (Caron et al., 2011).

In the current work, as presented in Chapter 4, ST was obtained in its amorphous state on spray drying. By lowering the inlet temperature compared to that used by Caron et al. (85°C to 78°C), the corresponding outlet temperature in the spray dryer was consequently reduced to a value (outlet temperature = ~50°C) below the T_g of the amorphous API, enabling the recovery of a completely amorphous powder. It is well known that the closer the temperature

of exposure of an amorphous system to the glass transition temperature the greater the possibility of inducing nucleation in the system because of increased molecular mobility (Hancock and Shamblin, 2001). It is hypothesised that in Caron et al.'s study the outlet temperature close to the T_g favoured the generation of some crystalline nuclei and since the more stable solid form (polymorph I being more stable than the amorphous form) had already nucleated, the tendency to convert the remaining less stable fraction during the duration/length of the spray drying process increased. A similar outcome was found in the present work for SD spray dried from ethanolic solutions with an inlet temperature of 120°C resulting in a corresponding outlet of 85°C , approximately 7 degrees higher than the T_g of amorphous SD. In this case the processed API solidified mainly as a crystalline material.

6.4 Comparison of solvent mediated polymorphic transformation and spray drying of ST

Sulphonamides exhibit interesting solid-state properties, including the ability for several of these drugs to exist in two or more polymorphic forms. Many drugs belonging to the class of sulphonamides were shown to give rise to polymorphism due to the presence of various hydrogen-bond donors and acceptors (Yang and Guillory, 1972). Despite being characterised by a similar chemical structure, SD is monomorphic (Maury et al., 1984), while ST is a highly polymorphic system, with five different polymorphs discovered and described so far (Chan et al., 1999).

The investigation of the behaviour of a highly polymorphic API upon spray drying and a comparison with that of its solidification from solvent evaporation were of interest as not

many studies have analysed the differences in the results deriving from the two processing techniques. In contrast, extensive research has been carried out on the crystallisation of sulfathiazole (ST) from different solvents with solvent evaporation techniques (Aaltonen et al., 2003; Anwar et al., 1989; Blagden et al., 1998; Khoshkhoo and Anwar, 1993; Parmar et al., 2007). Nevertheless there is a lack of consistency in the findings reported. For instance, several authors, albeit using the same solvent, produced different polymorphs.

ST can be isolated in five different polymorphic forms and its solidification from solution into a specific polymorph or into mixtures of polymorphs can be determined by the appropriate choice of: solvent, type of crystallisation process and specific process parameters. ST crystallisation from solution, regardless of the type of solvent employed, follows Ostwald's rule of stages, according to which, the first form to nucleate is always the highest free energy form. This is form I, which is characterised by the lowest activation energy of all the polymorphs (Blagden et al., 1998). According to Ostwald theory, this form should convert to the next most stable polymorph via its own dissolution and recrystallisation. The step by step process will continue, ending when the most stable form is present as a precipitate in the liquid medium (Threlfall, 2003).

According to Blagden et al. (1998), the solidification of a particular ST polymorph, other than the most stable form, is due to the fact that the molecules of solvent used in the process can inhibit nucleation and growth of the more stable subsequent form (Blagden et al., 1998). However, independently of the solvent chosen, form I is always the first form to nucleate from solution. Form I was seen to be based on structural basic units denominated as "α dimers" stabilised by 2 hydrogen bonds between the imine N2 and amino hydrogen H3. Conversely, the basic units characteristic of forms II, III, IV, denominated "β dimers", are

characterised by 2 distinct hydrogen bonds between one sulfate oxygen and aniline hydrogen (O2-H1) and aniline nitrogen to amino hydrogen (N1-H3) (Blagden et al., 1998). More recently, Parmar et al. (2007) calculated the theoretical energy released when the bonds in the α and β dimers are formed, defined as interaction energy. Following these calculations, Parmar demonstrated that β dimers were more stable than α dimers, confirming form I as the least stable of all ST polymorphs. ST from solution could solidify into pure form I when crystals were grown from n-propanol or n-butanol (Parmar et al., 2007). By calculating the thermodynamics of possible clustering of solvent molecules with sulfathiazole molecules, the authors explained that, with n-propanol and n-butanol, β dimerisation was inhibited because it was energetically disadvantageous compared to α dimerisation, and form I was the only polymorph that solidified from these solvents (Parmar et al., 2007). In contrast, the dissolution of ST in other solvents resulted in the solidification of other polymorphic forms or mixtures of ST polymorphs because β dimerisation was favoured. Form II, for example, was produced either from methanol (Parmar et al., 2007), boiling water (Khoshkhoo and Anwar, 1993), acetone (Aaltonen et al., 2003) and ethanol (Aaltonen et al., 2003); form III was obtained from 2-propanol (Parmar et al., 2007) or water (Khoshkhoo and Anwar, 1993) while form IV was favoured when crystals were grown from ethanol (Parmar et al., 2007), acetone (Khoshkhoo and Anwar, 1993) or water (Blagden et al., 1998).

Pure ethanol, acetone and mixtures of these organic solvents with water were used to prepare solutions of ST for spray drying in the current work, however, none of these solutions resulted in the production of the same polymorphs described above, obtained by using the corresponding solvents for crystallisation studies. The present study has however demonstrated that by accelerating the kinetics of solvent evaporation in a solidification

process, a drug can be induced to solidify in its metastable polymorph. Furthermore, it has been shown that spray drying may be used as an alternative technique to “classic” crystallisation from solvent evaporation, especially when dealing with highly polymorphic systems. Spray drying can be used to produce pure metastable polymorphs which traditionally may be hard to do with slow evaporation techniques. The production of only metastable (amorphous or polymorph I) forms of ST, despite the use of solvents which usually result in the production of different polymorphs, can be explained by the process of droplet evaporation which is faster compared to the characteristic times of crystallisation of the different polymorphs, as previously described in Chapter 4.

Another significant finding from this work is that by spray drying it is possible to obtain particles with no needle-like morphology. According to the literature, the morphology of sulfathiazole polymorph I and of several other metastable polymorphs is needle-like. This particular morphology in the pharma-industry is often considered adverse for secondary (drug product) processing as it frequently results in poor flowability. In our study we demonstrate the isolation by spray drying of spherical particles. The control of particle morphology in this manner may be applied to other active pharmaceutical ingredients.

6.5 (Water mediated) Recrystallisation from the amorphous state

Pharmaceutical solids may interact with water at each stage of pharmaceutical manufacturing and often a residual amount of water remains in the final solid dosage formulations. Pharmaceuticals may also be exposed to water during storage, if subjected to high humidity conditions or if dosage formulations contain hydrates capable of transferring moisture to other ingredients as a consequence of storage conditions. The physical and chemical

properties of pharmaceutical solids are critically dependent on the presence of moisture and specifically when the substance is in an amorphous phase. Water was a key factor in controlling the solid state nature of both APIs analysed (SD and ST) in the present pre-formulation studies.

Amorphous SD remained in the disordered state for a period of over 20 weeks when stored in desiccated conditions at 5°C. Regulatory guidelines require that physical stability is assessed at higher conditions of temperature and relative humidity. By increasing the temperature of storage to 25°C and 40°C, and the RH to 60% or 75%, respectively, Bragg peaks indicating the crystallisation of the API were clearly distinguishable on the PXRD pattern after only 1-3 days of storage.

The plasticising effect of water has been widely assessed by several studies (Levine and Slade, 1987; Ahlneck and Zografi, 1990; Burnett et al., 2004; Burnett et al., 2006). For example, Burnett et al. (2006) explained that water acts as a plasticiser by increasing molecular mobility, thus lowering the T_g and favouring crystallisation. Levine and Slade elucidated that the plasticising effect is due to the fact that water incorporated into an amorphous solid can greatly increase the free volume of the solid by reducing hydrogen bonding between the adjoining molecules of the solid with a corresponding reduction in its glass transition temperature (Levine and Slade, 1987).

Given that different solvents may plasticise amorphous systems to different extents, as a result of differing solubilities (Yoshioka and Tashiro, 2004), even the variation in storage temperature should be taken into account as the solubility and hydrophilicity of a substance varies with varying temperature. The physical stability at 60% RH of amorphous SD, for

example, was reduced from 4 weeks to 3 days when the temperature of storage was increased from 5°C to 25°C. These temperature values are both below the recommended temperature of storage for amorphous materials, dictated by the T_g -50°C (Yu, 2001 and Hancock et al., 1995), at which molecular mobility should be minimal. However, with an increase in temperature, it emerges that the solubility of a drug in water generally increases and, as a result, the plasticising effect of water is more apparent.

From the work described in Chapter 4, it was seen that the amorphous ST system can be tuned to recrystallise into a specific polymorphic form by controlling environmental storage conditions. The basis behind the recrystallisation of ST from the amorphous state is analogous to its solvent mediated recrystallisation from solution and both processes follow Ostwald's rule of stages. However this rule is not general (in effect, not all polymorphic systems behave in the same way). For instance, a comparison can be made here with the work of Yoshioka et al., (1994) on amorphous indomethacin. The author reported that indomethacin is able to crystallise from the amorphous state at temperatures below its T_g and that at a temperature below, or close to the T_g , it crystallises as the stable γ form. In contrast, at higher temperatures it mainly crystallises into the metastable α form (Yoshioka et al., 1994).

In another study by Andronis et al., 1997, it was shown that absorbed water vapour lowered the T_g , enhancing crystallisation and affecting the final polymorph of indomethacin produced. The authors showed that the crystallisation of the stable γ form was favoured at low water content while the metastable α form was favoured at higher water content (Andronis et al., 1997). In the present study, amorphous ST always crystallised as polymorph I, the least stable form among the various polymorphs, regardless of the

temperature of storage employed in the study. The behaviour characterising amorphous ST is different to that described for indomethacin. Under dry conditions, at or below 35% RH, therefore at low water content levels, full recrystallisation to form I, the most metastable polymorph, was produced. This was consistent with the crystallisation of amorphous ST into pure form I upon heating when subjected to DSC analysis. Nitrogen provides an inert water-free environment in the DSC oven and this kind of analysis always results in the crystallisation of the amorphous drug into form I. In contrast, an increase of the RH of storage to or above 55%, resulted in the crystallisation of mixtures of different polymorphs including the most stable form III.

6.6 Comparing hydration of crystalline and amorphous salts

Spray drying the salt forms of the two APIs appeared to be a promising strategy for stabilising amorphous drugs. Not only the melting point, but also the Tgs were greater than those of the corresponding non ionised drugs, which is generally indicative of an enhanced stability. However the hygroscopicity of the salt forms does affect their physical stability. By combining dynamic vapour sorption, thermal analysis and PXRD diffraction it was possible to monitor the structural changes in the solid state of the salt forms, leading to the formation of hydrates and the reversibility of these phenomena. PXRD patterns collected after equilibrating the materials at predetermined RH values enabled hydration and dehydration phases to be followed efficiently. DSC and TGA thermograms complemented the diffraction patterns as dehydration phenomena are characterised by heat flow variation and mass loss. Additionally, the relative hygroscopicities of amorphous STNa and SDNa were analysed by

the use of storage in humidity devices containing saturated salt solutions providing a relative humidity of 35, 60 and 75% at 25°C. SDNa converted from an amorphous powder to a hydrate crystal through a transient phase, characterised by the conversion into a sticky material on exposure to ambient humidity conditions. When stored in the humidity devices at 35% w/w, the salt appeared stable. On DVS analysis, the water vapour sorption profile for amorphous SDNa, showed that the amorphous salt directly converted to the dihydrate form, and the profile, as reflected by the weight change as a function of relative humidity, was in three stages. From 0 to 50% RH, the mass gain of water increased in a linear manner resulting in a water uptake (16%) higher than the stoichiometric amount of water required for the dihydrate form ($\text{SDNa}\cdot 2\text{H}_2\text{O}$) calculated at 12% (This phase probably represents the creation of the sticky material evident during exposure to ambient conditions). With a further increase of RH to 60%, the loss of water indicated the crystallisation of the amorphous material to the hydrated form, $\text{SDNa}\cdot 2\text{H}_2\text{O}$ (2nd stage). The third stage, after the phase transition to $\text{SDNa}\cdot 2\text{H}_2\text{O}$, was characterised by no water uptake, as indicated by a plateau until 90% RH. The $\text{SDNa}\cdot 2\text{H}_2\text{O}$ (dihydrate) was stable during desorption over a wide range of RH values from 90-10%. However it converted back to the anhydrous form when the DVS environment was set at 0% RH. In contrast, on exposure of the amorphous STNa to ambient conditions or when stored in the humidity chambers at RH values at or above 35% RH, the material undergoes amorphous deliquescence, transforming from a powder to a liquid viscous solution (Mikhailov et al., 2009). The transformation of the solid powder to the liquid solution was seen even when the amorphous salt was stored at RH conditions as low as that of 35%. This indicated that amorphous STNa was more hygroscopic than amorphous SDNa, with the latter appearing to be stable when stored at this 35% percentage RH. The

behaviour shown by the amorphous salt powders is in complete contrast to the water sorption behaviour of both unprocessed anhydrous crystalline substances where SDNa appeared to be a more hydrophilic substance than STNa. In fact, at very low RH conditions (20%), SDNa started to convert to the monohydrate form. In contrast, the STNa crystal structure remained unchanged and did not uptake any water up to 60% RH. Changes in the physical state of a substance can result in completely different hygroscopic behaviours which can affect performance or stability of the solid dosage form. These changes should be known, anticipated and ideally controlled.

6.7 Amorphous dispersions

Amorphous mixtures of both non ionised forms and corresponding sodium salts were produced by spray drying solutions of the two forms at different compositions from ethanol:water 9:1 v/v. Modulated scanning calorimetry detected a single T_g for all the spray dried composites, indicating that the two species form a molecular dispersion over the entire composition range. Stronger interactions between the species in the ST:STNa system compared to the SD:SDNa systems were noted. This was indicated by the positive deviation of T_g values from those predicted by the Gordon and Taylor equation and supported by the peak shifts detected by IR analysis. IR spectroscopy has shown that the two species can interact at a molecular level, through a combination of hydrogen bonding forming a one to two molar ratio system. In contrast, the system obtained by co-spray drying solutions of sulfadimidine and its corresponding salt form presented T_g values matching those predicted by the Gordon and Taylor equation. This indicated the lack of interactions as intense/strong as those in the case of the ST:STNa composites. The ΔT_g (T_{g,salt} - T_{g,acid}) is greater for sulfadimidine/sulfadimidine sodium compared to sulfathiazole/sulfathiazole sodium (76°C

versus 60°C). This suggests that the introduction of Na in composite systems results in a relatively greater potential reduction in molecular mobility for the molecules belonging to the SD:SDNa system compared to ST:STNa system. A lower molecular mobility may result in a reduced ability for the molecules in the system to interact, consequently resulting in T_g values that do not deviate significantly from those predicted by the Gordon-Taylor equation. IR analysis confirmed this hypothesis, as no significant peak shifts in the spectra of the composite were detected for SD:SDNa. A possible explanation is that in the latter system bonding between the molecules is of lower intensity compared to that in the ST:STNa system.

An increase in the physical stability upon storage in dry conditions relative to amorphous ST characterised ST:STNa samples. It has been shown in Chapter 4 that the crystallisation of amorphous ST takes place after one hour storage, whereas even the least stable among the co-spray dried mixtures of ST:STNa, obtained by adding only 10% w/w salt to the feed solution, remained amorphous up to 2 months post production when stored at 5 °C in dry conditions. Despite the lack of strong interaction between the species, the investigation of the physical stability upon storage in dry conditions demonstrated an increase of the stability also for SD:SDNa composites compared to SD spray dried alone. Composites of SD and SDNa were stable for over a year regardless of the composition, while SD processed alone crystallised after 5 months. The greater stability of the SD:SDNa system compared to the ST:STNa suggests that the physical stability of the composites reflects the dominating effect of recrystallisation of the acidic non ionised drug.

6.8 Main findings

- SD and ST can be transformed into an amorphous form on spray drying when the spray drier is operated in the open mode configuration, provided that drugs are in solution and the outlet temperature is below the T_g of the API.
- Amorphous ST can be tuned to crystallise into a specific polymorph by controlling the RH of storage.
- The crystallisation of amorphous ST in the solid state follows Ostwald's rule of stages.
- SDNa and STNa as model compounds for alkali salts of acidic drug compounds can be transformed into amorphous forms via spray drying.
- The amorphous forms of SDNa and STNa were characterised by glass transition temperatures of 155°C and 120°C, respectively. These values are 75 and 60 degrees higher than the T_g characterising the non ionised forms, suggesting that this property is strongly affected by the ionic interaction developed on amorphisation between the ions and the molecules.
- Due to increased T_g , the physical stability of the amorphous salt forms in dry conditions of storage is strongly enhanced compared to that of the amorphous non ionised forms.
- Exposure of the salt forms to water vapour induces crystallisation and the production of hydrates through viscous or liquid intermediate forms.

- Amorphous dispersions of SD:SDNa and ST:STNa could be produced over a wide composition range. The effect of inclusion of the sodium ion was to increase the T_g for the composite systems significantly up to 130 and 110 degrees for SD:SDNa and ST:STNa respectively
- Stronger molecular interaction seem to develop between the species in the ST:STNa system compared to the SD:SDNa system. Nevertheless an enhanced physical stability of the composites compared to the individual amorphous APIs was noted for both APIs.

6.9 Suggestions for future work

It would be worthwhile to continue this strand of research, in order to exploit the conclusions reached in the present study, in the following manner:

- Spray dry feed solutions prepared from solvents characterised by a lower boiling point compared to that of the solvents employed in this thesis. This would potentially enable the process temperature to be reduced below the T_g , which should result in the amorphous form being more easily obtained.
- Ascertain whether spray drying other APIs, which are known to present a needle-shape habit, could result in a morphology more suitable for downstream processing - i.e. spherical morphology.
- Analyse further the free acid-salt mixtures by means of solid state NMR to probe interactions and molecular mobility.

Co-formulate the amorphous salt forms or API/salt composite systems with excipients capable of competing for water retention in order to neutralise the plasticising effect of moisture on the ionised APIs.

References

References:

Aaltonen, J., Rantanen, J., Siiriä, S., Karjalainen, M., Jørgensen, A., Laitinen, N., Savolainen, M., Seitavuopio, P., Louhi-Kultanen, M., Yliruusi, J., 2003. Polymorph screening using near-infrared spectroscopy. *Analytical Chemistry* 75, 5267-5273.

Adamska, K., Voelkel, A., 2005. Inverse gas chromatographic determination of solubility parameters of excipients. *International Journal of Pharmaceutics* 304, 11-17.

Adsmund, D.A., Grant, D.J.W., 2001. Hydrogen bonding in sulfonamides. *Journal of Pharmaceutical Sciences* 90, 2058-2077.

Agrawal, A.M., Manek, R.V., Kolling, W.M., Neau, S.H., 2004. Water distribution studies within microcrystalline cellulose and chitosan using differential scanning calorimetry and dynamic vapor sorption analysis. *Journal of Pharmaceutical Sciences* 93, 1766-1779.

Ahlneck, C., Zografi, G., 1990. The molecular basis of moisture effects on the physical and chemical stability of drugs in the solid state. *International Journal of Pharmaceutics* 62, 87-95.

Airaksinen, S., Karjalainen, M., Shevchenko, A., Westermarck, S., Leppänen, E., Rantanen, J., Yliruusi, J., 2005. Role of water in the physical stability of solid dosage formulations. *Journal of Pharmaceutical Sciences* 94, 2147-2165.

Alvarez-Lorenzo, C., Gómez-Amoza, J.L., Martínez-Pacheco, R., Souto, C., Concheiro, A., 2000. Interactions between hydroxypropylcelluloses and vapour/liquid water. *European Journal of Pharmaceutics and Biopharmaceutics* 50, 307-318.

Ambarkhane, A.V., Pincott, K., Buckton, G., 2005. The use of inverse gas chromatography and gravimetric vapour sorption to study transitions in amorphous lactose. *International Journal of Pharmaceutics* 294, 129-135.

- Andronis, V., Yoshioka, M., Zografi, G., 1997. Effects of sorbed water on the crystallization of indomethacin from the amorphous state. *Journal of Pharmaceutical Sciences* 86, 346-357.
- Anwar, J., Tarling, S.E., Barnes, P., 1989. Polymorphism of sulfathiazole. *Journal of Pharmaceutical Sciences* 78, 337-342.
- Ashford, M., 2002. *Pharmaceutics-The science of dosage form design-* ed. Aulton M., 17, 234-252.
- Aulton, M., 2002. *Pharmaceutics-The science of dosage form design-* ed. Aulton M., 2, 15-32.
- Baird, J.A., Taylor, L.S., 2012. Evaluation of amorphous solid dispersion properties using thermal analysis techniques. *Advanced Drug Delivery Reviews* 64, 396-421.
- Baird, J.A., Van Eerdenbrugh, B., Taylor, L.S., 2010. A classification system to assess the crystallization tendency of organic molecules from undercooled melts. *Journal of Pharmaceutical Sciences* 99, 3787-3806.
- Bates, S., Zografi, G., Engers, D., Morris, K., Crowley, K., Newman, A., 2006. Analysis of amorphous and nanocrystalline solids from their X-ray diffraction patterns. *Pharmaceutical Research* 23, 2333-2349.
- Beckmann, W., Otto, W.H., 1996. Occurrence, stability, kinetics of crystallization and polymorphic transition of the A, B and C modification of abecarnil: Influence of supersaturation, temperature, solvents and impurities. *Chemical Engineering Research and Design* 74, 750-757.
- Blagden, N., Davey, R.J., Lieberman, H.F., Williams, L., Payne, R., Roberts, R., Rowe, R., Docherty, R., 1998. Crystal chemistry and solvent effects in polymorphic systems: Sulfathiazole. *Journal of the Chemical Society - Faraday Transactions* 94, 1035-1044.

- Bosma, M., Ten Brinke, G., Ellis, T.S., 1988. Polymer-polymer miscibility and enthalpy relaxations. *Macromolecules* 21, 1465-1470.
- Bradley, R.H., Andreu, A., Cassity, K., Osbeck, S., Andrews, R., Meier, M., Johnston, C., 2010. Dependence of water vapour adsorption on the polarity of the graphene surfaces of multi-wall carbon nanotubes. *Adsorption Science and Technology* 28, 903-912.
- Bravo-Osuna, I., Ferrero, C., Jiménez-Castellanos, M.R., 2005. Water sorption-desorption behaviour of methyl methacrylate-starch copolymers: effect of hydrophobic graft and drying method. *European Journal of Pharmaceutics and Biopharmaceutics* 59, 537-548.
- Brittain, H.G. (1999) Methods for the characterization of polymorphs and solvates. In *Polymorphism in Pharmaceutical Solids*. Brittain, H. (ed.), 1st ed., Marcel Dekker Inc., New York, USA. pp. 1-34.
- Brum, J., Burnett, D., 2011. Quantification of surface amorphous content using dispersive surface energy: The concept of effective amorphous surface area. *AAPS PharmSciTech* 12, 887-892.
- Buchi-B-290, 2007. technical specification B-290.
- Buckton, G., Ambarkhane, A., Pincott, K., 2004. The use of inverse phase gas chromatography to study the glass transition temperature of a powder surface. *Pharmaceutical Research* 21, 1554-1557.
- Buckton, G., Chidavaenzi, O.C., Koosha, F., 2002. The effect of spray-drying feed temperature and subsequent crystallization conditions on the physical form of lactose. *AAPS PharmSciTech* [electronic resource] 3.
- Buckton, G., Darcy, P., 1995. The use of gravimetric studies to assess the degree of crystallinity of predominantly crystalline powders. *International Journal of Pharmaceutics* 123, 265-271.

- Buckton, G., Gill, H., 2007. The importance of surface energetics of powders for drug delivery and the establishment of inverse gas chromatography. *Advanced Drug Delivery Reviews* 59, 1474-1479.
- Burnett, D.J., Thielmann, F., Booth, J., 2004. Determining the critical relative humidity for moisture-induced phase transitions. *International Journal of Pharmaceutics* 287, 123-133.
- Burnett, D.J., Thielmann, F. and Brum, J., 2009. Using the DVS to investigate moisture induced crystallisation kinetics. *SMS Application note* 42.
- Burnett, D.J., Thielmann, F., Sokoloski, T., Brum, J., 2006. Investigating the moisture-induced crystallization kinetics of spray-dried lactose. *International Journal of Pharmaceutics* 313, 23-28.
- Byrn, S., Pfeiffer, L.R., Ganey, L.M., Hoiberg, C., Poochikian, G., 1995. Pharmaceutical solids: A strategic approach to regulatory considerations. *Pharmaceutical Research* 12, 945-954.
- Caira, M.R., 2007. Sulfa drugs as model cocrystal formers. *Molecular Pharmaceutics* 4, 310-316.
- Capparella, M., Foster Iii, W., Larrousse, M., Phillips, D.J., Pomfret, A., Tuvim, Y., 1995. Characteristics and applications of a new high-performance liquid chromatography guard column. *Journal of Chromatography A* 691, 141-150.
- Caron, V., Tajber, L., Corrigan, O.I., Healy, A.M., 2011. A comparison of spray drying and milling in the production of amorphous dispersions of sulfathiazole/polyvinylpyrrolidone and sulfadimidine/ polyvinylpyrrolidone. *Molecular Pharmaceutics* 8, 532-542.
- Chan, F.C., Anwar, J., Cernik, R., Barnes, P., Wilson, R.M., 1999. Ab initio structure determination of sulfathiazole polymorph V from synchrotron X-ray powder diffraction data. *Journal of Applied Crystallography* 32, 436-441.

- Chidavaenzi, O.C., Buckton, G., Koosha, F., Pathak, R., 1997. The use of thermal techniques to assess the impact of feed concentration on the amorphous content and polymorphic forms present in spray dried lactose. *International Journal of Pharmaceutics* 159, 67-74.
- Clas, S.D., Dalton, C.R., Hancock, B.C., 1999. Differential scanning calorimetry: Applications in drug development. *Pharmaceutical Science and Technology Today* 2, 311-320.
- Corrigan, O.I., Holohan, E.M., Sabra, K., 1984. Amorphous forms of thiazide diuretics prepared by spray-drying. *International Journal of Pharmaceutics* 18, 195-200.
- Crocker, D., Hodnett, B.K., 2010. Mechanistic features of polymorphic transformations: The role of surfaces. *Crystal Growth and Design* 10, 2808-2816.
- Crusellas, J., 1942. The vapor pressure of some hydrates of sulfathiazole sodium. *Journal of the American pharmaceutical association* 31(5), 157-158.
- Cullity, B.D., 1978 *Elements of X-ray Diffraction*. 2nd ed., Addison and Wesley Publishing Company Inc., Reading, USA. pp. 33-106.
- Cuppen, H.M., Van Eerd, A.R.T., Meekes, H., 2004. Needlelike morphology of aspartame. *Crystal Growth and Design* 4, 989-997.
- Datta, S., Grant, D.J.W., 2004. Crystal structures of drugs: Advances in determination, prediction and engineering. *Nature Reviews Drug Discovery* 3, 42-57.
- Delgado, D.R., Vargas, E.F., Martínez, F., 2011. Thermodynamics of the mixing process of several sodium sulfonamides in ethanol + water cosolvent mixtures. *Estudio termodinámico del proceso de mezcla de algunas sulfonamidas sódicas en mezclas cosolventes etanol + agua* 18, 192-200.

Della Volpe, C., Siboni, S., 1997. Some reflections on acid-base solid surface free energy theories. *Journal of Colloid and Interface Science* 195, 121-136.

Dobry, D.E., Settell, D.M., Baumann, J.M., Ray, R.J., Graham, L.J., Beyerinck, R.A., 2009. A model-based methodology for spray-drying process development. *Journal of Pharmaceutical Innovation* 4, 133-142.

Dontireddy, R., Crean, A.M., 2011. A comparative study of spray-dried and freeze-dried hydrocortisone/ polyvinyl pyrrolidone solid dispersions. *Drug Development and Industrial Pharmacy* 37, 1141-1149.

DVS-training-guide, 2009. Experimental setup and data interpretation.

FDA, F.D.A., 2007. Guidance for Industry ANDAs: Pharmaceutical Solid Polymorphism.

Forbes, R.T., 1998. Water vapor sorption studies on the physical stability of a series of spray-dried protein/sugar powders for inhalation. *Journal of Pharmaceutical Sciences* 87, 1316-1321.

Gilani, K., Najafabadi, A.R., Darabi, M., Barghi, M., Rafiee-Tehrani, M., 2004. Influence of formulation variables and inhalation device on the deposition profiles of cromolyn sodium dry powder aerosols. *Daru* 12, 123-130.

Giron, D., 1998. Contribution of thermal methods and related techniques to the rational development of pharmaceuticals - Part 1. *Pharmaceutical Science and Technology Today* 1, 191-199.

Giron, D., 2001. Investigations of polymorphism and pseudo-polymorphism in pharmaceuticals by combined thermoanalytical techniques. *Journal of Thermal Analysis and Calorimetry* 64, 37-60.

Giron, D., Mutz, M., Gamier, S., 2004. Solid-state of pharmaceutical compounds impact of the ICH Q6 guideline on industrial development. *Journal of Thermal Analysis and Calorimetry* 77, 709-747.

- Grisedale, L.C., Jamieson, M.J., Belton, P.S., Barker, S.A., Craig, D.Q.M., 2011. Characterization and quantification of amorphous material in milled and spray-dried salbutamol sulfate: A comparison of thermal, spectroscopic, and water vapor sorption approaches. *Journal of Pharmaceutical Sciences* 100, 3114-3129.
- Grossjohann, C., Eccles, K.S., Maguire, A.R., Lawrence, S.E., Tajber, L., Corrigan, O.I., Healy, A.M., 2012. Characterisation, solubility and intrinsic dissolution behaviour of benzamide: Dibenzyl sulfoxide cocrystal. *International Journal of Pharmaceutics* 422, 24-32.
- Hancock, B.C., Shamblin, S.L., 1998. Water vapour sorption by pharmaceutical sugars. *Pharmaceutical Science and Technology Today* 1, 345-351.
- Hancock, B.C., Shamblin, S.L., Zografi, G., 1995. Molecular mobility of amorphous pharmaceutical solids below their glass transition temperatures. *Pharmaceutical Research* 12, 799-806.
- Hancock, B.C., Zografi, G., 1994. The relationship between the glass transition temperature and the water content of amorphous pharmaceutical solids. *Pharmaceutical Research* 11, 471-477.
- Hancock, B.C., Zografi, G., 1997. Characteristics and Significance of the Amorphous State in Pharmaceutical Systems. *Journal of Pharmaceutical Sciences* 86, X1-12.
- Hiatt, A.N., Ferruzzi, M.G., Taylor, L.S., Mauer, L.J., 2008. Impact of deliquescence on the chemical stability of vitamins B 1, B 6, and C in powder blends. *Journal of Agricultural and Food Chemistry* 56, 6471-6479.
- Hiatt, A.N., Taylor, L.S., Mauer, L.J., 2011. Effects of co-formulation of amorphous maltodextrin and deliquescent sodium ascorbate on moisture sorption and stability. *International Journal of Food Properties* 14, 726-740.

Hilden, L.R., Morris, K.R., 2004. Physics of Amorphous Solids. *Journal of Pharmaceutical Sciences* 93, 3-12.

Huang, L.F., Tong, W.Q., 2004. Impact of solid state properties on developability assessment of drug candidates. *Advanced Drug Delivery Reviews* 56, 321-334.

Hu, Y., Erxleben, A., Ryder, A.G., McArdle, P., 2010. Quantitative analysis of sulfathiazole polymorphs in ternary mixtures by attenuated total reflectance infrared, near-infrared and Raman spectroscopy. *Journal of Pharmaceutical and Biomedical Analysis* 53, 412-420.

ICH Topic Q3C (R4) Impurities: Guideline for Residual Solvents, 2009

Islam, M.I.U., Langrish, T.A.G., 2010. The effect of different atomizing gases and drying media on the crystallization behavior of spray-dried powders. *Drying Technology* 28, 1035-1043.

Janssens, S., Anné, M., Rombaut, P., Van den Mooter, G., 2009. Spray drying from complex solvent systems broadens the applicability of Kollicoat IR as a carrier in the formulation of solid dispersions. *European Journal of Pharmaceutical Sciences* 37, 241-248.

Janssens, S., Van Den Mooter, G., 2009. Review: Physical chemistry of solid dispersions. *Journal of Pharmacy and Pharmacology* 61, 1571-1586.

Jouppila, K., Kansikas, J., Roos, Y.H., 1998. Crystallization and X-ray diffraction of crystals formed in water-plasticized amorphous lactose. *Biotechnology Progress* 14, 347-350.

K.R. Morris, N.R.-H., 1993. Hydrates. *Encyclopedia of pharmaceutical technology*, Marcel Dekker, New York, 393-440.

- Karmwar, P., Graeser, K., Gordon, K.C., Strachan, C.J., Rades, T., 2012. Effect of different preparation methods on the dissolution behaviour of amorphous indomethacin. *European Journal of Pharmaceutics and Biopharmaceutics* 80, 459-464.
- Kaushal, A.M., Chakraborti, A.K., Bansal, A.K., 2008. FTIR studies on differential intermolecular association in crystalline and amorphous states of structurally related non-steroidal anti-inflammatory drugs. *Molecular Pharmaceutics* 5, 937-945.
- Kaushal, A.M., Gupta, P., Bansal, A.K., 2004. Amorphous drug delivery systems: Molecular aspects, design, and performance. *Critical Reviews in Therapeutic Drug Carrier Systems* 21, 133-193.
- Kedward, C.J., Macnaughtan, W., Mitchell, J.R., 2000. Crystallization kinetics of amorphous lactose as a function of moisture content using isothermal differential scanning calorimetry. *Journal of Food Science* 65, 324-328.
- Kerč, J., Srčič, S., 1995. Thermal analysis of glassy pharmaceuticals. *Thermochimica Acta* 248, 81-95.
- Khoshkhoo, S., Anwar, J., 1993. Crystallization of polymorphs: the effect of solvent. *Journal of Physics D: Applied Physics* 26.
- Langer, E., Kamiiska-Bach, G., 2011. Inverse gas chromatography characterization of coatings. *JCT CoatingsTech* 8, 46-51.
- Langrish, T.A.G., 2007. New engineered particles from spray dryers: Research needs in spray drying. *Drying Technology* 25, 971-983.
- Lappalainen, M., Pitkänen, I., Harjunen, P., 2006. Quantification of low levels of amorphous content in sucrose by hyperDSC. *International Journal of Pharmaceutics* 307, 150-155.

Lee, C.H.a.S., 2002. Large-scale aspects of salt formation: Processing of intermediates and final products. *Handbook of pharmaceutical salts. Properties, selection and use* 8, 191-220.

Levine H. and Slade L., 1987, Water as a Plasticizer: Physicochemical Aspects of Low Moisture Polymeric Systems,” in *Water Science Reviews*, F. Franks Ed. (Cambridge University Press, Cambridge, UK), pp. 179–185.

Likussar, W., Boltz, D.F., 1971. Theory of continuous variations plots and a new method for spectrophotometric determination of extraction and formation constants. *Analytical Chemistry* 43, 1265-1272.

Liu, Y., Bhandari, B., Zhou, W., 2006. Glass transition and enthalpy relaxation of amorphous food saccharides: A review. *Journal of Agricultural and Food Chemistry* 54, 5701-5717.

Löbmann, K., Strachan, C., Grohganz, H., Rades, T., Korhonen, O., Laitinen, R., 2012. Co-amorphous simvastatin and glipizide combinations show improved physical stability without evidence of intermolecular interactions. *European Journal of Pharmaceutics and Biopharmaceutics* 81, 159-169.

Lu, Q.L., Yang, G., Gu, H., 2005. Phase quantification of two chlorothalonil polymorphs by X-ray powder diffraction. *Analytica Chimica Acta* 538, 291-296.

Master, K., 2002. *Spray drying in practice*. SprayDryConsult International ApS. Denmark.

Maury, L., Rambaud, J., Pauvert, B., 1985. Physicochemical and structural study of sulfamethazine. *Journal of Pharmaceutical Sciences* 74, 422-426

McArdle, P., Hu, Y., Lyons, A., Dark, R., 2010. Predicting and understanding crystal morphology: the morphology of benzoic acid and the polymorphs of sulfathiazole. *CrystEngComm* 12, 3119-3125.

McCrone, W.C., 1965 *Physics and Chemistry of the Organic Solid State*. eds. D. Fox, M. M. Labes and A. Weissberger, Interscience Publishers, London 2, 725-767.

Mikhailov, E., Vlasenko, S., Martin, S.T., Koop, T., Pöschl, U., 2009. Amorphous and crystalline aerosol particles interacting with water vapor: Conceptual framework and experimental evidence for restructuring, phase transitions and kinetic limitations. *Atmospheric Chemistry and Physics* 9, 9491-9522.

Mortko, C.J., Sheth, A.R., Variankaval, N., Li, L., Farrer, B.T., 2010. Risk assessment and physicochemical characterization of a metastable dihydrate API phase for intravenous formulation development. *Journal of Pharmaceutical Sciences* 99, 4973-4981.

Najafabadi, A.R., Gilani, K., Barghi, M., Rafiee-Tehrani, M., 2004. The effect of vehicle on physical properties and aerosolisation behaviour of disodium cromoglycate microparticles spray dried alone or with L-leucine. *International Journal of Pharmaceutics* 285, 97-108.

Newell, H.E., Buckton, G., Butler, D.A., Thielmann, F., Williams, D.R., 2001. The use of inverse phase gas chromatography to study the change of surface energy of amorphous lactose as a function of relative humidity and the processes of collapse and crystallisation. *International Journal of Pharmaceutics* 217, 45-56.

Newell, H.E., Buckton, G., Butler, D.A., Thielmann, F., Williams, D.R., 2001a. The use of inverse phase gas chromatography to measure the surface energy of crystalline, amorphous, and recently milled lactose. *Pharmaceutical Research* 18, 662-666.

Newman, A.W., Reutzel-Edens, S.M., Zografí, G., 2008. Characterization of the "hygroscopic" properties of active pharmaceutical ingredients. *Journal of Pharmaceutical Sciences* 97, 1047-1059.

Nolan, L., 2008. title. Research thesis, Trinity College Dublin, Dublin.

Oakley, D.E., 1997. Produce uniform particles by spray drying. *Chemical Engineering Progress* 93, 48-54.

Paluch, K.J., Tajber, L., Amaro, M.I., Corrigan, O.I., Healy, A.M., 2012. Impact of process variables on the micromeritic and physicochemical properties of spray-dried microparticles - Part II.

Physicochemical characterisation of spray-dried materials. *Journal of Pharmacy and Pharmacology*.

Parmar, M.M., Khan, O., Seton, L., Ford, J.L., 2007. Polymorph selection with morphology control using solvents. *Crystal Growth and Design* 7, 1635-1642.

Price, G.J., 1988. Calculation of solubility parameters from inverse gas chromatography. Publ by ACS, Toronto, Ont, Can, pp. 1009-1013.

Puri, V., Dantuluri, A.K., Kumar, M., Karar, N., Bansal, A.K., 2010. Wettability and surface chemistry of crystalline and amorphous forms of a poorly water soluble drug. *European Journal of Pharmaceutical Sciences* 40, 84-93.

Qian, F., Huang, J., Hussain, M.A., 2010. Drug-polymer solubility and miscibility: Stability consideration and practical challenges in amorphous solid dispersion development. *Journal of Pharmaceutical Sciences* 99, 2941-2947.

Rodríguez-Hornedo, N., Murphy, D., 1999. Significance of controlling crystallization mechanisms and kinetics in pharmaceutical systems. *Journal of Pharmaceutical Sciences* 88, 651-660.

Rodríguez-Spong, B., Price, C.P., Jayasankar, A., Matzger, A.J., Rodríguez-Hornedo, N., 2004. General principles of pharmaceutical solid polymorphism: A supramolecular perspective. *Advanced Drug Delivery Reviews* 56, 241-274.

Rubino, J.T., 1989. Solubilities and solid state properties of the sodium salts of drugs. *Journal of Pharmaceutical Sciences* 78, 485-489.

Saleki-Gerhardt, A., Ahlneck, C., Zografi, G., 1994. Assessment of disorder in crystalline solids. *International Journal of Pharmaceutics* 101, 237-247.

Schultz, J., Lavielle, L., Martin, C., 1987. The role of the interface in carbon-fiber epoxy composites. *Journal of Adhesion* 23, 45-60.

Shah, B., Kakumanu, V.K., Bansal, A.K., 2006. Analytical techniques for quantification of amorphous/crystalline phases in pharmaceutical solids. *Journal of Pharmaceutical Sciences* 95, 1641-1665.

Socrates, G., 2001. Infrared and Raman characteristic group frequencies. Tables and charts. John Wiley & Sons, Chichester.

Tajber, L., Corrigan, O.I., Healy, A.M., 2005. Physicochemical evaluation of PVP-thiazide diuretic interactions in co-spray-dried composites - Analysis of glass transition composition relationships. *European Journal of Pharmaceutical Sciences* 24, 553-563.

Tang, X.C., Pikal, M.J., Taylor, L.S., 2002. A spectroscopic investigation of hydrogen bond patterns in crystalline and amorphous phases in dihydropyridine calcium channel blockers. *Pharmaceutical Research* 19, 477-483.

Taylor, L.S., 1998. Sugar-polymer hydrogen bond interactions in lyophilized amorphous mixtures. *Journal of Pharmaceutical Sciences* 87, 1615-1621.

Taylor, L.S., Williams, A.C., York, P., 1998. Particle size dependent molecular rearrangements during the dehydration of trehalose dihydrate-in situ FT-Raman spectroscopy. *Pharmaceutical Research* 15, 1207-1214.

Tewes, F., Tajber, L., Corrigan, O.I., Ehrhardt, C., Healy, A.M., 2010. Development and characterisation of soluble polymeric particles for pulmonary peptide delivery. *European Journal of Pharmaceutical Sciences*, 41, 2, 2010, 337-352.

Tewes, F., Gobbo, O.L., Amaro, M.I., Tajber, L., Corrigan, O.I., Ehrhardt, C., Healy, A.M., 2011. Evaluation of HP β CD-PEG microparticles for salmon calcitonin administration via pulmonary delivery. *Molecular Pharmaceutics* 8, 1887-1898.

Threlfall, T., 2003. Structural and Thermodynamic Explanations of Ostwald's Rule. *Organic Process Research and Development* 7, 1017-1027.

Threlfall, T.L., 1995. Analysis of organic polymorphs: A review. *The Analyst* 120, 2435-2460.

Tong, P., Taylor, L.S., Zografi, G., 2002. Influence of alkali metal counterions on the glass transition temperature of amorphous indomethacin salts. *Pharmaceutical Research* 19, 649-654.

Tong, P., Zografi, G., 1999. Solid-state characteristics of amorphous sodium indomethacin relative to its free acid. *Pharmaceutical Research* 16, 1186-1192.

Tong, P., Zografi, G., 2001. A study of amorphous molecular dispersions of indomethacin and its sodium salt. *Journal of Pharmaceutical Sciences* 90, 1991-2004.

Towler, C.S., Li, T., Wikstrom, H., Remick, D.M., Sanchez-Felix, M.V., Taylor, L.S., 2008. An investigation into the influence of counterion on the properties of some amorphous organic salts. *Molecular Pharmaceutics* 5, 946-955.

Van Campen, L., Zografi, G., Carstensen, J.T., 1980. An approach to the evaluation of hygroscopicity for pharmaceutical solids. *International Journal of Pharmaceutics* 5, 1-18.

Van Oss, C.J., Good, R.J., Chaudhury, M.K., 1988. Additive and nonadditive surface tension components and the interpretation of contact angles. *Langmuir* 4, 884-891.

Van Oss, C.J., Good, R.J., 1989. Surface tension and the solubility of polymers and biopolymers. The role of polar and apolar interfacial free energies. *Journal of macromolecular science. Chemistry A26*, 1183-1203.

Vehring, R., 2008. Pharmaceutical particle engineering via spray drying. *Pharmaceutical Research* 25, 999-1022.

Yang, S.S., Guillory, J.K., 1972. Polymorphism in sulfonamides. *Journal of Pharmaceutical Sciences* 61, 26-40.

Yang, X.L., Liu, J., Yang, L., Zhang, X.Y., 2005. Synthesis, characterization, and susceptibility of bacteria of selenium dioxide complexes with sulfadruugs. *Synthesis and Reactivity in Inorganic, Metal-Organic and Nano-Metal Chemistry* 35, 761-766.

Yoshioka, M., Hancock, B.C., Zograf, G., 1994. Crystallization of indomethacin from the amorphous state below and above its glass transition temperature. *Journal of Pharmaceutical Sciences* 83, 1700-1705.

Yoshioka, A., Tashiro, K., 2004. Solvent effect on the glass transition temperature of syndiotactic polystyrene viewed from time-resolved measurements of infrared spectra at the various temperatures and its simulation by molecular dynamics calculation. *Macromolecules* 37, 467-472.

Yu, L., 2001. Amorphous pharmaceutical solids: Preparation, characterization and stabilization. *Advanced Drug Delivery Reviews* 48, 27-42.

Zdziennicka, A., Jańczuk, B., 2010. Behavior of cationic surfactants and short-chain alcohols in mixed surface layers at water-air and polymer-water interfaces with regard to polymer wettability. II. Wettability of polymers. *Journal of Colloid and Interface Science* 350, 568-576.

Zeitler, J.A., Newnham, D.A., Taday, P.F., Threlfall, T.L., Lancaster, R.W., Berg, R.W., Strachan, C.J., Pepper, M., Gordon, K.C., Rades, T., 2006. Characterization of temperature-induced phase transitions in five polymorphic forms of sulfathiazole by terahertz pulsed spectroscopy and differential scanning calorimetry. *Journal of Pharmaceutical Sciences* 95, 2486-2498.

Zhang, C.L., Wang, F.A., Wang, Y., 2007. Solubilities of sulfadiazine, sulfamethazine, sulfadimethoxine, sulfamethoxydiazine, sulfamonomethoxine, sulfamethoxazole, and sulfachloropyrazine in water from (298.15 to 333.15) K. *Journal of Chemical and Engineering Data* 52, 1563-1566.

APPENDICES

APPENDIX I

All experiments are listed as discussed in each chapter. Key : EtOH = Ethanol, Ac= Acetone, OM = open mode configuration, CM = closed mode configuration, N₂ = nitrogen gas drying medium, Air = compressed air drying medium.

Table 1. Spray drying conditions for sulfadimidine systems

System (API)	Solvent (% v/v)	Spray Drying Mode	Solid Conc (%w/v)	Drying Gas	Inlet Temp (°C)	Outlet Temp (°C)	Pump rate (%)	Gas-flow rate L/hr	Aspirator %
Sulfadimidine	H ₂ O	OM	0.1	Air	120	64-65	30	473	100
Sulfadimidine	EtOH:H ₂ O (90:10)	OM	0.5	Air	120	84-86	30	473	100
Sulfadimidine	EtOH:H ₂ O (90:10)	OM	0.5	Air	78	49-51	30	473	100
Sulfadimidine	EtOH:H ₂ O (80:20)	OM	0.5	Air	78	50-52	30	473	100
Sulfadimidine	EtOH:H ₂ O (70:30)	OM	0.5	Air	78	47-50	30	473	100
Sulfadimidine	EtOH:H ₂ O (60:40)	OM	0.5	Air	78	48-50	30	473	100
Sulfadimidine	Ac	CM	0.5	N ₂	78	51-52	30	473	100
Sulfadimidine	Ac:H ₂ O (90:10)	CM	0.5	N ₂	78	49-51	30	473	100

System (API)	Solvent (% v/v) Volume	Spray Drying Mode	Solid Conc (%w/v)	Drying Gas	Inlet Temp (°C)	Outlet Temp (°C)	Pump rate (%)	Gas-flow rate L/hr	Aspirator %
Sulfadimidine	Ac:H ₂ O (70:30)	CM	0.5	N ₂	78	49-51	30	473	100
Sulfadimidine Sodium	H ₂ O	OM	0.5	Air	130	66-67	30	473	100
Sulfadimidine Sodium	H ₂ O	OM	0.5	Air	140	73-75	30	473	100
Sulfadimidine Sodium	H ₂ O	OM	0.5	Air	160	94-96	30	473	100
Sulfadimidine Sodium	EtOH:H ₂ O (90:10)	OM	0.5	Air	78	48-52	30	473	100
Sulfadimidine Sodium	EtOH:H ₂ O (80:20)	OM	0.5	Air	78	50-55	30	473	100
Sulfadimidine Sodium	EtOH:H ₂ O (70:30)	OM	0.5	Air	78	49-51	30	473	100
Sulfadimidine Sodium	EtOH:H ₂ O (60:40)	OM	0.5	Air	78	48-50	30	473	100
Sulfadimidine Sodium	Ac:H ₂ O (90:10)	CM	0.5	N ₂	78	54-55	30	473	100
Sulfadimidine Sodium	Ac:H ₂ O (80:20)	CM	0.5	N ₂	78	52-53	30	473	100

System (API)	Solvent (% v/v) Volume	Spray Drying Mode	Solid Conc (%w/v)	Drying Gas	Inlet Temp (°C)	Outlet Temp (°C)	Pump rate (%)	Gas-flow rate L/hr	Aspirator %
Sulfadimidine Sodium	Ac:H ₂ O (70:30)	OM	0.5	N ₂	78	50-52	30	473	100
Sulfadimidine Sodium	Ac:H ₂ O (60:40)	OM	0.5	N ₂	78	50-52	30	473	100
Sulfathiazole	EtOH	OM	0.5	Air	78	52-56	30	473	100
Sulfathiazole	EtOH:H ₂ O (90:10)	OM	0.5	Air	78	49-55	30	473	100
Sulfathiazole	EtOH:H ₂ O (80:20)	OM	0.5	Air	78	48-52	30	473	100
Sulfathiazole	EtOH:H ₂ O (70:30)	OM	0.5	Air	78	45-50	30	473	100
Sulfathiazole	EtOH:H ₂ O (90:10)	CM	0.5	N ₂	85	51	30	473	100
Sulfathiazole	EtOH:H ₂ O (70:30)	CM	0.5	N ₂	78	48-49	30	473	100
Sulfathiazole	Ac	CM	0.5	N ₂	78	58-59	30	473	100
Sulfathiazole	Ac:H ₂ O (90:10)	CM	0.5	N ₂	78	49-54	30	473	100

System (API)	Solvent (% v/v) Volume	Spray Drying Mode	Solid Conc (%w/v)	Drying Gas	Inlet Temp (°C)	Outlet Temp (°C)	Pump rate (%)	Gas-flow rate L/hr	Aspirator %
Sulfathiazole	Ac:H ₂ O (80:20)	CM	0.5	N ₂	78	48-50	30	473	100
Sulfathiazole	Ac:H ₂ O (70:30)	CM	0.5	N ₂	78	47-50	30	473	100
Sulfathiazole	Ac	CM	1.2	N ₂	78	57-58	30	473	100
Sulfathiazole	Ac:H ₂ O (90:10)	CM	3	N ₂	78	54-55	30	473	100
Sulfathiazole	Ac:H ₂ O (80:20)	CM	2.45	N ₂	78	49-50	30	473	100
Sulfathiazole	Ac:H ₂ O (70:30)	CM	1.95	N ₂	78	50-51	30	473	100
Sulfathiazole sodium	H ₂ O	OM	0.5	Air	160	98-99	30	473	100
Sulfathiazole sodium	EtOH	OM	0.5	Air	160	105-106	30	473	100
Sulfathiazole sodium	EtOH:H ₂ O (90:10)	OM	0.5	Air	160	102-108	30	473	100

System (API)	Solvent (% v/v) Volume (mls)	Spray Drying Mode	Solid Conc (%w/v)	Drying Gas	Inlet Temp (°C)	Outlet Temp (°C)	Pump rate (%)	Gas-flow rate L/hr	Aspirator %
Sulfathiazole sodium	EtOH:H ₂ O (80:20)	OM	0.5	Air	160	98-103	30	473	100
Sulfathiazole sodium	EtOH:H ₂ O (70:30)	OM	0.5	Air	160	98-100	30	473	100
Sulfathiazole sodium	EtOH	CM	0.5	N ₂	160	107	30	473	100
Sulfathiazole sodium	EtOH:H ₂ O (90:10)	CM	0.5	N ₂	160	103-106	30	473	100
Sulfathiazole sodium	EtOH:H ₂ O (80:20)	CM	0.5	N ₂	160	98-101	30	473	100
Sulfathiazole sodium	EtOH:H ₂ O (70:30)	CM	0.5	N ₂	160	98-100	30	473	100
Sulfathiazole sodium	Ac:H ₂ O (90:10)	CM	0.5	N ₂	160	98-100	30	473	100
Sulfathiazole sodium	Ac:H ₂ O (80:20)	CM	0.5	N ₂	160	98	30	473	100
Sulfathiazole sodium	Ac:H ₂ O (70:30)	CM	0.5	N ₂	160	97-98	30	473	100